

DESIGN OF LIGHTWEIGHT ASSISTIVE EXOSKELETONS FOR INDIVIDUALS WITH MOBILITY DISORDERS

BY

MICHAEL GEOFFREY MCKINLEY

A DISSERTATION SUBMITTED IN PARTIAL SATISFACTION OF THE

REQUIREMENTS FOR THE DEGREE OF

DOCTOR OF PHILOSOPHY

IN

MECHANICAL ENGINEERING

IN THE

GRADUATE DIVISION

OF THE

UNIVERSITY OF CALIFORNIA, BERKELEY

COMMITTEE IN CHARGE:

PROFESSOR HOMAYOON KAZEROONI

PROFESSOR DAVID DORNFELD

PROFESSOR RUZENA BAJCSY

SPRING 2014

Design of Lightweight Assistive Exoskeletons for Individuals with Mobility Disorders

Copyright © 2014

By

Michael Geoffrey McKinley
www.mckgyver.com



Abstract

Design of Lightweight Assistive Exoskeletons for Individuals with Mobility Disorders

by

Michael Geoffrey McKinley

Doctor of Philosophy in Mechanical Engineering

University of California, Berkeley

Professor Homayoon Kazerooni, Chair

There are over 270,000 people in the United States suffering from spinal cord injury. Currently, the wheelchair is the most commonly prescribed mobility solution for these individuals. Unfortunately, numerous health problems can be developed as a side effect of extended sitting. Studies have indicated that standing and walking for wheelchair bound individuals can improve overall health and mitigate these secondary health risks. Several passive walking devices exist, however these approaches are impractical due to the high metabolic cost associated with walking. Powered lower extremity exoskeletons have the capacity to substantially improve overall health and mobility of paralyzed individuals. The practicality of previous mobile medical exoskeletons has been limited due to cumbersome walking dynamics, high system mass and high cost.

This work introduces the Steven Exoskeleton, a lightweight minimally actuated assistive exoskeleton developed as a device that can be intuitively adopted by manual wheelchair users. This device builds off of the successes of several generations of low cost medical exoskeletons developed at the UC Berkeley Robotics and Human Engineering Laboratory.

Several elements of exoskeleton gait have been refined for the Steven Exoskeleton allowing better control of walking speed with more fluid walking dynamics. By smoothing hip trajectories and increasing stride length it has been possible to increase overall speed and pilot comfort. New hardware allows tunable hip and spine flexibility, improving pilot performance and adaptability. Through hardware and control refinement, comfortable walking speed has been increased to 0.48m/s from a previous maximum of 0.27m/s. Higher walking speed makes the device more useful for locomotion and allows greater independence in society.

The Steven Exoskeleton was designed to bridge the gap between seated and standing operation by assisting the user in a new range of postures. This approach expands pilot capabilities while seated and increases overall utility as a tool. This work also discusses a new approach to increase the reliability, and safety of standup and sit-down. Consistent standup and sit-down enables individuals to be self-sufficient with the possibility of full operation without a spotter. The adaptability of this device has enabled testing in laboratory and real world environments with pilots exhibiting a variety of medical conditions. The success of the Steven Exoskeleton and associated control and hardware adaptions moves devices of this nature closer to widespread adoption by paraplegics.

Table of Contents

Table of Contents.....	2
List of Figures	5
List of Tables	9
Acknowledgements.....	10
Chapter 1: Introduction and Motivation	11
1.1 The Impact of Spinal Cord Injury.....	11
1.2 Prior Art	12
1.2.1 Passive Devices	12
1.2.2 Active Devices	13
1.3 Thesis Contributions.....	14
1.3.1 Steven Exoskeleton: Developing the Medical Exoskeleton as a Practical Tool.....	14
1.3.2 Electronics Development for Exoskeletons	15
1.3.3 Achieving a Better Fit with Exoskeleton Systems.....	15
Chapter 2: Exoskeleton Systems for Individuals with Mobility Disorders	16
2.1 An Overview of Medical Exoskeleton Systems Developed a the Human Engineering Laboratory	16
2.1.1 Austin Exoskeleton (Mechanical Gait Generation).....	16
2.1.2 Austin II Exoskeleton (Dynamic Leg Articulation).....	17
2.1.3 Ryan.....	18
2.1.4 Steven	19
2.1.5 Daniel	19
Chapter 3: An Introduction to the Steven Exoskeleton.....	21
3.1 Exoskeleton Structure	22
3.1.1 Design for Integration with a Wheelchair.....	22
3.1.2 Torso Module.....	22
3.1.3 Orthotic Legs.....	23
3.1.4 Adjustable Legs	24
3.1.5 Key Features for Future Leg Brace Revisions.....	24
3.1.6 Wrap-Spring Knee	26
3.1.7 Hip Actuators	27

3.2	Steven Electronics	28
3.2.1	Electronics Board	28
3.2.2	Batteries.....	28
3.3	Exoskeleton Operation.....	29
3.3.1	User Interface and Finite State Machine	29
3.3.2	Guarding Against Unwanted State Changes.....	31
3.3.3	Steven Exoskeleton Gait	32
Chapter 4:	Passive Knee Gait	33
Chapter 5:	Exoskeleton Gait Generation for Variable Speed Walking	35
5.1	Definition of Terms.....	35
5.2	Approximating a Normal Human Walking Gait.....	36
5.3	Walking Continuously.....	39
5.3.1	Continuous Walking Through Gait Delay Modulation.....	39
5.3.2	More Haste, Less Speed.....	41
5.4	Designing an Exoskeleton Gait Based on Healthy Walking Biomechanics	42
5.5	Changing Walking Speed.....	43
5.6	Determining a Starting Point for a New Exoskeleton Pilot	43
5.7	Applying the Variable Gait Method to the Steven Exoskeleton	44
5.7.1	Practical Approach to Determining Gait as a Function of Speed	46
5.7.2	Practical Approach to Accelerating.....	46
5.7.3	Speed Comparison	47
Chapter 6:	Overcoming Barriers to Widespread Adoption: Creating a Device for Public Transit	
	49	
6.1	Addressing Independence with Robotic Exoskeletons	49
6.2	Using the Exoskeleton to Enhance Seated Abilities.....	50
6.2.1	Offering Support While Seated.....	51
6.2.2	Interaction with Objects on the Floor.....	51
6.3	Standing and Sitting Trajectories	52
6.3.1	Ineffective Sit to Stand.....	52
6.3.2	Sit to Stand: Developing a Better Standup Trajectory.....	52
6.3.3	Ineffective Sit-down Trajectory	54
6.3.4	Developing a Better Method for Sit-down	55
Chapter 7:	Tailoring the Right Fit: Making an Exoskeleton Best Suit Its Pilot	57

7.1	Mechanical Sizing	57
7.1.1	Exoskeleton Dimensions	57
7.1.2	Location and Construction of Key Pads	57
7.2	Posture While Seated.....	60
7.3	Posture for Static Balance and Walking	60
7.3.1	Comparison of Standing Posture between Steven and Austin Exoskeletons.....	62
Chapter 8:	Electronics for Exoskeleton Systems	63
8.1	Main Board Design.....	64
8.1.1	Constraints on Electronics Design.....	64
8.1.2	High Power Systems.....	64
8.1.3	Low Power Systems	65
8.1.4	Layout.....	66
8.1.5	Keeping Track of Data on the Exoskeleton	66
8.1.6	Battery Charging	67
Chapter 9:	Developing a Lightweight Handheld User Interface.....	68
9.1	Comparison to Other User Interface Approaches	68
9.2	User Interface Simplicity	68
9.3	Impact of Power Requirements on User Interface Design	69
Chapter 10:	Taking the Next Steps.....	73
10.1	Reduction in Mass	73
10.2	Simplified Donning	74
10.3	Working with Contracture and Spasticity	74
10.4	Moving Faster.....	74
10.4.1	Hardware Modifications	74
10.4.2	User Interface Modifications	74
Chapter 11:	Concluding Remarks.....	75
Chapter 12:	Bibliography	76
Appendix A: Media Featuring My Work	82	
Patents and Publications.....	85	
Media Featuring My Work	85	
Appendix B: The Austin Exoskeleton	88	

List of Figures

Figure 1 : (Left to right) 1) 1943 Dunlop: Once a box of rust, now a precision instrument. 2) The basement lab where it all began. 3) I use my grandfather's needle-nose pliers when I require soldering perfection.....	10
Figure 2: Spinal cord injury level and associated extremity function.....	12
Figure 3: Passive walking aids. a) Reciprocating Gait Orthosis (RGO) image from [21]. b) Long Leg Brace. c) Ankle Foot Orthosis (AFO) image from [22].	13
Figure 4: Active mobile medical exoskeleton prior art.....	13
Figure 5 : Austin Exoskeleton with mechanically generated gait.....	16
Figure 6 : Austin 2 Exoskeleton. Transmission decoupled for swing phase dynamic leg articulation.....	17
Figure 7: Playing in Berkeley California with the Ryan Exoskeleton.....	18
Figure 8 : Test pilot standing comfortably with the Steven Exoskeleton.....	19
Figure 9 : The Steven Exoskeleton.....	21
Figure 10: Modular elements of the Steven Exoskeleton.	21
Figure 11: The Steven Exoskeleton is quickly assembled around the exoskeleton pilot. A) Components laid out. B) Leg Braces attached. C) Torso Connected.	22
Figure 12: Pilot performing a sitting pivot transfer to get into the Austin Exoskeleton from a wheelchair.....	22
Figure 13: Steven Exoskeleton adjustment range.....	23
Figure 14: Adjustable compliant elements.....	23
Figure 15: Comparison of fixed length and adjustable legs.	24
Figure 16: Comparison of ankle brace designs.....	24
Figure 17: Ankle degrees of freedom.	25
Figure 18: Flexibility of insole design affords greater stability due to predictable contact with the ground.	26
Figure 19: Wrap-Spring – free swing operation. Figure from [34].	27
Figure 20: Wrap-Spring knee design. Image from [34].....	27
Figure 21 : AS5145b magnetic encoder module.....	27
Figure 22: Steven Exoskeleton hip actuator. Figure adapted from [38].	28
Figure 23: Steven Exoskeleton electronics.	28
Figure 24: Steven Exoskeleton finite state machine.....	29
Figure 25: Conditions for changing speed while walking.	30
Figure 26: User Interface embedded in forearm crutch.....	31
Figure 27: Bilateral transfemoral amputee walking on level ground with unactuated knee prosthesis.....	33
Figure 28: Comparison of dynamically coupled knee flexion to knee flexion developed by mechanical gait generation, and normal CGA walking data. Figure from [45]. This data was taken using the Austin 2 which was configured for both Mechanical Gait Generation and Dynamic swing.	34
Figure 29: Steven Exoskeleton Passive Knee Gait. Knees are locked against flexion at all times except during swing phase.	34

Figure 30: Definition of joint angles. $\theta_{\text{Tors}o}$ is the angle between torso and vertical reference frame. θ_{Hip} is the angle between torso centerline and thigh centerline, θ_{Knee} is the angle between thigh centerline and shank centerline. Positive and negative angles correspond to flexion and extension respectively.	35
Figure 31 : Definition of walking gait phases. Adapted from [46].....	36
Figure 32 : Definition of stride length and stride time.	36
Figure 33 Healthy Walking CGA Data from [47].	37
Figure 34: Overlay of sinusoidal approximation on CGA walking data. Red and blue are left and right CGA data respectively.	37
Figure 35: Sinusoid based approximation of hip trajectory for a continuous walking gait with constant cadence and step length. Solid line and dashed line represent right and left hips respectively.....	39
Figure 36: Illustration of walking gait with delay during double stance.	40
Figure 37: Step length geometry.	41
Figure 38: Smooth Gait vs. Modulated Gait.	42
Figure 39: Theoretical exoskeleton gait plotted against healthy adult walking. Data from [48] and [52]. Dashed lines represent lines of constant velocity. Relationship between cadence and stride length changes at higher speeds as an individual transitions from walking to running gait.	43
Figure 40: Comparison of Steven Exoskeleton gait and gait proposed in [37]. Note elimination of inflection point after maximum hip flexion resulting in smoother knee extension. New gait is designed to produce a longer stride at base speed.	45
Figure 41: One stride of the Steven Exoskeleton gait.	45
Figure 42: Variation of gait trajectory as step frequency increases. Note the slope of early and late swing phase increases for faster walking. This property provides adequate toe clearance as stride length increases.....	46
Figure 43: Steven Exoskeleton Gait Acceleration. First step with a long delay, subsequent steps accelerate to top speed. Note as step frequency increases, so too does stride length.....	47
Figure 44 : Comparison of Exoskeleton Walking Speeds.....	48
Figure 45 : Public Transit- Reimagining public education one exoskeleton at a time. Billboard featuring the Steven Exoskeleton installed outside of Oracle Arena in Oakland California; May 1, 2014.	49
Figure 46 : Muscle groups used for spinal extension.	50
Figure 47 : Normal force of shoulder straps compensates for lack of erector spinae functionality.	51
Figure 48: Exoskeleton seated Support. a) The user's torso is stabilized by hip actuators while seated in an upright posture. b) The user can effortlessly reach the floor by commanding the exoskeleton to bend forward. c) Reaching the floor requires substantial upper body strength without the exoskeleton.....	51
Figure 49 : Legacy standup state transition diagram.....	52
Figure 50: Comparison of Old and New Standup Postures A) Posture used in [37] B) New Posture C) Comparison.	53
Figure 51 : State transition diagram for new standup procedure.....	54
Figure 52 : State transitions for legacy approach to sit-down.....	54

Figure 53 : User falling forward after making contact with wheelchair due to insufficient erector spinae musculature. 1) Begin sit-down. 2) Touchdown on wheelchair. 3) Pilot falls forward.....	55
Figure 54 : State transitions for torque controlled sit-down method.....	55
Figure 55: Sit down: A) Positioned relative to wheelchair. B) Crutches placed beneath seated COM. C) Sit-down completed without repositioning crutches to support torso. The pilot is able to complete this maneuver without the assistance of a spotter.	56
Figure 56: Pad forces acting on user to maintain posture while wearing exoskeleton. Pad forces are low when standing in an erect posture as loads are efficiently transferred through the pilot's skeletal structure. Pad forces increase during standup and sit-down.	58
Figure 57 : Comparison of shoulder strap placement. Less tissue pressure and better control result from fixing straps above the shoulder.....	58
Figure 58: Cross section illustrating lumbar pad construction. Roho pad pressure should be minimized to minimize pad interface pressure.	59
Figure 59 : Multi cell Roho inflatable pad [71].	59
Figure 60: Tibial Tuberosity.....	60
Figure 61: Tuning hip and ankle angles.	61
Figure 62 : Tuning of ankle angle for knee stability during stance phase.	61
Figure 63: Comparison of standing posture between Steven (left) and Austin (right) exoskeletons. Note the pilot of the Steven Exoskeleton can stand hands free.	62
Figure 64 : Electronics for the Austin Exoskeleton.	63
Figure 65 : Miniaturized electronics for the Ryan assistive exoskeleton system.	63
Figure 66 : Daniel Exoskeleton control module.	63
Figure 67 : Polarity protection and power switching. High efficiency P-channel MOSFETs used for polarity protection and power switching to minimize part count and resistive losses. Heavy and light line thicknesses used to denote high and low current pathways respectively.....	65
Figure 68: Exoskeleton Electronics System Configuration: Heavy lines indicate flow of power; light lines indicate flow of data.....	66
Figure 69: Exoskeleton battery pack voltage measurement. A) Voltage divider for monitoring pack voltage. B) Overvoltage protection of microprocessor analog input.....	67
Figure 70: Freedom of motion afforded by a wireless User Interface. A) Leaning a crutch nearby to get hands free. B) Getting into a car and stowing crutches nearby.....	69
Figure 71: User interface information diagram.	70
Figure 72: Schematic of low power wireless user interface.	70
Figure 73: Schematic of high efficiency low power voltage regulator for wireless user interface.	71
Figure 74: Physical Implementation of low power wireless user interface board.	71
Figure 75: User Interface Embedded in Forearm Crutch.....	72
Figure 76 : A pilot of the Ryan Exoskeleton explores beyond the lab.	73
Figure 77 : System overview of the Austin Exoskeleton.....	88
Figure 78 : Austin Exoskeleton crew April 2011. (Left to right) Jason Reid, controls; Austin Whitney, pilot; Michael McKinley, hardware and electronics design; Wayne Tung, hardware and padding design.....	89
Figure 79 : Austin Exoskeleton mechanical gait generation MGG. Knee trajectory encoded in hardware.....	90

Figure 80 : Austin Exoskeleton Standup - Trajectory encoded in hardware. 91

List of Tables

Table 1: Average yearly expenses of SCI (Table from[2])	11
Table 2: Summary of active medical exoskeletons.....	14
Table 3: Steven Exoskeleton control as regulated by finite state machine.....	30
Table 4: Description of state change conditions.	31
Table 5 : Dimensionless numbers for gait scaling. Table from [55].....	44
Table 6: Comparison of walking speed across several exoskeleton systems.....	48
Table 7: 6 Bar linkage during standup and sit-down.	53
Table 8: Comparison of Old and New UI.....	70

Acknowledgements

Professor Kazerooni, it has been an honor and a pleasure to work with you over the last five years. Thank you for the opportunity to grow as a student and as an engineer. From day one I felt like I belonged in the Berkeley Human Engineering Lab, and I look forward to bringing our exoskeleton technologies into the world.

I would like to extend thanks to my dissertation and qualifying exam committees for the invaluable lessons you have helped me learn about myself while at Berkeley. Thank you for your insight Professors Dornfeld, Bajcsy, Lieu, and Dharan.

Steven, Austin, Daniel, and Ryan thank you for being a part of my life. You guys have been amazing partners as we developed these projects; your dedication creativity and indomitable spirit has given these exoskeletons a life of their own. You guys have been great friends and provide tremendous inspiration, insight, and enthusiasm.

Thank you everyone at the Human Engineering and Robotics Laboratory (HEL). Especially, I want to thank Wayne Tung, Jason Reid, Minerva Pillai, Yoon Jeong, and Bradley Perry for the dedication and energy that you have imparted into our projects over the last five years. Thanks for all the awesome photography Lee, and your sense of humor Stephen. Also thank you to all of the HEL undergraduate researchers for your dedication and willingness to learn.

Heather, thanks for all the great windsurfing, bike rides, and cookies; these things seem to fix any research problems. I want to extend thanks to Russell, Chris, Carl, Peter, and the rest of my Cal Sailing Club comrades and thanks to Berkeley, Treasure Island, Chrissy Field, and 3rd Avenue for being so awesome. Thanks Berkeley Climbing Crew for providing lots of great times and, thank you John for helping me continue the search for real bagels in the Bay Area.

Thanks to all of my teachers and advisers who helped form many facets of my education. Thanks Ross Kowalski, Robert Webster, Chris Connors, Michael McGuire, and Mark Dunn for opening my world to microprocessors, programming, CAD, physics, and leadership. Professors Danai, Rothstein, Soules, Grosse, and Rinderle, thanks for pushing my academic limits, and getting me started with research as an undergraduate. Thank you Rick, Miles, Mick, Gordon, and Dennis for helping me develop my hands as a machinist, and further my ability to bring ideas into the world.

Finally, I want to extend a special thanks to my family for helping me get to where I am today. Stephen and Jonathan, thanks for being awesome friends, colleagues, collaborators, and competitors. Mom and Dad, thanks for encouraging the continuous flow of crazy projects that came out of our first lab. Thanks to my grandfather for teaching me how to solder (almost 2 decades ago), Aunt Marilyn and Uncle Jack for exposing me to metalsmithing techniques, and Uncle Jim for introducing me to the metal lathe. The tools, techniques, and inspiration you all provided gave me a solid foundation to stand on.



Figure 1 : (Left to right) 1) 1943 Dunlop: Once a box of rust, now a precision instrument. 2) The basement lab where it all began. 3) I use my grandfather's needle-nose pliers when I require soldering perfection.

Chapter 1: Introduction and Motivation

1.1 The Impact of Spinal Cord Injury

In the United States there are over 270,000 individuals suffering from spinal cord injury (SCI) with 12,000 new cases annually [1]. Of these cases an estimated 43% of SCI result in paraplegia. Average yearly costs associated with SCI are reported in [2] and are tabulated in Table 1.

Table 1: Average yearly expenses of SCI (Table from[2])

Severity of Injury	Average Yearly Expenses (2013 US\$)	
	First Year	Each Subsequent Year
High Tetraplegia (C1-C4)	1,044,197	181,328
Low Tetraplegia (C5-C8)	754,524	111,237
Paraplegia	508,904	67,415
Incomplete motor function at any level	340,787	41,393

SCI has numerous detrimental long term health consequences due to extensive time confined to a wheelchair [3]. Some of the most common conditions include:

- Muscle atrophy[4], spasticity [5], decreased joint range of motion and contracture [6]
- Pressure ulcer development [7]
- Bone mineral loss and osteoporosis [8]
- Increased risk of urinary tract infection (UTI) [9]
- Bowel and digestive dysfunction [10]
- Reduced respiratory [11] and cardiovascular functions [12]

Several studies have linked higher risk of mortality to increased levels of time sitting [13]. Additionally, the population with SCI faces reduced life expectancy due to increased risk of renal failure, pneumonia, and septicemia[1]. Some of these medical conditions can be mitigated through frequent bouts of assisted standing and walking [2].

As illustrated in Figure 2 residual nerve function varies with the level and severity of spinal cord injury. Typically, individuals with higher injuries (upper thoracic or cervical spine) will suffer from increased levels of impairment as they will be left with reduced functionality below their injury level[14]. The assistive devices discussed in this dissertation require some form of stability aid for balance. Unfortunately, this means that these machines are only useful for individuals with complete motor control of their arms and enough torso control to assist with overall balance. These devices are not necessarily contraindicated for high level (upper thoracic) paraplegics; however, these individuals will require additional assistance during training and operation.

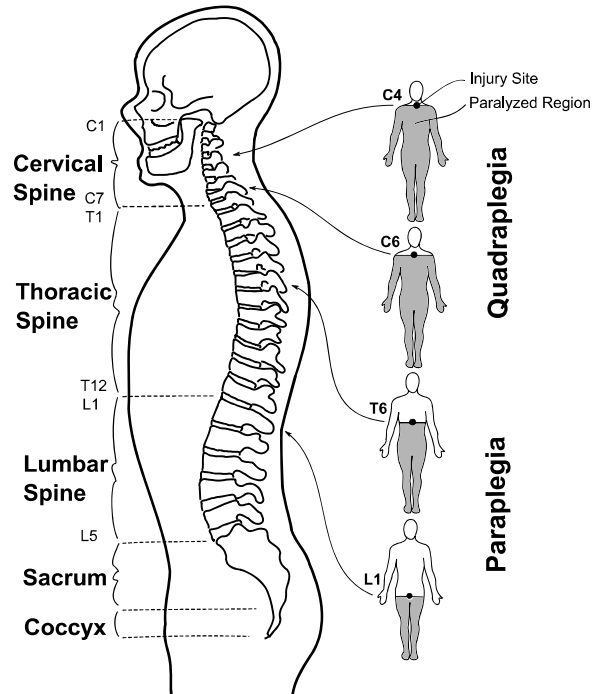


Figure 2: Spinal cord injury level and associated extremity function.

1.2 Prior Art

1.2.1 Passive Devices

Several passive devices such as leg braces and the reciprocating gait orthosis (RGO) have been developed to aid paraplegics with standing and walking[15]. As pictured in Figure 3, these devices assist by constraining lower extremity joint motion so that residual upper body muscles can be used for locomotion. This approach requires substantial upper body strength and crutches or a walker for balance. Unfortunately, ambulation through this method is highly inefficient; when compared to healthy walking at 1m/s, ambulation with the RGO requires up to 14 times more energy [16]. Additional information regarding RGO functionality and user adoption rates can be found in [17].

It is possible to reduce the metabolic cost of ambulation with the RGO or other passive orthotics through the introduction of functional electrical stimulation (FES) [18]. Numerous hybrid orthotic devices that use some form of mechanical bracing in conjunction with muscle stimulation are described in the literature [19]. The effect of FES on muscle activation is not consistent across individuals and is contraindicated for some paraplegics [20]. At this time devices developed at the UC Berkeley Human Robotics and Engineering Lab have not incorporated FES systems.

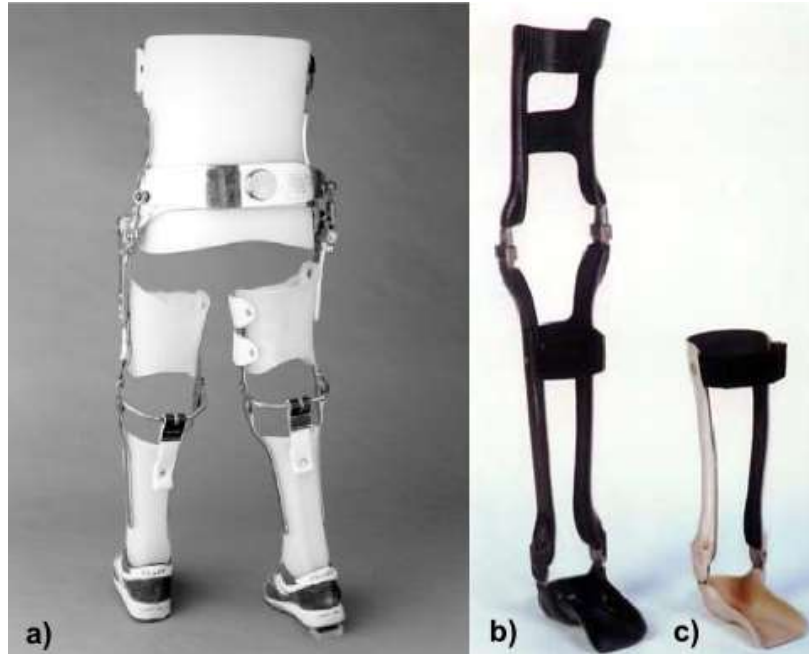


Figure 3: Passive walking aids. a) Reciprocating Gait Orthosis (RGO) image from [21]. b) Long Leg Brace. c) Ankle Foot Orthosis (AFO) image from [22].

1.2.2 Active Devices



Figure 4: Active mobile medical exoskeleton prior art.

Several active mobile medical exoskeleton systems have been developed to provide gait assistance for paraplegics (illustrated in Figure 4). The devices all aim to reduce the metabolic cost of walking compared to passive devices by providing torque at the joints (device specifications are summarized in Table 2). ReWalk [23], eLegs [24], and Indego [25], three of the most widely known devices marketed towards paraplegics, are similar in that they use four powered degrees of freedom (one at each hip, and one at each knee) to provide a walking gait. The user interface designs of these devices rely on some form of posture measurement to interpret the user's intent. eLegs uses an over shoe binding to constrain the pilot's feet relative to the device, while Indego and ReWalk both use in-shoe orthosis designs.

By using a total of ten actuators to control hip, knee, and ankle in the frontal and sagittal planes the Rex Exoskeleton is the only device to be completely self-balancing [26]. As each step is commanded, the user is moved through a series balanced postures so that the total center of mass is always over the stance foot [27]. This approach to self-balancing comes at the cost of much slower walking and substantially higher mass than other devices. However, Rex is the only device available for individuals suffering from quadriplegia as it does not require balance aids [28].

The Austin Exoskeleton represents the first medical exoskeleton developed by the UC Berkeley Human Engineering Lab. The Austin system was designed to forgo the cost and complexity of a system with knee actuators in favor of a mechanical gait generation system [29]. This device served as a baseline for subsequent systems proposed in this thesis.

Table 2: Summary of active medical exoskeletons.

Exoskeleton	Powered Degrees of Freedom		Stability Aid	Weight	Approximate Cost	Required Upper Body Strength	Foot Fixture Method	User Interface
	#	Location						
Austin Exoskeleton	2	1 at each Hip	Walker / Crutches	50 lbs. (23kg)	n/a	Moderate/ High	Outsole Binding	2 button wireless
Indego	4	1 at each Hip 1 at each Knee	Walker / Crutches	27 lbs. (12.2kg)	n/a	Moderate	Insole	Postural through Estimated Center of Pressure
ReWalk	4	1 at each Hip 1 at each Knee	Walker / Crutches	45 lbs. (20.4kg)	\$100,000	Moderate	Insole	Postural via Torso angle
eLegs	4	1 at each Hip 1 at each Knee	Walker / Crutches	45 lbs. (20.4kg)	\$100,000	Moderate	Outsole Binding	Postural via arm placement
Rex	10	2 at each Hip 1 at each Knee 2 at each Ankle	None	85 lbs. (38.6kg)	\$150,000	Minimal	Outsole Binding	Joystick

At this time, few articles have been published discussing the efficacy of powered exoskeleton devices. Currently, papers discuss early performance of ReWalk ([23], [30]), and anecdotal evidence regarding performance of eLegs [31] and Rex [32]. Several design problems including independence, ambulation energy, reliability, and system cost remain unsolved at this time by commercially available exoskeleton systems [33].

1.3 Thesis Contributions

The objective of this research is to develop exoskeleton systems which provide pilots with mobility solutions that are practical and self-sufficient. These systems have moved beyond cumbersome early prototypes, and are poised for independent use. The contributions presented in this thesis can be categorized in the following sections:

1.3.1 Steven Exoskeleton: Developing the Medical Exoskeleton as a Practical Tool

The Steven Exoskeleton represents the most recent step for modular full body exoskeletons developed in the Human Engineering Lab. Several advances over previous devices have been implemented. New features and adaptations include: 1) A new gait strategy that allows better

control in tight environments, and smoother top speed in open environments. 2) A new strategy for commanding the exoskeleton for intuitive, seamless, and predictable speed transitions. 3) New postures and features that allow paraplegic individuals to interact with their environment more easily.

1.3.2 Electronics Development for Exoskeletons

The author has developed several iterations of power and control electronics used in the Austin, Austin II, Ryan, RGO, Steven, and Daniel exoskeletons. Sections on electronics discuss requirements and development of power and control electronics, user interface electronics, power management, and data logging.

1.3.3 Achieving a Better Fit with Exoskeleton Systems

A number of lessons have been learned over several exoskeleton design iterations regarding best fitting of an exoskeleton system to a pilot. Specific areas addressed in these sections include: 1) Padding designs to optimize user comfort and promote skin integrity. 2) Strapping placement to best provide support and control to exoskeleton pilots. 3) Positioning of exoskeleton joints, and selection of rigid link lengths to best suit exoskeleton pilot dimensions. 4) Crutch length selection for best posture. 5) Joint angle settings and shoe selection to best improve stability for minimally actuated exoskeletons.

Chapter 2: Exoskeleton Systems for Individuals with Mobility Disorders

2.1 An Overview of Medical Exoskeleton Systems Developed at the Human Engineering Laboratory

The author has contributed to the development of several medical exoskeleton systems while working in Professor Kazerooni's Human Engineering and Robotics Laboratory (HEL) at UC Berkeley. A brief description of each exoskeleton is presented in the following sections.

2.1.1 Austin Exoskeleton (Mechanical Gait Generation)



Figure 5 : Austin Exoskeleton with mechanically generated gait.

Austin I	Mass	Gait	Knee	Assistive Objective
2010	50 lbs.	Mechanically Driven	Locking Gas Spring	Complete T10 or lower

The Austin exoskeleton was the first minimally actuated medical exoskeleton developed by the HEL team. The Austin Exoskeleton was comprised of a rigid metal frame (to support the pilot's torso and legs) with actuators located only at each hip. A Mechanical Gait Generation (MGG) system developed by Tung and McKinley produced a normal walking gait by automatically transferred power from the hip motors to articulate the knees [29]. Additionally, the MGG was designed to couple hip and knee motion to provide power during sitting and standing. More detailed information about this system can be found in [34]. Throughout development and testing of this exoskeleton several mechanical knees were designed to achieve different walking characteristics. Ultimately, the most stable knee system used with the MGG concept was designed around a locking gas damper (as discussed in [35]). Although the Austin Exoskeleton worked well to provide paraplegic pilots with ambulation assistance, it was clear that at 50lbs (23kg) the Austin system was too heavy for widespread adoption.

2.1.2 Austin II Exoskeleton (Dynamic Leg Articulation)

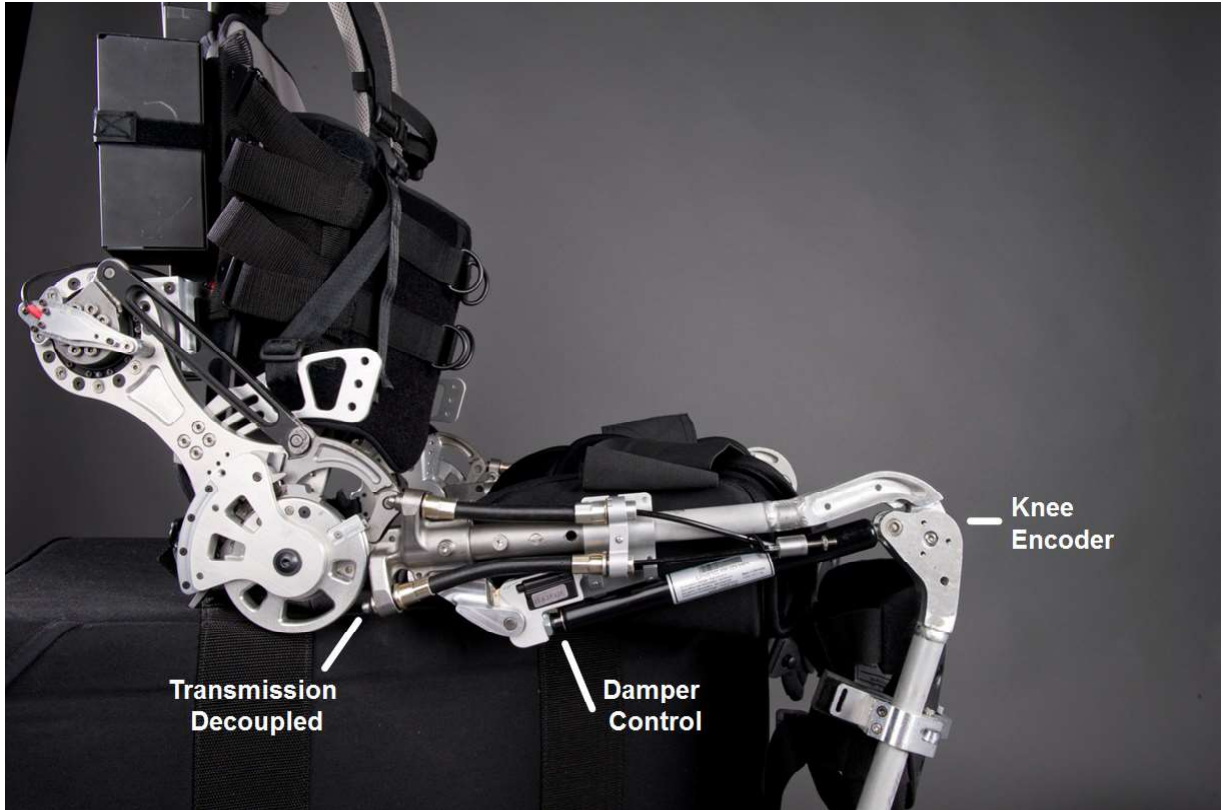


Figure 6 : Austin 2 Exoskeleton. Transmission decoupled for swing phase dynamic leg articulation.

Austin II	Mass	Gait	Knee	Assistive Objective
2011	45 lbs.	Dynamic	Ratchet Knee	Complete T10 or lower

The MGG concept was dropped in favor of Dynamic Leg Articulation (DLA) in an effort to reduce system weight and complexity [36]. DLA obviates the need for a traditional mechanical coupling between the hip and knee by treating the leg system as a two link pendulum. Instead of strictly coupling hip and knee rotation by a fixed ratio, a trajectory is chosen for the hip that creates a desired flexion response at the knee. Not only does this system achieve required joint trajectories for walking, but the resultant gait is more natural as the mechanism is no longer constrained to a fixed coupling. A new mechanism was designed for the knee that allows computer control of knee locking [34]. Overall system mass was slightly reduced from the previous system by eliminating some of the MGG system. Additional images and diagrams of the Austin Exoskeleton can be found in the Appendix.

2.1.3 Ryan



Figure 7: Playing in Berkeley California with the Ryan Exoskeleton.

Ryan	Mass	Gait	Knee	Assistive Objective
2011	22 lbs.	Dynamic	Wrap-Spring Knee	Complete T12 or lower

The Ryan exoskeleton was developed as an ultra-lightweight exoskeleton using the DLA concept discovered with the Austin 2 system. New electronics and knee hardware were developed as necessary to explore the full potential of the lightweight system. The Ryan exoskeleton proved to be a substantially more efficient form of ambulation allowing long distance and duration tests [37]. An efficient user interface was designed to address power consumption issues found with the Austin UI's.

2.1.4 Steven



Figure 8 : Test pilot standing comfortably with the Steven Exoskeleton.

Steven	Mass	Gait	Knee	Assistive Objective
2012	31 lbs.	Dynamic	Wrap-Spring Knee	Complete T6 or lower

Initially, the Steven Exoskeleton was developed as a modular version of the Ryan system. This approach allowed the system to be quickly adapted to a broad range of SCI patients. The Torso was designed as an adjustable unit that could be tuned to fit many body types [38]. New hardware was developed that allowed tunable stiffness of spine and leg supports to enable cooperation between pilot and machine. The user interface and control were further refined to address speed and independence issues identified in previous systems. The Steven Exoskeleton and associated design challenges are the focus of this dissertation.

2.1.5 Daniel

Daniel	Mass	Gait	Knee	Assistive Objective
2013	15 lbs.	Dynamic	None	Partial T12 or lower

The Daniel system is the first device developed for an incomplete spinal lesion. The hardware for this device is a stripped down version of the Steven torso module. New electronics were designed to allow further separation of the torso module for use with a hemiplegic patient. The control system developed by Bradley Perry is designed to amplify the capabilities of an individual with partial paralysis.

These devices are unified by a desire to reduce cost and complexity. With all of these exoskeleton devices it was observed that pilots were able to ambulate more naturally and more efficiently with systems that allowed the most direct and predictable voluntary control. This observation further validates the decision to eliminate knee actuation in favor of a passive mechanism for level ground walking with individuals exhibiting flaccid paralysis or partial muscular control. This finding is similar to the observation that some transfemoral amputees prefer non-microprocessor controlled legs as they allow more voluntary knee control over active prosthetics [39].

Chapter 3: An Introduction to the Steven Exoskeleton

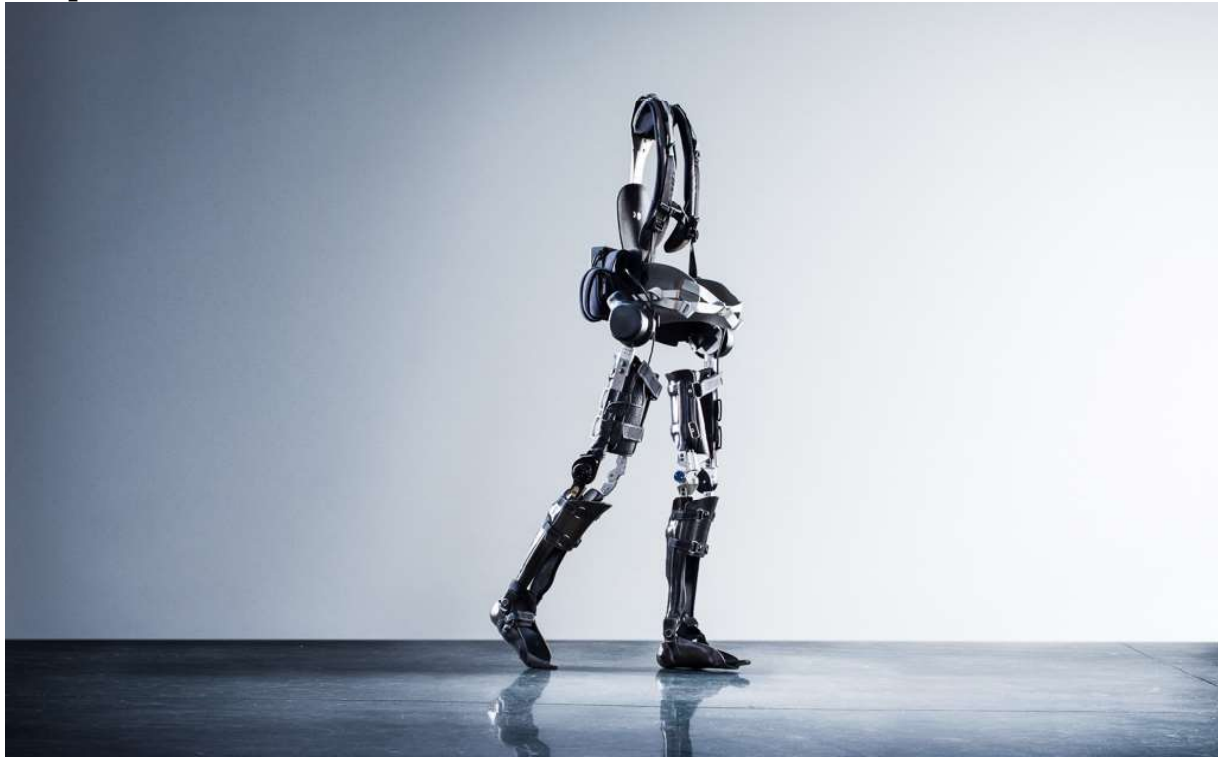


Figure 9 : The Steven Exoskeleton.

The Steven Exoskeleton (Figure 9) represents the best features of several iterations of mobility enhancement systems designed by the Human Engineering Laboratory at UC Berkeley. The Steven Exoskeleton is a semi-active assistive robotic system that consists of a flexible torso structure coupled at the hips to long leg braces (Figure 10). The system was developed to minimize weight while maintaining maximum maneuverability. Motors provide power at the hips while brakes at the knees govern when the knees are locked (to support weight) or unlocked (to swing freely). Batteries and computers are located near the waist of the system where they are out of the way. Crutches or a walker are used for balance, and the user commands the device through a wireless crutch mounted interface.



Figure 10: Modular elements of the Steven Exoskeleton.

3.1 Exoskeleton Structure

3.1.1 Design for Integration with a Wheelchair

The Steven Exoskeleton was designed to allow easy donning and doffing while remaining seated in one's wheelchair. The exoskeleton breaks down into three components (torso, right and left legs), all light enough to be manipulated and adjusted from a wheelchair as illustrated in Figure 11. This approach differs from previous designs where the exoskeleton remains fully assembled at all times. The modular approach obviates the need for the user to perform a sitting pivot transfer from his/her wheelchair into the exoskeleton (illustrated in Figure 12). Sitting pivot transfers require that the pilot have substantial upper body strength and control in order to lift and pivot themselves from the wheelchair into the adjacent exoskeleton [40]. By eliminating the sitting pivot transfer requirement, the exoskeleton is made accessible to a broader user group.

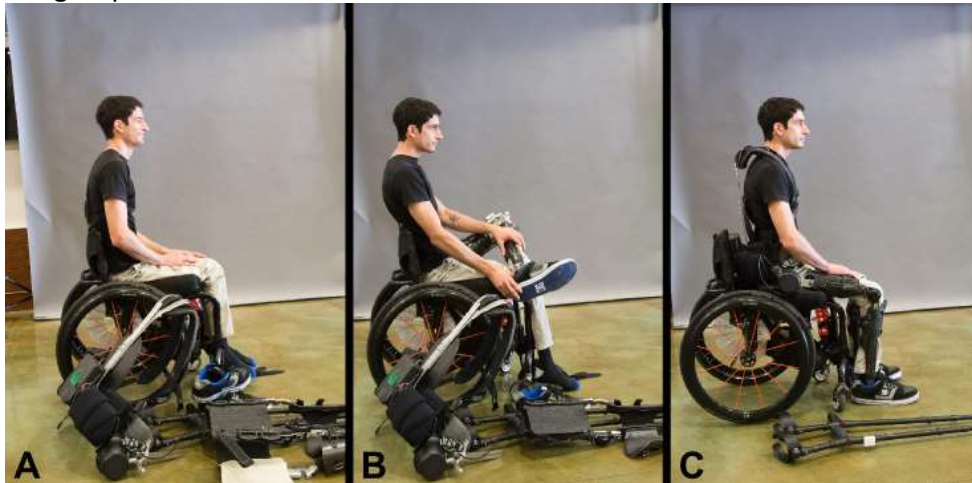


Figure 11: The Steven Exoskeleton is quickly assembled around the exoskeleton pilot. A) Components laid out. B) Leg Braces attached. C) Torso Connected.



Figure 12: Pilot performing a sitting pivot transfer to get into the Austin Exoskeleton from a wheelchair.

3.1.2 Torso Module

The torso structure of the Steven Exoskeleton was designed in collaboration with Patrick Barnes during the fall of 2012. The torso structure is adjustable to accommodate a broad range of body dimensions as illustrated in Figure 13. As illustrated in Figure 14, a number of exoskeleton torso components were designed to allow tunable flexibility. Flexible aluminum shoulder supports were designed to allow rotational compliance between the upper body and the lower frame.

Back support stiffness can be tuned to match the injury level of each pilot to stabilize during spinal flexion and extension (as discussed in chapter 6.2). Laterally flexible stainless steel couplings connect the torso to the legs. This flexibility affords stability during walking by allowing the user to shift weight more easily than with a rigidly coupled system. Additional details regarding the construction of the torso module can be found in [38].

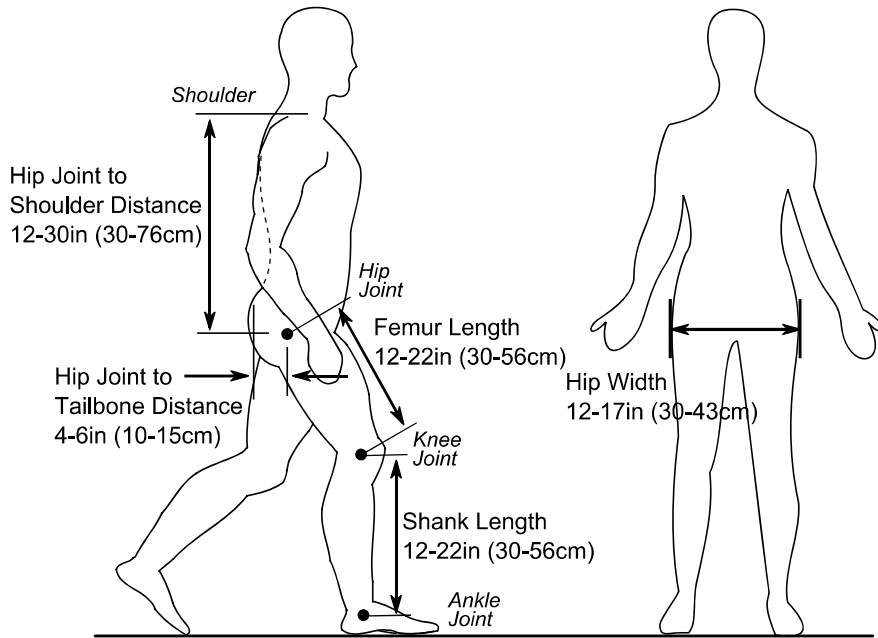


Figure 13: Steven Exoskeleton adjustment range.

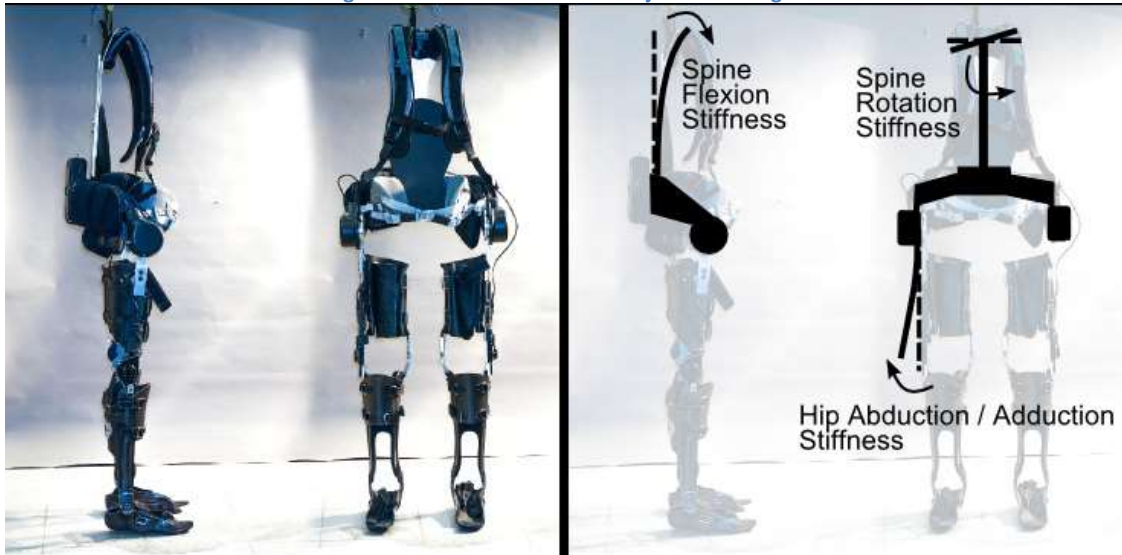


Figure 14: Adjustable compliant elements.

3.1.3 Orthotic Legs

Long leg braces (typically custom molded to the user's legs) are a standard orthotics technology prescribed to people with mobility disorders. Leg braces (illustrated in Figure 10) are coupled to the Steven Exoskeleton at the hip to provide support during standing and walking. At the knee,

a wrap-spring clutch is used to control knee motion during walking. The wrap-spring knee was designed as a drop in replacement for standard orthotic knee components (design details can be found in [34]). Orthotic legs braces are a mature, readily available technology. They offer a lightweight, low profile leg support system that can be easily worn under clothing, and inside standard shoes.

3.1.4 Adjustable Legs

It is often practical to test a new pilot with the Steven Exoskeleton before custom molding a set of braces. For this reason, an adjustable set of legs was designed to allow easy fitting to a broad range of users. These legs are not ideal for long duration use as they are considerably heavier and more cumbersome due to the included adjustment features. Figure 15 offers a visual comparison of fixed and adjustable leg braces.

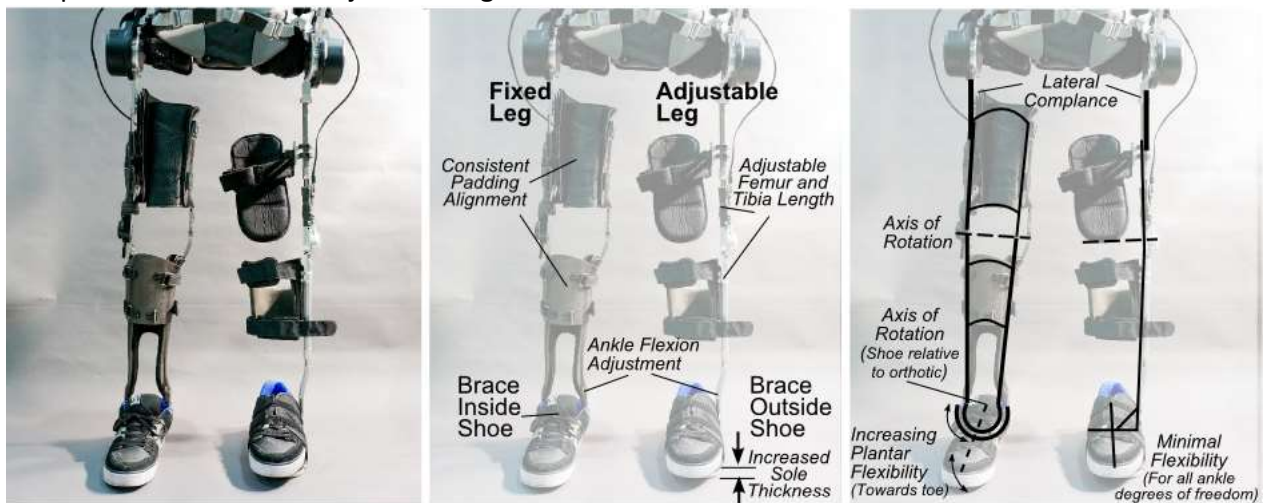


Figure 15: Comparison of fixed length and adjustable legs.

3.1.5 Key Features for Future Leg Brace Revisions

Ankle Foot Orthosis (AFO)



Figure 16: Comparison of ankle brace designs.

Several iterations of leg brace systems have been developed for the Steven Exoskeleton. Figure 16 illustrates a comparison between the insole and external ankle designs commonly used with the Steven Exoskeleton. The exoskeleton ankle is designed to protect the pilot's ankle by limiting abduction/adduction, plantar/dorsiflexion, and inversion/eversion (see Figure 17)

while aiding in stability and swing phase ground clearance during walking. Additionally it has been observed that tuning ankle flexibility parameters can positively affect gait efficiency and improve stability [41]. There are several variables that need to be balanced for a successful AFO design:

1. Ankle abduction/adduction and mid-foot flexibility

The neutral point of the ankle should be adjustable to so that the erect standing balance point can be adjusted (in conjunction with standing hip angle as discussed in chapter 7.3) to suit pilot preference. Generally, the ankle is angled in a slightly toe-down orientation so that the knee is kinematically extended and the pilot balances on the mid-foot region. The AFO mid-foot region mimics the functionality of healthy foot muscles by providing stiffness while standing and walking. If the mid-foot and ankle stiffness is too compliant the pilot will lose swing leg toe clearance during stance.

2. Forefoot flexibility

The forefoot flexes to allow load to be transferred to the ball of the foot while walking. If this area is too rigid (as in some outsole designs), balance becomes difficult as load is taken by a small region near the toes (see Figure 18).

3. Ankle Inversion/Eversion and ground interface

The AFO should protect the ankle against ankle inversion/eversion while allowing the foot to align with the walking surface. The insole design performs this function by allowing slight rotation between shoe and orthotic while keeping the ankle aligned (illustrated in Figure 18). Maintaining a large contact region with the ground provides better traction and helps pilots avoid inadvertent rotation in the transverse plane while walking.

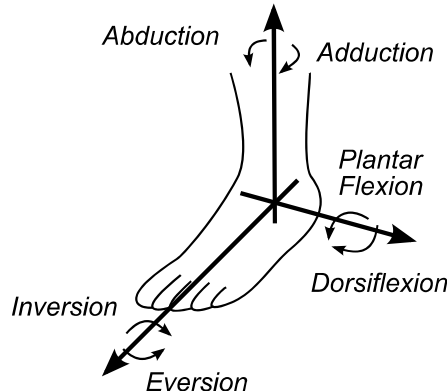


Figure 17: Ankle degrees of freedom.

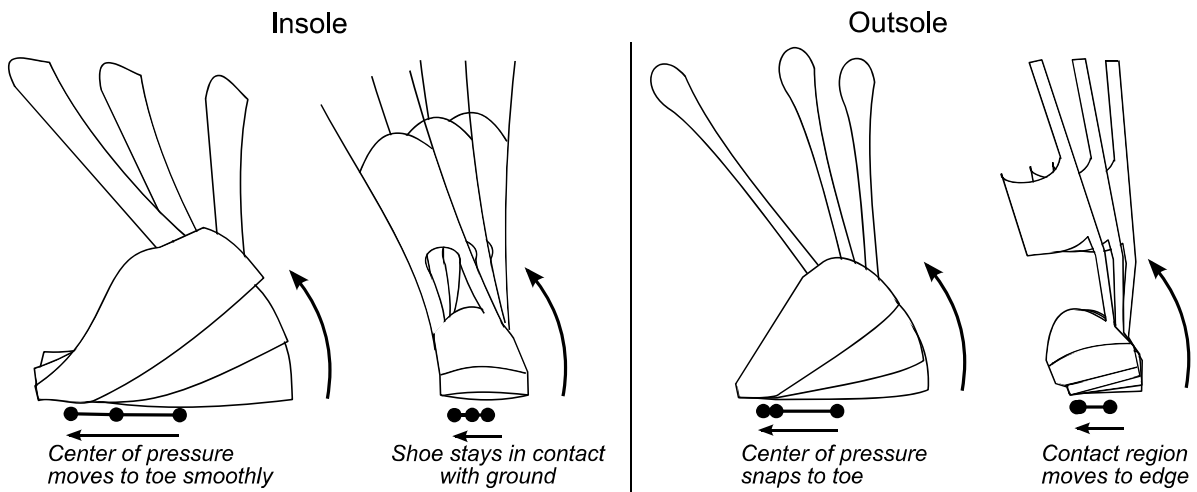


Figure 18: Flexibility of insole design affords greater stability due to predictable contact with the ground.

Knee Pad and Thigh Pad

A rigid heavily padded structure is required to keep the pilot's knee coaxially aligned with the exoskeleton knee joint. Pilot mass is transferred efficiently through the anatomic knee joint during stance (and resultant pad/knee tissue forces are kept low) if knee alignment is maintained during stance phase.

The thigh pad is critical for keeping pilot and exoskeletal hips aligned during standup and sit-down. If the thigh pad does not maintain alignment during standup, the pilot will sag out of the exoskeleton posing problems for balance and increasing the likelihood of pressure sores.

Leg Quick Connect

The leg quick connect allows the exoskeleton to be assembled around the user as three independent modules. The current design for the connector between leg brace and torso requires careful alignment and is difficult for a single person to assemble. A future revision should address these shortcomings.

3.1.6 Wrap-Spring Knee

The Steven Exoskeleton uses a wrap-spring clutch to provide torque at the knee. The advantage of the wrap-spring over other mechanical brake designs is the ability to lock at any angle, always provide free knee extension, and unlock smoothly while loaded. As illustrated in Figure 19, the wrap-spring consists of two coaxial cylindrical shafts elements coupled by a coil spring. In this design the spring behaves as a band brake, gripping the shafts if rotated in one direction and releasing the shafts if rotated in the other direction. By manipulating the free end of the spring it is possible to increase or decrease coupling torque; however this relationship is not linear [42]. The wrap-spring clutch knee pictured in Figure 20 is used for fixed and adjustable leg brace designs. The device used with the Steven Exoskeleton is the result of several design iterations to provide the right balance of size, torque performance, and locking/unlocking properties. Additional details regarding optimization and analysis of this design can be found in [34].

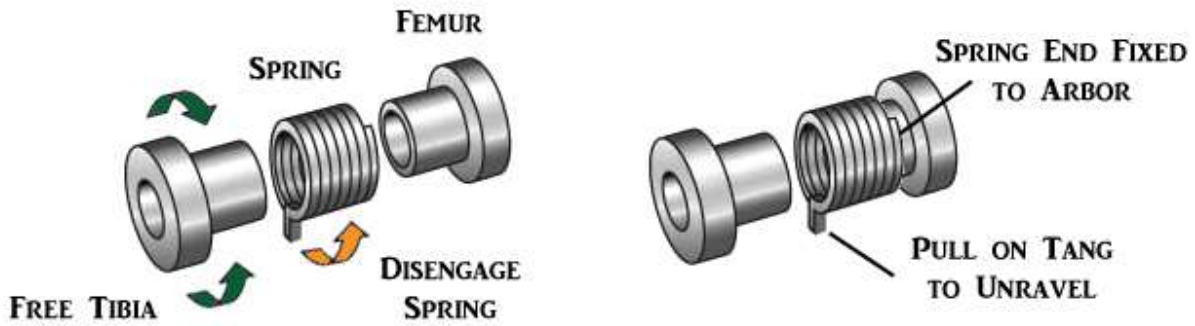


Figure 19: Wrap-Spring – free swing operation. Figure from [34].

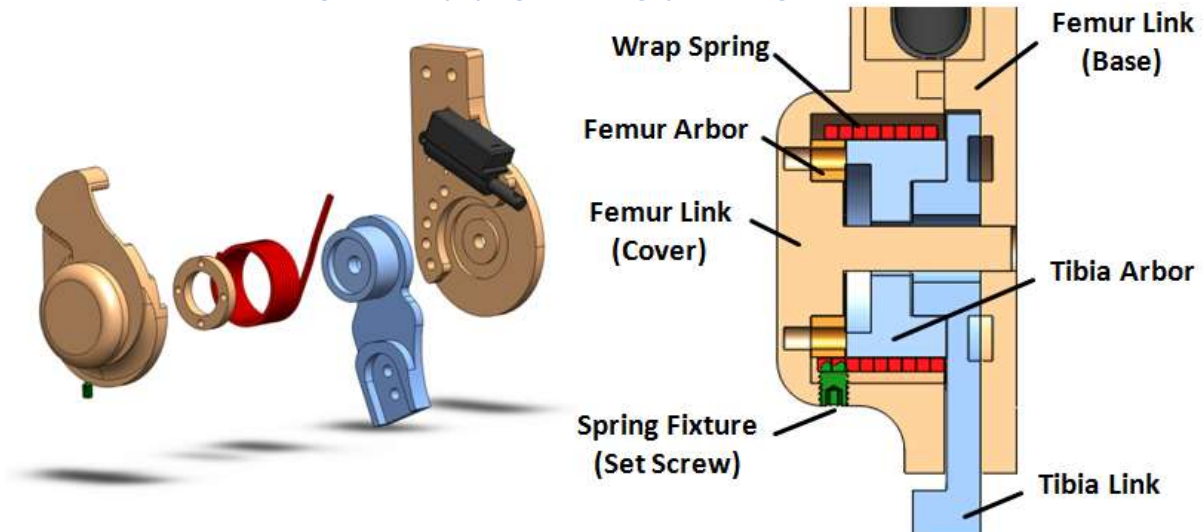


Figure 20: Wrap-Spring knee design. Image from [34]

3.1.7 Hip Actuators

The Steven Exoskeleton hip actuators are comprised of a Maxon EC-90-flat electric motor, a Harmonic Drive (SHD-20-100-2SH) 100-to-1 transmission, and an Austria Microsystems AS5145b 12 bit absolute magnetic encoder (see Figure 21). The actuator was designed to provide 95Nm of momentary peak torque, 49Nm of continuous torque, and a no load speed of 2.2 radians per second. Total actuator mass is approximately 3lbs (1.4kg). The actuator assembly measures 3.8in (9.7cm) in diameter and 2.8in (7.2cm) in thickness including covers. The overall thickness can be reduced by 0.38in (1cm) with further integration of the motor and harmonic drive.

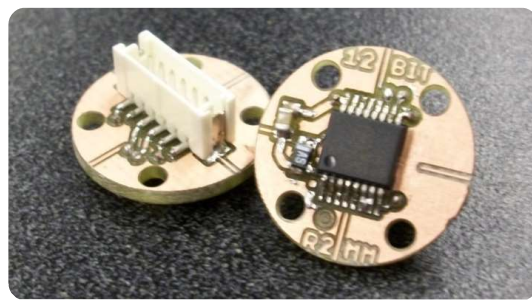


Figure 21 : AS5145b magnetic encoder module.

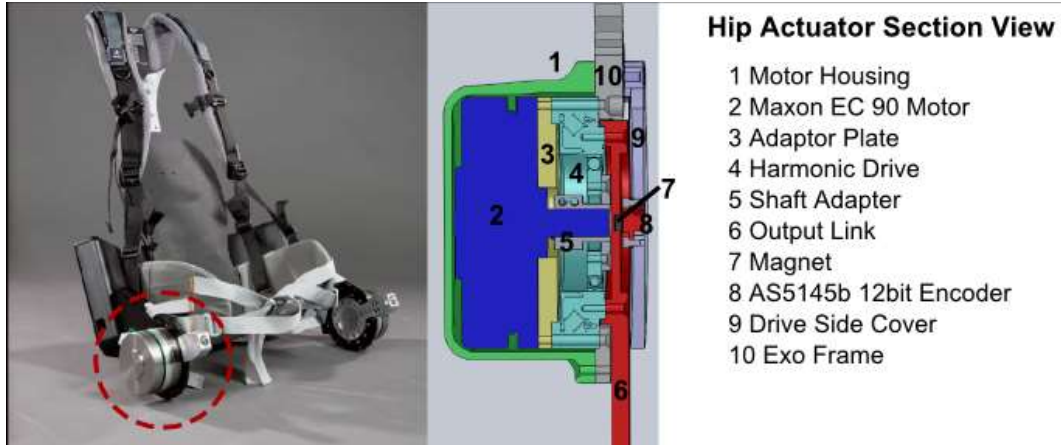


Figure 22: Steven Exoskeleton hip actuator. Figure adapted from [38].

3.2 Steven Electronics

3.2.1 Electronics Board

The Steven Exoskeleton electronics system consists of a main control board, associated sensor boards, and a wireless user interface. The Steven electronics main board (see Figure 23) is built around two MBED LPC1768 prototyping modules. Hip motors are controlled through two Copley Bantam BTM-090-10 amplifiers. Wireless User Interface communication is achieved by 900 MHz Xbee Radios, and optional Bluetooth or 2.4 GHz Xbee communication is available for off-board data logging/processing. Hip actuator position feedback is provided by AS5145b 12bit Absolute Magnetic Encoders. The knee is activated by 12v 63:1 Firgelli PQ 12 linear actuators with built-in feedback potentiometers, and controlled with DC motor driver ICs. A 9 degree of freedom Razor IMU (SparkFun SEN-10736) is used to measure torso angle, and safeguard operation in certain postures. Additional information about electronics development can be found in Chapter 8.

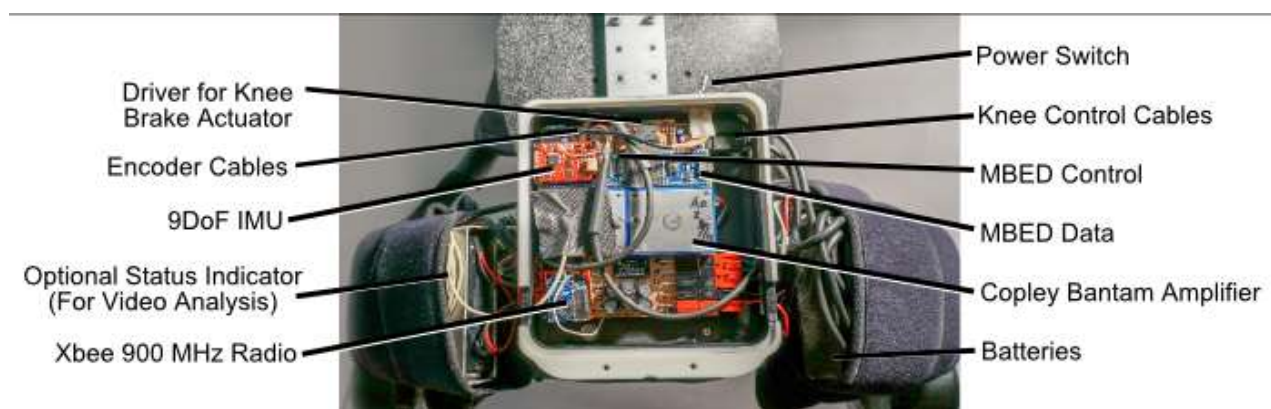


Figure 23: Steven Exoskeleton electronics.

3.2.2 Batteries

The Steven Exoskeleton uses a pair of 25.9v nominal 2.1Ah Lithium Polymer Battery packs connected in series to produce 51.8v nominal. These packs are capable of delivering enough

power for approximately 4 hours of continuous walking or 8 hours of average use (standing and walking while stopping to talk or work at a counter). Each pack weighs 0.9 lbs. and measures 5.9" x 4.25" x 1.0" (15cm x 10.8cm x 2.5cm).

3.3 Exoskeleton Operation

3.3.1 User Interface and Finite State Machine

Operation of the Steven Exoskeleton is governed by the finite state machine illustrated in Figure 24 and described in Table 3. All states are accessed through the use of a wireless crutch mounted User Interface (UI) consisting of a forward button and a backward button (illustrated in Figure 26). The FSM can be imagined as set of options arranged in two dimensions so that the pilot has at most two choices at any given time (move forward or move backward through states). States are changed through the forward and backward buttons. Some additional gating conditions in the form of verification clicks and time constraints (described in Table 4) are in place to avoid accidental state changes. Additionally, it is important to ensure that the pilot does not fall backwards during standup. Currently, this failure mode is avoided by measuring absolute torso angle during standup through the use of a torso mounted Inertial Measurement Unit (IMU).

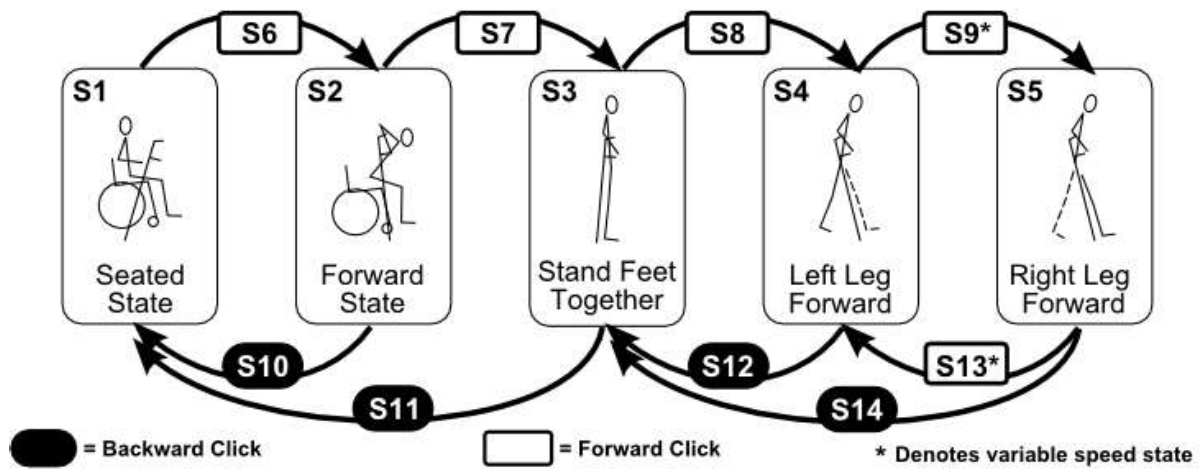


Figure 24: Steven Exoskeleton finite state machine.

Table 3: Steven Exoskeleton control as regulated by finite state machine.

State		Action	Posture Set-point or Trajectory During Action
S1	Sitting	Static	Seated Balance Posture
S2	Sitting Bent Forward	Static	Balanced Ready to Standup
S3	Standing Feet Together	Static	Erect Balanced Posture
S4	Left Foot Forward	Static	Slight Bend Forward
S5	Right Foot Forward	Static	Slight Bend Forward
S6	Bend Forward	Motion	Linear from S1 to S2
S7	Stand Up	Motion	Sinusoidal from S2 to S3
S8	Take Half Step	Motion	Sinusoidal
S9*	Right Foot Swing	Motion	Right Foot Swing Trajectories
S10	Sit Upright	Motion	Linear from S2 to S1
S11	Sit Down	Motion	Linear from S3 to S2
S12	Feet Together	Motion	Linear from S4 to S3
S13*	Left Foot Swing	Motion	Left Foot Swing Trajectories
S14	Feet Together	Motion	Linear from S4 to S3

States S9* and S13*(Right Foot Swing and Left Foot Swing respectively) are special states that can command a plurality of possible hip trajectories to enable variable speed walking. As indicated in Table 4, States S9* and S13*are gated by a Forward Click with the condition that the last step was taken less than 15 seconds previously (this ensures that the user cannot accidentally trigger a step while standing and talking). Walking starts with speed V0 (time since last step is > than Time Threshold). As long as steps are triggered at a rate slower than the Time Threshold, S9* and S13* will remain in V0. If steps are triggered at a rate *faster* than the Time Threshold, velocity will increase with each step until maximum velocity is achieved. If steps are triggered at a rate *slower* than the Time Threshold, velocity will return to V0. This process is illustrated in Figure 25. The system for variable speed walking was designed with the assumption that paraplegic pilots are either navigating tightly constrained environments (offices, kitchens, etc.) requiring tight control and low speed, or traversing larger distances (hallways, sidewalks, etc.) requiring high speed and less control over step placement.

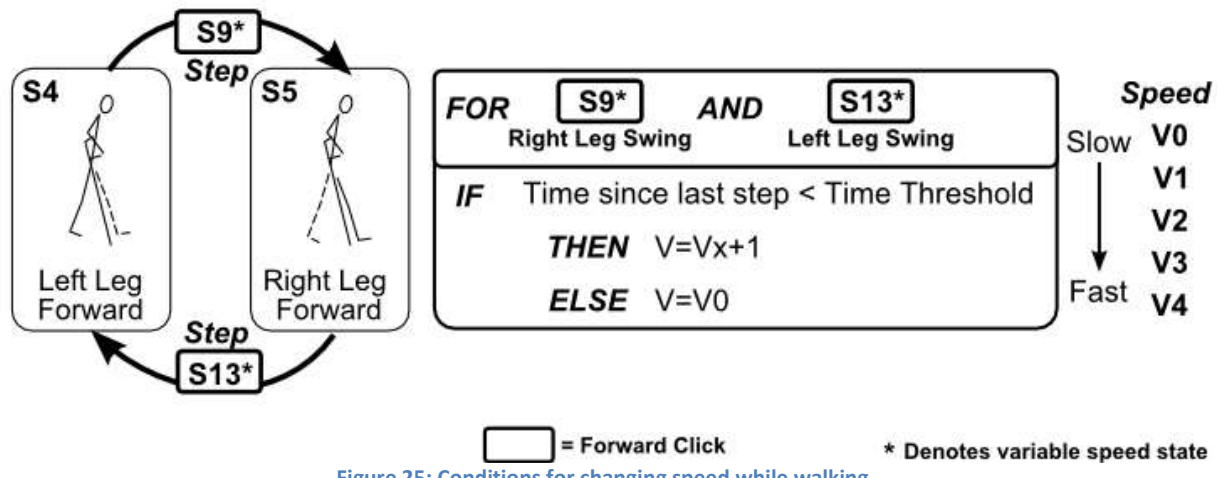


Figure 25: Conditions for changing speed while walking.

Table 4: Description of state change conditions.

State Change	Transition State	Gate Condition
S1 to S2	S6	Bend Forward
S2 to S1	S10	Sit Upright
S2 to S3	S7	Stand Up
S3 to S1	S11	Sit Down
S3 to S4	S8	Take Half Step
S4 to S3	S12	Feet Together
S4 to S5	S9*	Right Foot Swing
S5 to S4	S13*	Left Foot Swing
S5 to S3	S14	Feet Together

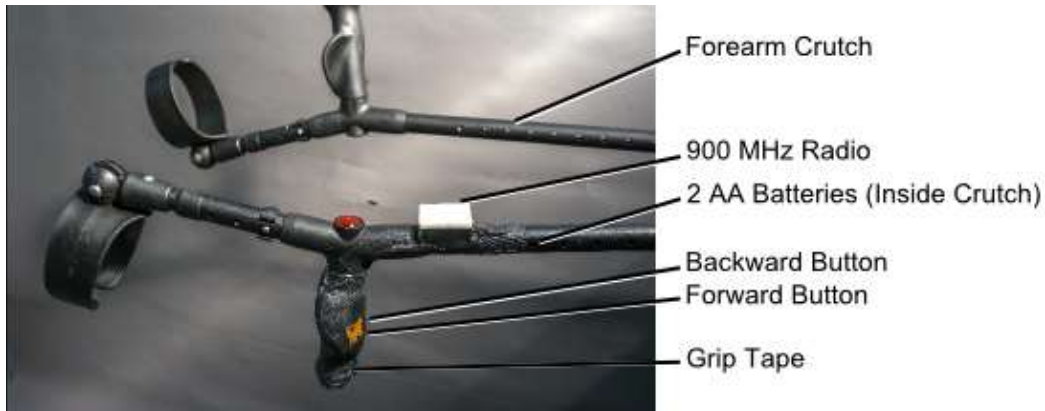


Figure 26: User Interface embedded in forearm crutch.

3.3.2 Guarding Against Unwanted State Changes

To avoid accidental motions, several state changes are gated by additional conditions as described in Table 4.

Standing

It is often convenient for a pilot to talk or work while standing in place. The FSM automatically locks against state changes after 15 seconds of inactivity to avoid accidental steps. This allows the pilot to let go of the crutches so that he/she can be hands free. To unlock the FSM the pilot presses the forward button, waits 1 second and then presses the forward button again. An audible tone confirms that the FSM was successfully unlocked.

Stand to sit

To command sit-down the pilot must press and hold the back button for more than 1 second, wait for audible feedback, release the button, and then confirm the command.

Sit to Stand

To command standup the pilot must press and hold the forward button for more than 1 second, wait for audible feedback, release the button, and then confirm the command. Additionally, if the pilot's torso angle moves out of a safe range during standup, the system will make an audible tone and automatically transition back to sitting. This avoids the possibility of falling backwards while standing up.

3.3.3 Steven Exoskeleton Gait

The Steven Exoskeleton walks using a passive knee gait that was designed specifically for exoskeleton systems without motor actuation at the knees. When applied properly, this approach generates a natural looking gait with adequate toe clearance for level ground walking [36]. The current approach to passive knee walking is discussed in the subsequent chapters.

Chapter 4: Passive Knee Gait

The ReWalk [23], eLegs [24], Indego [25], and Rex Exoskeletons [27] all use some form of actuation at the knee to achieve knee flexion while walking. The Austin Exoskeleton produced knee flexion by relying on a mechanical gait generation system in place of a knee actuator [29]. The Steven Exoskeleton forgoes the use of a motor or mechanical coupling at the knee in favor of a passive brake mechanism to stabilize knee motion during load bearing phases of walking. The resultant passive knee gait was inspired by the gait of bilateral transfemoral amputees who walk with passive knee prostheses illustrated in Figure 27.



Figure 27: Bilateral transfemoral amputee walking on level ground with unactuated knee prosthesis.

Using passive prosthetics, bilateral transfemoral amputees are capable of walking with gaits that are similar to, although less efficient than able bodied individuals [43]. It has been shown that this gait requires more energy than able bodied walking [44]. It is hypothesized that an efficient exoskeleton gait can be produced by relying on hip actuation to provide both knee flexion and reduction of metabolic cost (compared to passive systems). Figure 28 illustrates a comparison between knee flexion produced by transfemoral inspired dynamic coupling, Austin Exoskeleton mechanical gait generation, and normal CGA walking data.

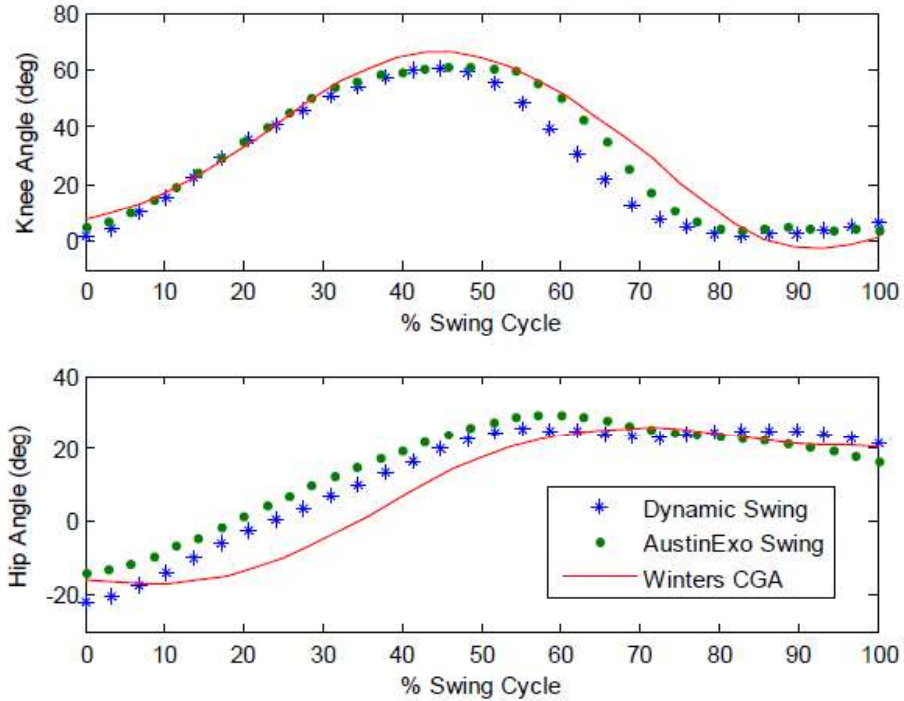


Figure 28: Comparison of dynamically coupled knee flexion to knee flexion developed by mechanical gait generation, and normal CGA walking data. Figure from [45]. This data was taken using the Austin 2 which was configured for both Mechanical Gait Generation and Dynamic swing.

Reid proposed a form of passive knee locomotion optimized for maximum toe clearance during walking [36]. As with exoskeletons, prosthetics have numerous actuated and passive designs. In one study it was noted that some amputees preferred passive prosthetic knees over active models as it offered them better voluntary knee control [39]. Likewise, passive knee gaits hold several advantages over actuated systems including the possibility for better control over voluntary foot placement, reduced system mass, and decreased system complexity. Figure 29 is an illustration of the Steven Exoskeleton passive knee gait.



Figure 29: Steven Exoskeleton Passive Knee Gait. Knees are locked against flexion at all times except during swing phase.

Chapter 5: Exoskeleton Gait Generation for Variable Speed Walking

Previous exoskeleton gaits as discussed in [1] and [5] do not allow a pilot to easily adjust walking speed. From extensive testing with numerous individuals, it is clear that pilots desire fine control in tight environments (such as offices and kitchens) with the ability to increase speed when walking for long distances in unobstructed environments (hallways, sidewalks). The transition from stationary to full speed should be intuitive, predictable, and natural. The following sections describe the approach taken to develop variable speed gaits for the Steven Exoskeleton.

5.1 Definition of Terms

As illustrated in Figure 30 joint angles are defined with positive values indicating joint flexion, and negative values indicating joint extension. For example, an individual standing with an erect posture would have hip and knee angles of 0 degrees, and an individual in a seated position would have hip and knee angles of approximately 90 degrees.

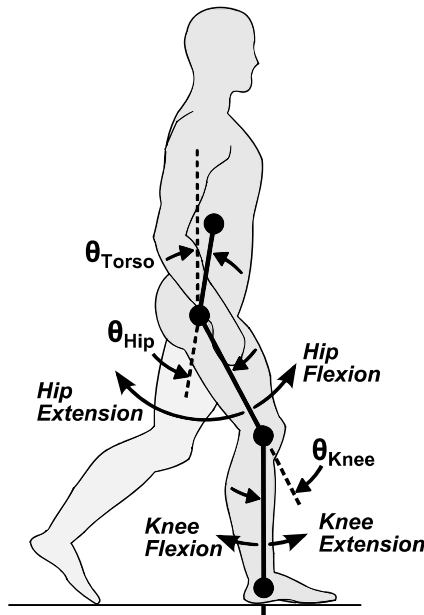


Figure 30: Definition of joint angles. θ_{Torso} is the angle between torso and vertical reference frame. θ_{Hip} is the angle between torso centerline and thigh centerline, θ_{Knee} is the angle between thigh centerline and shank centerline. Positive and negative angles correspond to flexion and extension respectively.

Healthy human gait can be defined as a sequence of repeating phases as illustrated in Figure 31. Commonly a walking gait is subdivided into stance phase and swing phase [46]. Stance phase occurs when a foot is in contact with the ground, and swing phase when the foot is not contacting the ground. When both feet are on the ground simultaneously an individual is in double stance.

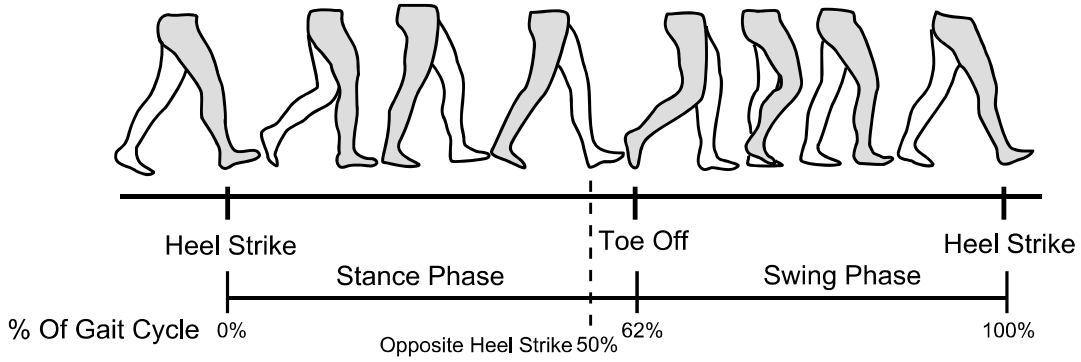


Figure 31 : Definition of walking gait phases. Adapted from [46].

As illustrated in Figure 32 one stride is a complete cycle of a reference leg (e.g. heel strike to heel strike of the right leg). The stride length L_s is the distance measured from heel strike to heel strike of the same foot, and stride time is the time it takes to complete this cycle. Additionally, step length is the distance measured from one heel strike to the next of subsequent feet and is therefore half of one stride.

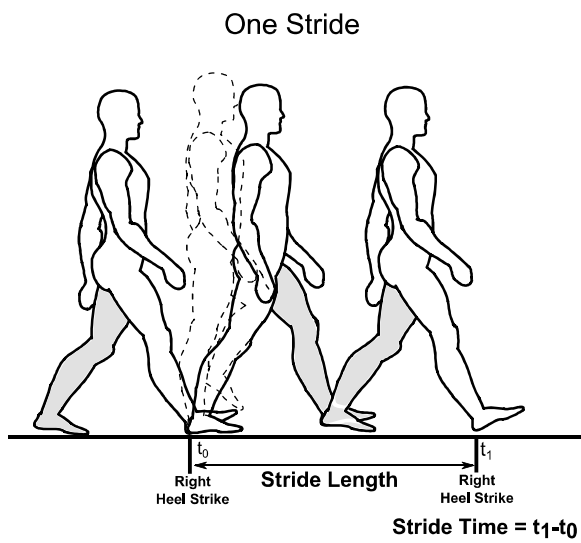


Figure 32 : Definition of stride length and stride time.

An individual's cadence is defined as the total number of strides taken per minute which can be written as:

$$\text{cadence} = \frac{\text{strides}}{\text{minute}} = \frac{\text{strides}}{60 \text{ seconds}} = \frac{2 * \text{steps}}{60 \text{ seconds}} \quad (5-1)$$

5.2 Approximating a Normal Human Walking Gait

Right and left hip angles for a normal human walking gait [47] are plotted as a function of time in Figure 33. It can be seen that the left and right legs follow similar trajectories, but with a 180 degree phase shift as heel-strike of the opposing leg occurs at approximately 50% of the gait cycle.

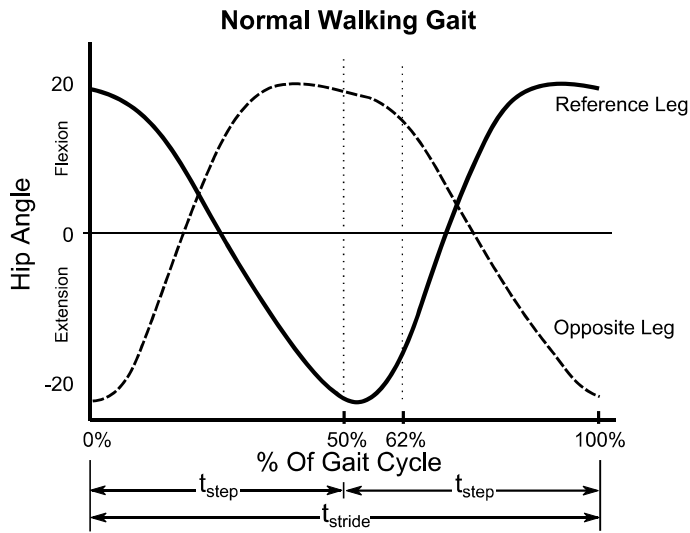


Figure 33 Healthy Walking CGA Data from [47].

As commonly defined in gait literature, toe off occurs at approximately 62% of the gait cycle (illustrated in Figure 33). For discussion, the gait cycle can be approximated as two sinusoids of similar amplitude but of differing periods (as illustrated in Figure 34 swing phase has a slightly shorter period, and stance phase a slightly longer period).

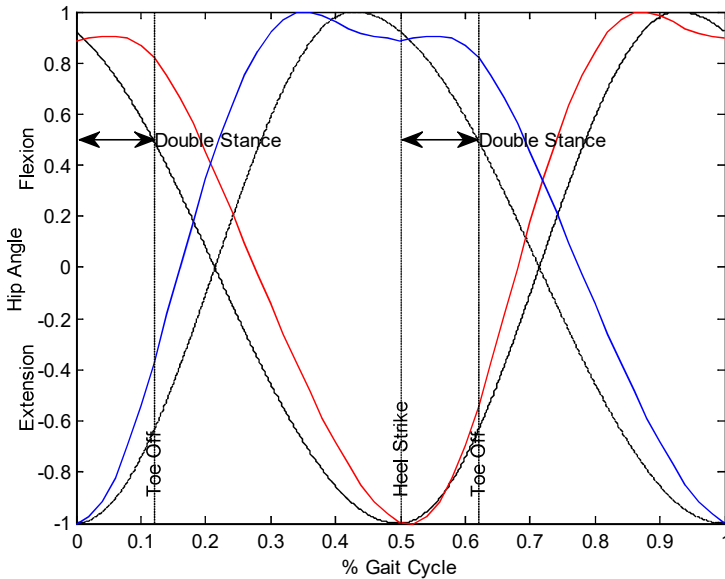


Figure 34: Overlay of sinusoidal approximation on CGA walking data. Red and blue are left and right CGA data respectively.

With t_{stance} equal to the duration of stance phase, the angular frequency of the sinusoid associated with stance phase can be written as:

$$\omega_{stance} = \frac{2\pi}{t_{stance}} \quad (5-2)$$

Likewise if t_{swing} is the duration of swing phase, the angular frequency of the sinusoid associated with swing phase can be written as:

$$\omega_{swing} = \frac{2\pi}{t_{swing}} \quad (5-3)$$

For a given stride amplitude A, the right hip trajectory can be expressed in terms of time from:

$$t = 0 \text{ to } t_{step} \text{ where } t_{step} = t_{swing} + t_{stance} \quad (5-4)$$

Right hip trajectory can be expressed as:

$$\theta(t)_{Right\ Hip} = \begin{cases} -A * \cos(\omega_{swing}t), & 0 \leq t < t_{swing} \\ A * \cos(\omega_{stance}(t - t_{swing})), & t_{swing} \leq t < (t_{swing} + t_{stance}) \end{cases} \quad (5-5)$$

The left hip trajectory is phase shifted 180 degrees from the right hip. One way to describe the phase shift between the right and left hips is to say that the left hip trajectory starts after the right hip, by a delay of $t_{delay} = \frac{t_{step}}{2}$. The left hip trajectory can be written as:

$$\theta(t)_{Left\ Hip} = \begin{cases} A * \cos\left(\omega_{stance}\left(t - t_{swing} + \frac{t_{step}}{2}\right)\right), & 0 \leq t < \frac{t_{step}}{2} \\ -A * \cos\left(\omega_{swing}\left(t - \frac{t_{step}}{2}\right)\right), & \frac{t_{step}}{2} \leq t < t_{swing} + \frac{t_{step}}{2} \\ A * \cos\left(\omega_{stance}\left(t - t_{swing} - \frac{t_{step}}{2}\right)\right), & t_{swing} + \frac{t_{step}}{2} \leq t < t_{step} \end{cases} \quad (5-6)$$

Additionally, in Figure 33 it can be seen that:

$$\frac{t_{stride}}{2} = t_{stance} + t_{swing} = t_{step} \quad (5-7)$$

Where t_{stride} and t_{step} are the times it takes to execute a full stride and an individual step respectively. Furthermore, one can approximate the amount of time spent in double stance as:

$$T_{double\ stance\ per\ stride} = T_1 - T_2 \quad (5-8)$$

If stride length is known, stride velocity can be written as:

$$V_{stride} = \frac{l_{stride}}{t_{stride}} = l_{stride} * \frac{C}{60} \quad (5-9)$$

where l_{stride} is the stride length, t_{stride} is the stride time, and C is the stride cadence.

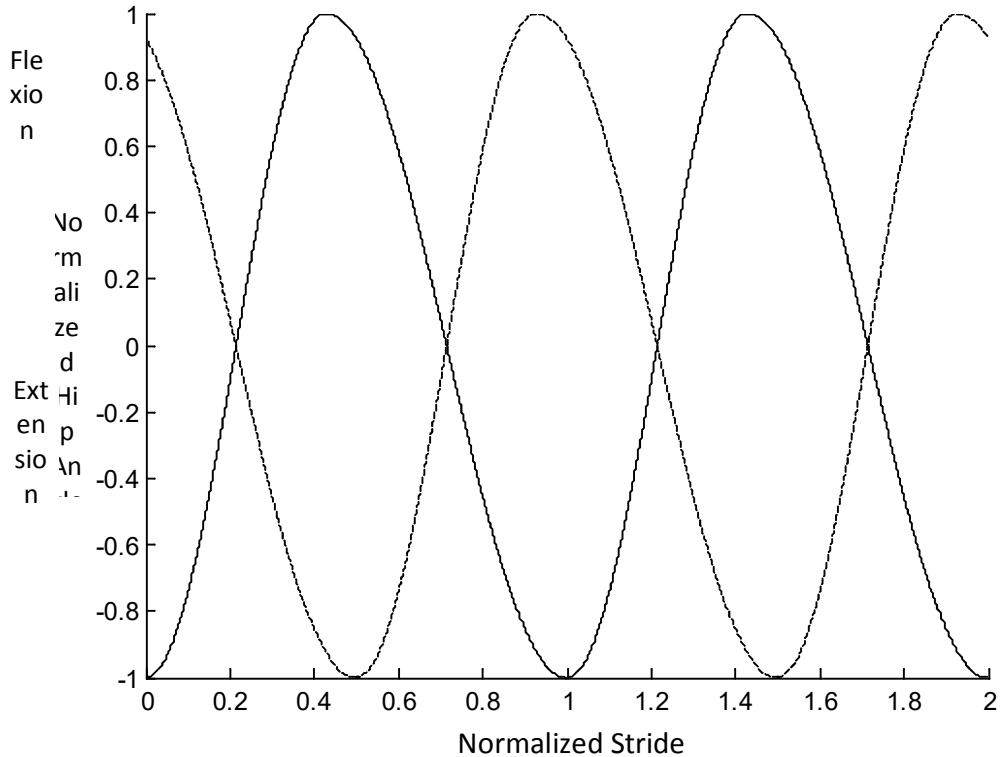


Figure 35: Sinusoid based approximation of hip trajectory for a continuous walking gait with constant cadence and step length. Solid line and dashed line represent right and left hips respectively.

5.3 Walking Continuously

As illustrated in Figure 35, the gait cycle is repeated continuously as an individual walks, smoothly transitioning from one step to the next. A trajectory of this nature feels natural for healthy constant velocity walking, where moving from one place to another is effortless and balance is second nature. However, maintaining balance is an ever present concern for a paraplegic pilot wearing an assistive exoskeleton. For a paraplegic pilot it feels natural to take one step at a time when walking at low speeds and when navigating the obstacles of a home or office.

5.3.1 Continuous Walking Through Gait Delay Modulation

The approach to continuous gait generation described in [37] was to prescribe a single walking gait and allow the user to pause for any period of time between steps. Figure 36 is an illustration of what CGA gait data would look like if treated in this fashion (where t_{delay} is the time between steps).

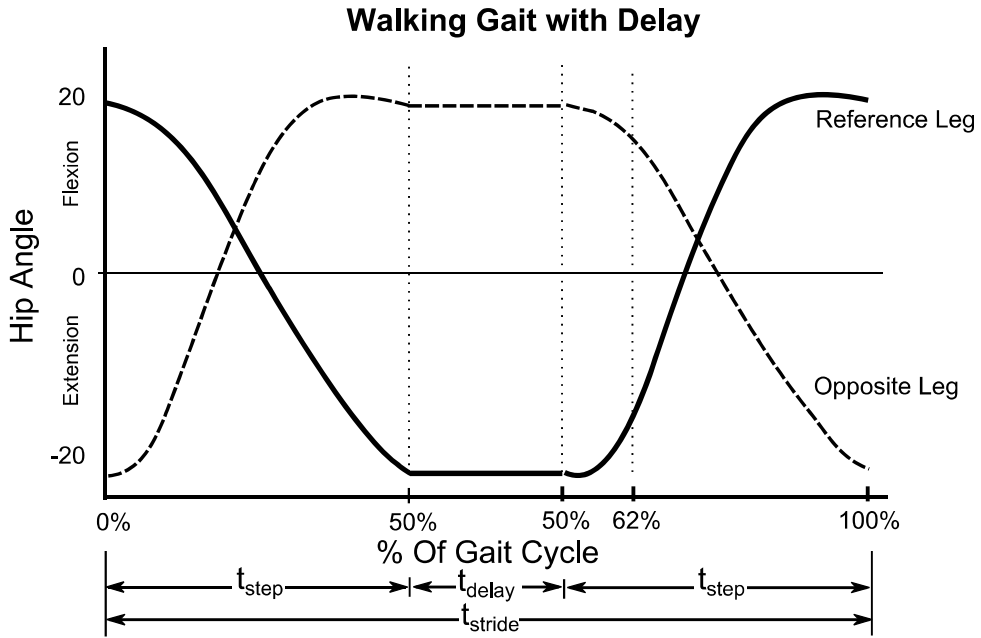


Figure 36: Illustration of walking gait with delay during double stance.

If t_{delay} is the pause between steps, stride time can be expressed as:

$$t_{stride} = 2 * t_{step} + t_{delay} \quad (5-10)$$

Through this method average walking velocity can be adjusted by varying the delay between steps. This approach to controlling walking velocity will be referred to as Gait Delay Modulation (GDM), as it is analogous to controlling the velocity of a DC motor through pulse width modulation. GDM average stride velocity can be written as:

$$V_{avg} = \frac{l_{stride}}{t_{stride} + t_{delay}} \quad (5-11)$$

With GDM not only is commanded hip trajectory constant, but by geometry, commanded step length also remains constant assuming full knee extension before heel strike (illustrated in Figure 37).

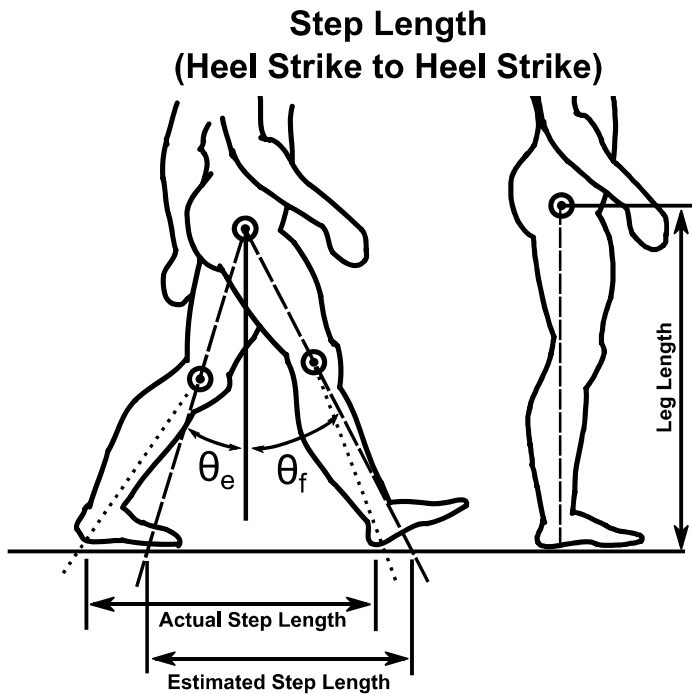


Figure 37: Step length geometry.

The objective (and primary advantage) of the GDM approach is to provide the exoskeleton pilot with a *predictable* hip trajectory that remains constant for all steps taken. System predictability is important to patient safety as it reduces the possibility of falls due to unplanned motions. GDM also avoids the complexity of trying to accurately determine self-selected walking characteristics (e.g. desired stride length and velocity). To achieve an average velocity, stride length is kept constant and delay between steps is varied.

5.3.2 More Haste, Less Speed

Although it has been demonstrated that paralyzed exoskeleton users can ambulate with a GDM gait [37], there are a number of disadvantages associated with walking in this manner. As long as $t_{\text{delay}} > 0$ each step includes a brief acceleration from rest, followed by an immediate deceleration. This means that the user does not smoothly gain momentum and maintain constant velocity as one would during healthy walking. Frequent acceleration and deceleration means that the user is always experiencing a jerky walking gait even when moving slowly. Furthermore, when walking at low speeds a large percentage of the time between steps is spent ironing out the kinematic and dynamic mess left by the previous step. A more desirable walking trajectory (as illustrated in Figure 38) achieves the same average velocity without enduring the jerky motions associated with the rapid acceleration and deceleration of GDM. The smooth trajectory illustrated in Figure 38 is achieved by scaling the period of the walking gait to match the desired cadence of the user.

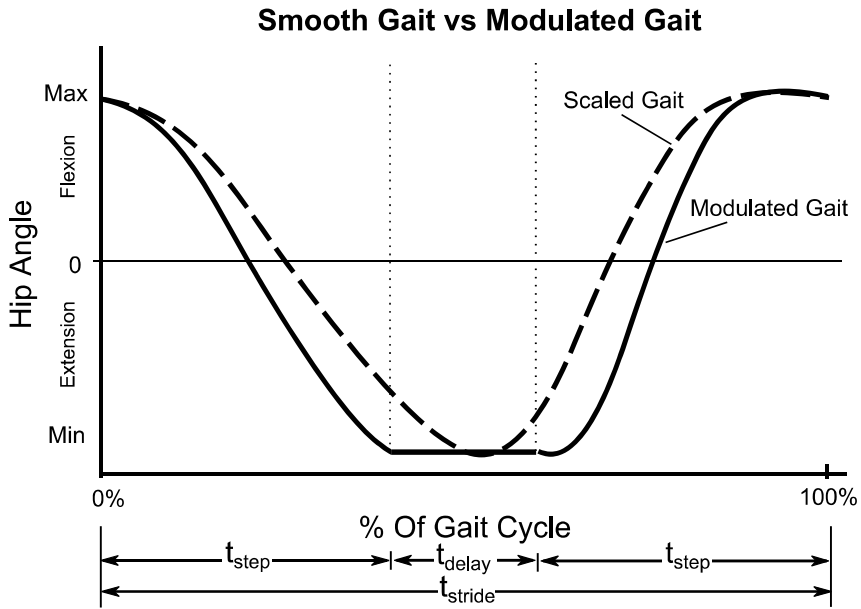


Figure 38: Smooth Gait vs. Modulated Gait.

Simply scaling the gait period does not address all of the problems with walking smoothly at different speeds. As speed increases this gait does not look natural when compared to normal walking; more importantly this gait does not *feel* natural to the pilot. Pilots have indicated that their step length feels too small with increasing speed (as they approach $t_{delay} = 0$) with the GDM method. It is clear that the exoskeleton pilot should be comfortable when executing both low speed and high speed motions.

5.4 Designing an Exoskeleton Gait Based on Healthy Walking Biomechanics

Theoretically, a healthy individual could achieve any desired walking velocity V_{avg} by selecting any combination of stride length l_{stride} and stride time t_{stride} that satisfies the condition:

$$V_{avg} = \frac{l_{stride}}{t_{stride}} \quad (5-12)$$

However, it has been observed by [48], [49], [50], and [51] that self-selected human walking is generally characterized by a linear correlation between stride length and cadence (illustrated in Figure 39). This relationship can also be seen in self-selected transfemoral amputee walking [43]. Normally, stride length increases with cadence, which means that walking with the same stride length for all cadences feels increasingly unnatural with increasing speed. The relationship between stride length and cadence for GDM is a horizontal line as plotted in Figure 39. It is evident that when commanding a constant trajectory for all cadences, natural walking and GDM walking become increasingly different with increasing speed.

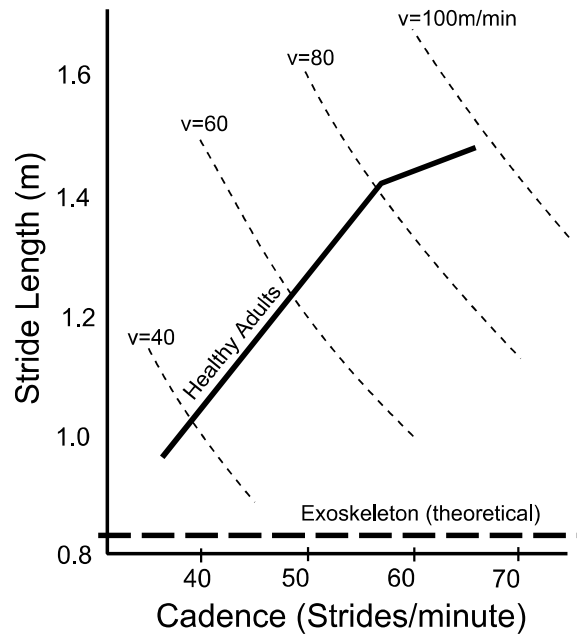


Figure 39: Theoretical exoskeleton gait plotted against healthy adult walking. Data from [48] and [52]. Dashed lines represent lines of constant velocity. Relationship between cadence and stride length changes at higher speeds as an individual transitions from walking to running gait.

5.5 Changing Walking Speed

By approximating an exoskeleton gait with a sine wave, we are able to generate a new gait at any desired cadence by simply selecting the duration of each stride t_{stride} . Furthermore, we have direct control over the length of each stride by tuning the amplitude A , of our sinusoid. Taking into account the relationship between cadence and stride length in healthy human walking, we can say that amplitude A is proportional to cadence by a scaling factor such that:

$$A \cong \text{cadence} * \text{gait scale} \quad (5-13)$$

This approach is consistent with human walking data presented in [53] in which it was observed that stride length is linearly correlated with speed. By determining an appropriate gait scaling factor for a given user, we are able to generate natural feeling gaits for any desired walking speed. Changing speeds can be accomplished by linking successively faster trajectories as illustrated in Figure 43.

5.6 Determining a Starting Point for a New Exoskeleton Pilot

Small people tend to walk with smaller steps at a higher step rate than larger people. This observation can be expressed as variation in the relationship between stride length and cadence as a function of height [50]. The strategy for the Steven Exoskeleton has been to fine-tune gait parameters based on user preferences. When tailoring a gait to a new exoskeleton user it would be useful to be able to scale gait as a function of pilot dimensions. This would expedite the tuning process for a given user. Several common techniques for scaling gait as a function of body dimensions are compared in [54]. A method of gait scaling by dimensionless

numbers is discussed in detail in [55] and the relevant equations for this approach are listed in Table 5. We could scale healthy gait characteristics and previously tuned exoskeleton characteristics as a function of pilot leg length in order to estimate a healthy objective gait and a starting gait for a given user.

Table 5 : Dimensionless numbers for gait scaling. Table from [55].

Variable	Symbol	Dimension	Dimensionless number
Mass	m	M	$\hat{m} = \frac{m}{m_0}$
Length	l	L	$\hat{l} = \frac{l}{l_0}$
Time	t	T	$\hat{t} = \frac{t}{\sqrt{l_0/g}}$
Velocity	v	$L T^{-1}$	$\hat{v} = \frac{v}{\sqrt{g * l_0}}$

m_0 = Subject Body Mass. l_0 = Pilot Leg Length (measured from hip joint to floor).

$g = 9.81 m/s^2$ acceleration due to gravity

We can use the dimensionless analysis approach to scale target cadence, stride length, and velocity as a function of leg length l_0 (where leg length is measured from hip joint to the floor).

$$\text{Normalized Velocity} = \frac{\text{Velocity}}{\sqrt{g * l_0}} \quad (5-14)$$

$$\text{Normalized Stride Length} = \frac{\text{Stride Length}}{l_0} \quad (5-15)$$

$$\text{Normalized Cadence} = \frac{\text{Cadence(strides/min)}}{60(sec/min)} * \frac{\text{sec}}{\sqrt{l_0/g}} \quad (5-16)$$

This approach of gait scaling based on dimensionless numbers is relevant for the Steven Exoskeleton as it provides a good starting point for a new pilot of known dimensions. Some manual tuning would be expected in order to account for individual preference. In practice it is generally necessary to start slower than expected, and adapt gait as a new pilot becomes more comfortable.

5.7 Applying the Variable Gait Method to the Steven Exoskeleton

The Steven Exoskeleton utilizes a passive dynamic method for achieving knee flexion during walking. In designing a hip trajectory for walking we need to attain adequate toe clearance and step length while minimizing jerky motions imposed on the user. Reid [37] discusses the theory behind calculating a minimally actuated gait for optimal toe clearance. It was observed that with the dynamic contributions of the Exoskeleton pilot, it is possible to achieve the same toe clearance and knee extension with a simpler less jerky gait (illustrated in Figure 40).

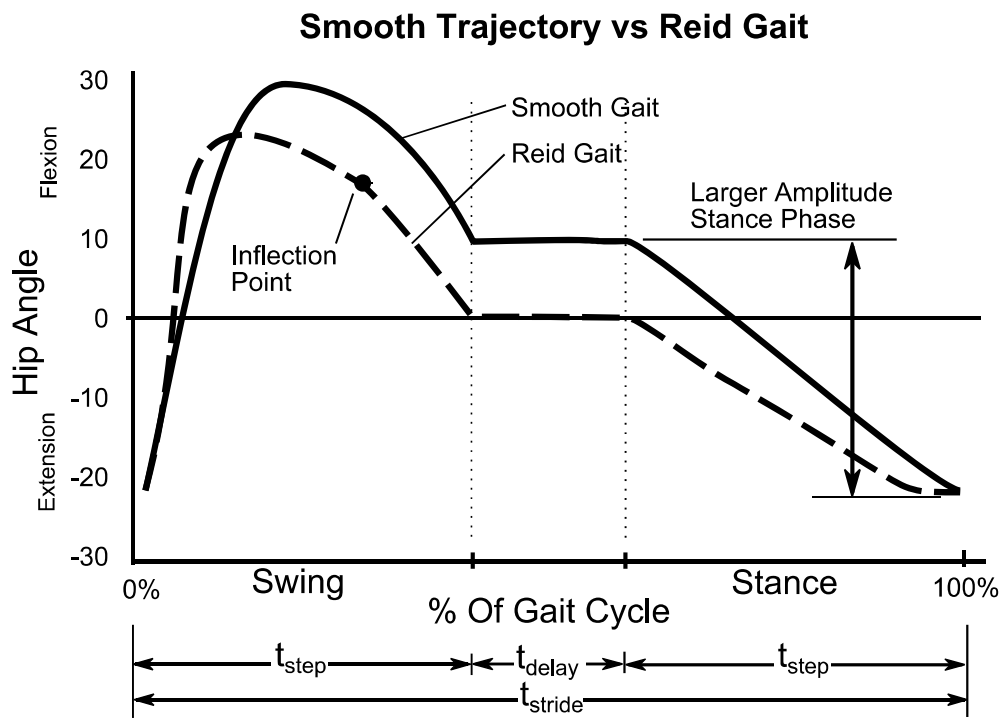


Figure 40: Comparison of Steven Exoskeleton gait and gait proposed in [37]. Note elimination of inflection point after maximum hip flexion resulting in smoother knee extension. New gait is designed to produce a longer stride at base speed.

Figure 41 illustrates one full stride using the Steven Exoskeleton gait at constant speed.

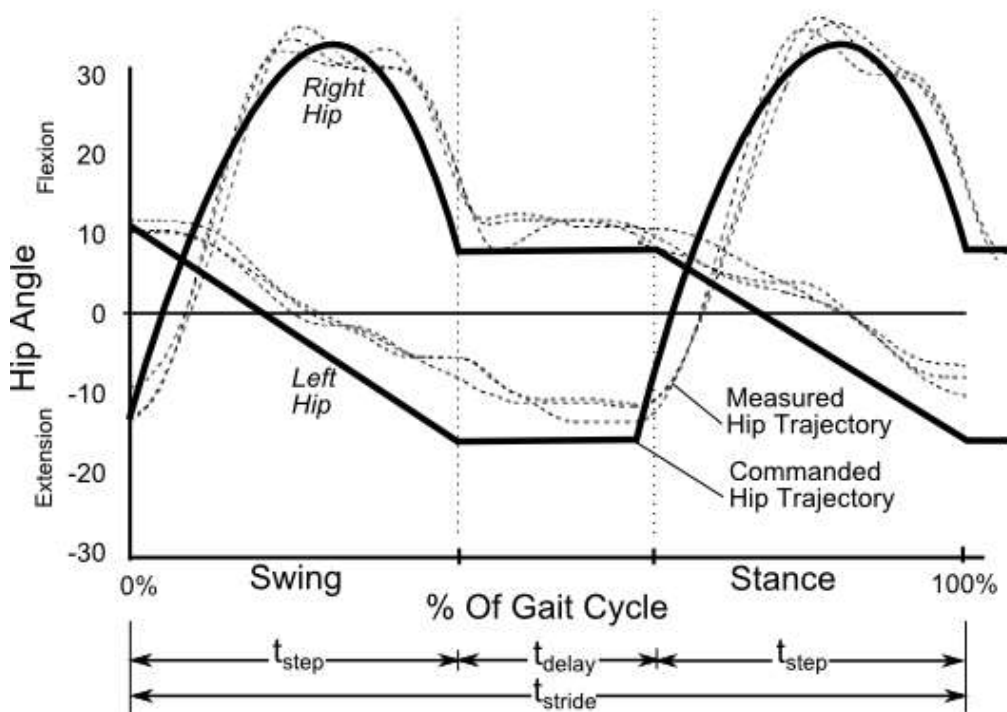


Figure 41: One stride of the Steven Exoskeleton gait.

5.7.1 Practical Approach to Determining Gait as a Function of Speed

To ensure pilot safety, gaits were tested at a single speed before adapting them for multispeed walking. The pilot would walk with a gait of a given Amplitude and Period until he found an optimal speed. After recording the self-selected walking speed for a given gait, a new gait with different Amplitude and Period was tested. In this way we were able to ensure that the exoskeleton pilot would feel natural as the exoskeleton was transitioned from one speed to another.

5.7.2 Practical Approach to Accelerating

In testing it was observed that most walking falls into two categories: Slow speed walking to negotiate tight environments, and high speed walking to traverse open spaces. With the Steven Exoskeleton, steps are commanded through a crutch mounted user interface. By measuring the time between step commands it is possible to change gait trajectory based on commanded step frequency. A threshold step command frequency was selected and was used as a gating condition to transition between finite state machine (FSM) states.

Steps commanded at a rate slower than the threshold frequency keep the FSM in a slow speed loop. When the step frequency threshold is exceeded (as illustrated in Figure 25), the gait automatically accelerates with each step until a top speed is attained. Upon pausing or bringing feet together, the gait resets back to a slow speed. The proposed method of gait acceleration assumes that pilot pauses are relatively large for negotiating tight environments and small for continuous walking.

An audible beep is sounded to alert the pilot to automatic finite state machine transitions (changing in and out of high speed mode). Figure 43 is an example of the transition process. The gait starts with a slow speed (steps are deliberate with a long delay period). As the commanded step frequency exceeds the gating threshold, the FSM automatically transitions into higher speed walking. Note the commanded step amplitude increases as period decreases (illustrated in Figure 42).

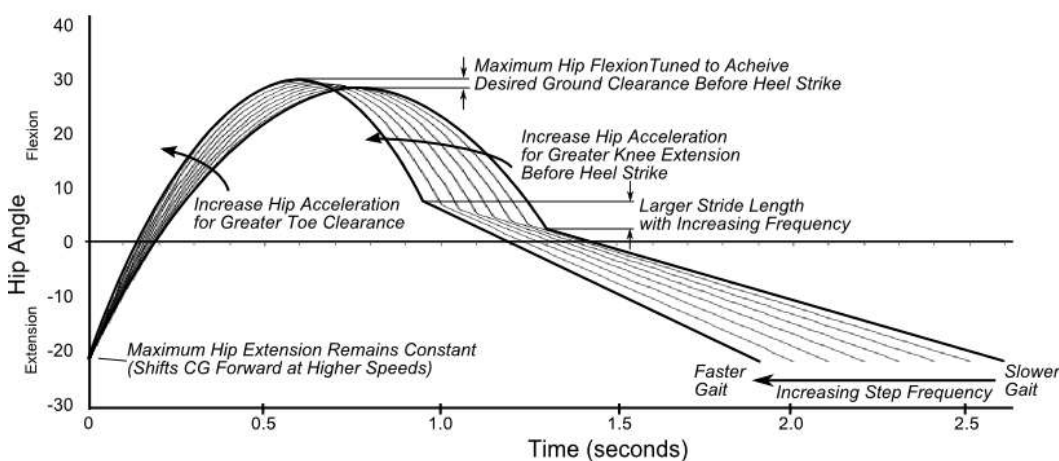


Figure 42: Variation of gait trajectory as step frequency increases. Note the slope of early and late swing phase increases for faster walking. This property provides adequate toe clearance as stride length increases.

This approach has been well received by the exoskeleton test pilot and has yielded predictable stable walking in both high speed and low speed maneuvers. User feedback indicated that this method was intuitive to learn, and the system seemed to respond in a natural manner. Figure 43 illustrates representative gait data as an exoskeleton pilot accelerates from rest to full speed. Over the course of several steps, the walking gait trajectory automatically changes so that stride length can increase as step frequency increases.

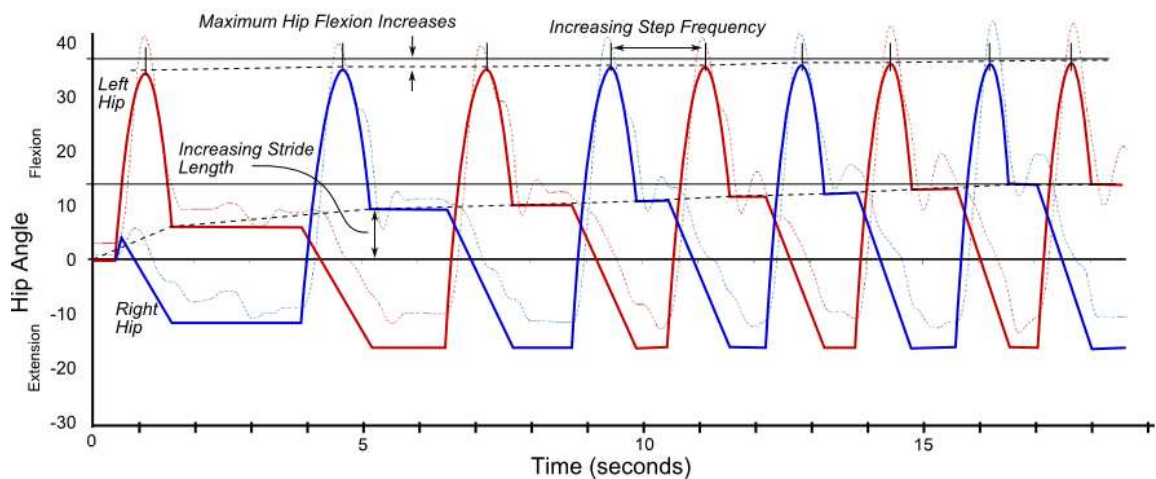


Figure 43: Steven Exoskeleton Gait Acceleration. First step with a long delay, subsequent steps accelerate to top speed. Note as step frequency increases, so too does stride length.

5.7.3 Speed Comparison

It is interesting to understand how assistive exoskeleton systems can be used as a tool in everyday life. Maximum sustainable speed is one meaningful measure of performance as speed allows a user to safely navigate real world scenarios with time constraints such as crossing a street or getting into an elevator. To get a rough understanding of maximum sustainable speed, an exoskeleton test pilot was asked to walk on a treadmill at a brisk pace for 3 minutes using the Steven Exoskeleton. The pilot was instructed to adjust the pace so that he felt fast yet comfortable. Walking velocity was measured over this interval and averaged to $0.48 (0.68 \times 10^{-2})$ m/s. This measurement stands as a rough measure for comparison between several other existing systems. Table 6 offers a comparison of the Steven Exoskeleton fast pace comfortable walking speed, to the walking speeds of healthy individuals and several other exoskeleton systems. The Steven Exoskeleton has the potential to be a substantially faster device as a more practical tool than many of the medical exoskeletons developed so far. More importantly, the Steven Exoskeleton has the potential to operate independently in society. As a benchmark 0.49 m/s was reported as a minimum ambulation velocity necessary to safely cross an average crosswalk [56].

Table 6: Comparison of walking speed across several exoskeleton systems.

	Measured Walking Speed (m/s)
Healthy Gait [57]	1.30
Crosswalk Minimum [56]	0.49
Steven Exoskeleton	0.475
Ryan Exoskeleton [37]	0.27
Vanderbilt Exoskeleton [25]	0.22
eLegs [58]	0.19
Austin Exoskeleton	0.15
Rex [28]	0.05
Garden Snail [59]	0.013

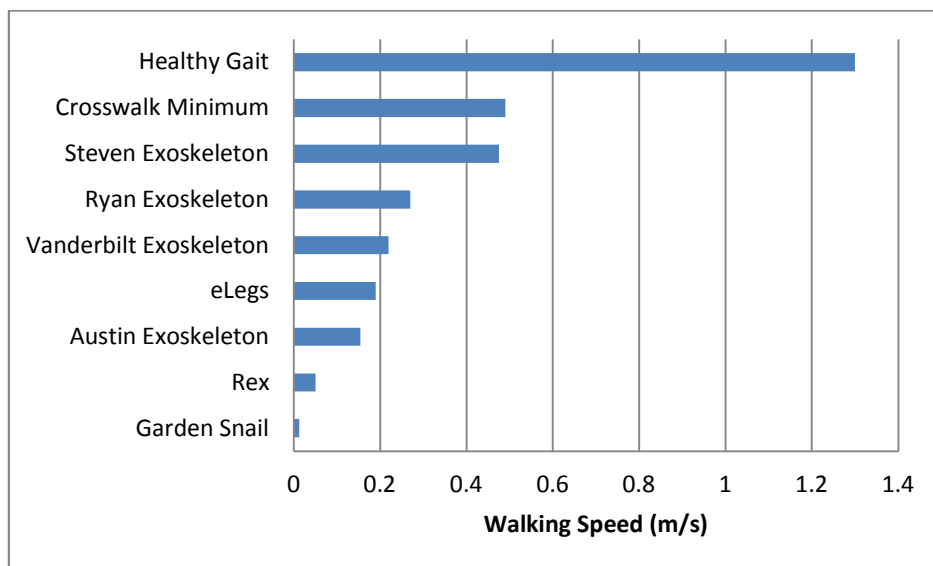


Figure 44 : Comparison of Exoskeleton Walking Speeds.

Chapter 6: Overcoming Barriers to Widespread Adoption: Creating a Device for Public Transit



Figure 45 : Public Transit- Reimagining public education one exoskeleton at a time. Billboard featuring the Steven Exoskeleton installed outside of Oracle Arena in Oakland California; May 1, 2014.

6.1 Addressing Independence with Robotic Exoskeletons

The objective of this research is to provide paralyzed or mobility impaired individuals with a tool that can enable them in their normal activities. A successful device is not only capable of achieving basic power and torque requirements, but also integrates naturally into daily life. In some circumstances wheelchairs are capable of faster and more efficient locomotion than healthy walking[60]. It is naive to expect that an assistive exoskeleton could be capable of completely replacing the wheelchair in daily activities. Instead, the assistive exoskeleton should be used as an opportunity to provide enhanced abilities to basic wheelchair operation. An assistive exoskeleton must integrate seamlessly with existing wheelchair technologies in order to provide a practical mobility solution.

One of the biggest challenges faced by paralyzed individuals in daily life is interfacing with the world from a seated position [61]. As discussed in [62], the maximum reach envelope (MRE) of wheelchair bound individuals is restricted by the seated posture and reduced muscle capacity. An exoskeleton should allow users to easily access counters and vertical shelves by enabling

them to stand up and sit down effortlessly. Furthermore, a successful device should be capable of enhancing the abilities of a paralyzed individual while seated in a wheelchair. Some of these capabilities have been designed into the Steven Exoskeleton, and are described in the following sections.

6.2 Using the Exoskeleton to Enhance Seated Abilities

The Steven Exoskeleton offers the opportunity to enhance the capabilities of the seated wheelchair user as it is small and light enough to stay out of the way during daily activities. Typically a T12 complete paraplegic does not have control of muscles necessary to fully stabilize his/her torso in the seated position [63]. Considerable effort is spent maintaining unbalanced seated positions [64]. Although individuals with SCI can compensate for atrophied erector spinae muscles by using latissimus dorsi and trapezius pars ascendens muscle groups (see Figure 46) , this is often not enough to fully stabilize the torso while seated [65]. Frequently individuals recruit arm strength to support his/her torso (so that he/she does not fall out of his/her wheelchair) while picking things up from the floor (illustrated in Figure 48 c). As illustrated in Figure 47, the Exoskeleton is capable of acting as the pilot's core muscles (abdominal and spinal) and can enable some new seated capabilities.

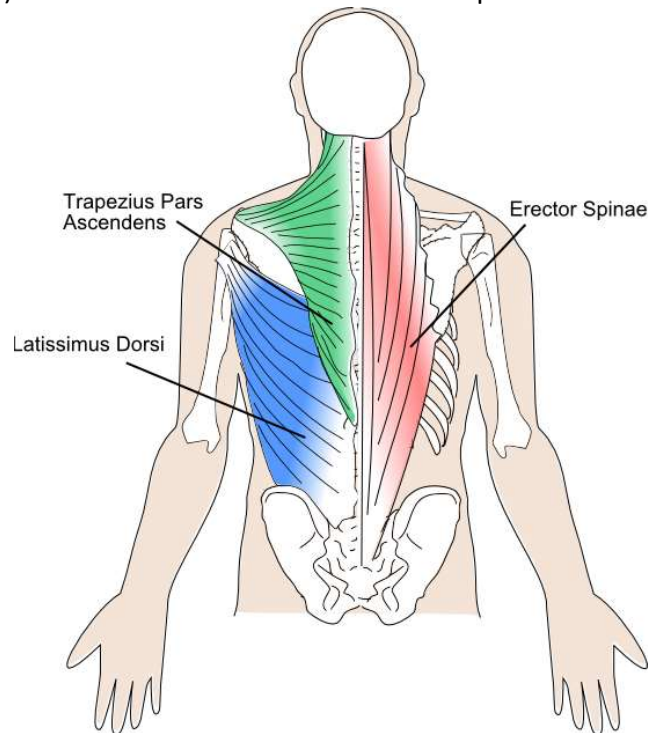


Figure 46 : Muscle groups used for spinal extension.

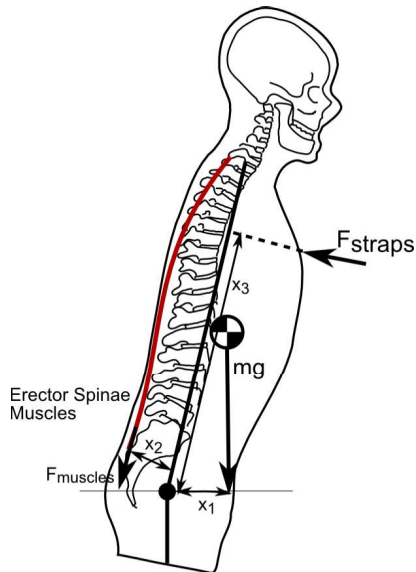


Figure 47 : Normal force of shoulder straps compensates for lack of erector spinae functionality.

The importance of shoulder straps increases as erector spinae muscle strength decreases:

$$\sum M_{Hip} = mgx_1 - F_{muscles}x_2 - F_{straps}x_3 \quad (6-1)$$

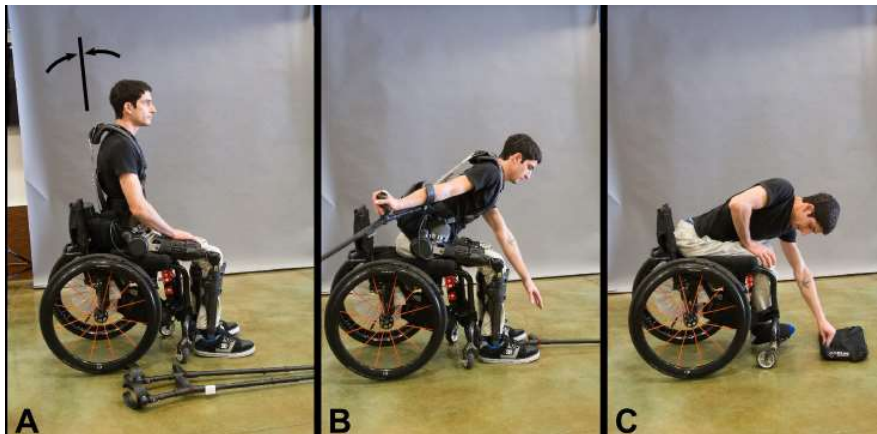


Figure 48: Exoskeleton seated Support. a) The user's torso is stabilized by hip actuators while seated in an upright posture. b) The user can effortlessly reach the floor by commanding the exoskeleton to bend forward. c) Reaching the floor requires substantial upper body strength without the exoskeleton.

6.2.1 Offering Support While Seated

The posture of the Steven Exoskeleton is actively controlled while seated. By providing a low level restorative torque to keep the pilot's torso upright, the pilot gets an added sense of stability while seated in his wheelchair and is able to manipulate heavy objects with both hands (illustrated in Figure 48 a).

6.2.2 Interaction with Objects on the Floor

A bent forward posture has been developed that allows the user to be supported in the exoskeleton while having both hands free to manipulate objects on the floor (see Figure 48 b). The pilot commands the Exoskeleton to move into this posture by pressing the step forward

button on the control crutch. After completing his/her task (e.g. tying one's shoes) the back button is pushed to effortlessly move back into the erect seated posture.

6.3 Standing and Sitting Trajectories

Knee joint torque is typically required for healthy standing and sitting. Although the Steven Exoskeleton does not provide actuation at the knees, it is still possible to sit and stand with minimal effort. Several changes have been made to increase the safety and comfort of the pilot during the standing and sitting procedures.

6.3.1 Ineffective Sit to Stand

Using the standup approach presented in [37], the pilot starts in an unpowered seated position (approximately 90 degrees as illustrated in Figure 50a), with crutches in a position that allows support (and hopefully leverage to stand up). When the user initiates the standup sequence the knees lock (to guard against flexion and allow free extension) and the motors are position controlled through a linear ramp from sitting to standing (Figure 49). This approach is strenuous and exceedingly difficult for an exoskeleton pilot to master. If standup was mistimed, the pilot would be unable to standup and would end up in a reclining position.

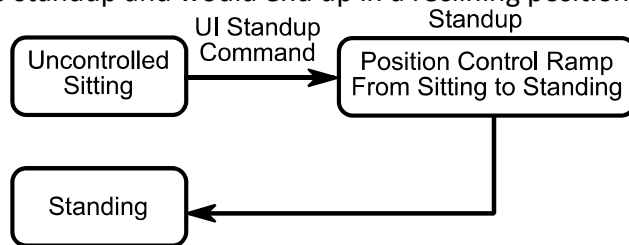


Figure 49 : Legacy standup state transition diagram.

When a healthy individual stands up (without the use of his/her arms) the torso is first flexed and then extended in an effort to move his/her center of mass (CoM) as close to the center of support as possible [66]. It has been observed that people with reduced muscle capacity increase torso flexion and angular velocity in an effort to bring the CoM closer to ones center of support and to increase momentum [67]. The standup method presented in [37] proceeds at a fixed pace and places the Exoskeleton's CoM far behind the base of support. This burdens the Exoskeleton pilot with the majority of the work as he/she wrestles the machine into the standing position.

6.3.2 Sit to Stand: Developing a Better Standup Trajectory

Movement of the center of mass from seated to standing is accomplished through the combination of joint torques and angular momentum generated by torso movement. Posture must be carefully considered to reduce user effort during stand up. As the Steven Exoskeleton cannot generate positive knee work some postures available to healthy individuals must be reconsidered for use with a minimally actuated exoskeleton. We can gain insight from strategies used by amputees and individuals with impaired muscle strength. For example, transfemoral amputees approach the problem by bending the torso farther forward, and executing standup faster[68]. By positioning CoM properly one is able to reduce required knee moments [69], and mechanical demand is redistributed to other muscle groups [70].

By changing the starting posture and also the control trajectory, it is possible to make better use of the pilot's muscle contributions during standup. A new approach to standup was developed that considers the observations in the literature. To start the standup sequence, the user bends over into a forward position (see Figure 50b). The new standup method is considerably easier for the pilot because the CoM is farther forward and shoulders and elbows are in better posture. This position has two benefits: 1) The torso is bent further forward meaning that the motors contribute to lifting the CoM instead of pushing the torso backward during the standup process. 2) The exoskeleton pilot's shoulders are in a more advantageous posture which enabling contribution of larger muscle groups. Additionally, by placing the crutches closer to the feet the range of motion afforded by the elbows and shoulders allow the pilot to standup fully without repositioning the crutches.

Note that in the previous posture (illustrated Figure 50a) the line of force through the crutch nearly passes through the hip. This alignment gives less advantage to the pilot's own muscle groups and means that the motors are acting to force the pilot backwards.

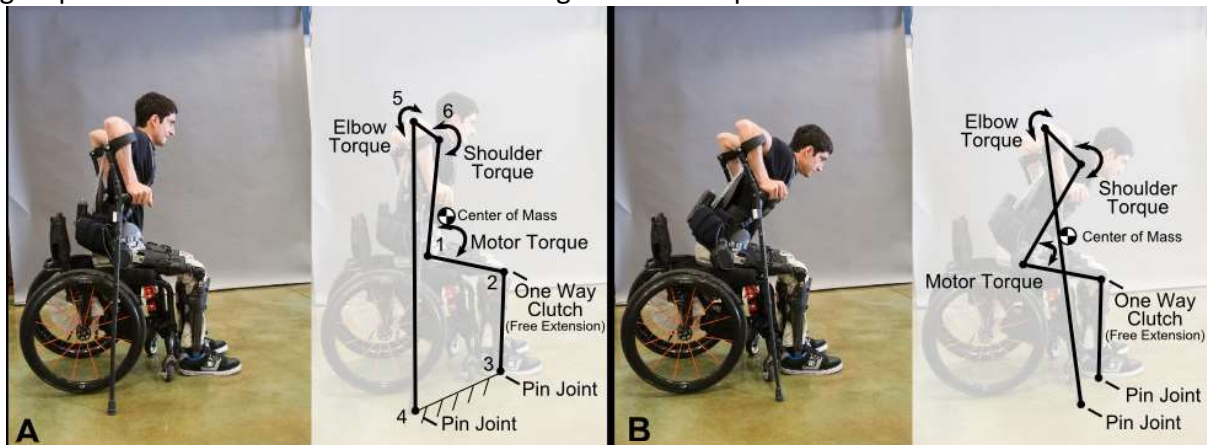


Figure 50: Comparison of Old and New Standup Postures A) Posture used in [37] B) New Posture C) Comparison.

Figure 50 illustrates the difference between the proposed standup posture (b) and the posture developed in [37] (a). Both cases rely on the same 6 bar linkage (as defined in Table 7 and illustrated in Figure 50a) consisting of Tibia, Femur, Torso, Humerus, Crutch, and Ground. Four of the six joints are constrained, (2 by the user's muscles (elbow and shoulder), one each at the hip motor and knee clutch).

Table 7: 6 Bar linkage during standup and sit-down.

Joint		Constraint	Contribution to Standup/Sit-down	Linkage Element	Description
1	Hip Actuator	Constrained	Torque or Position Controllable	1-2	Femur
2	Knee Joint	Partially Constrained	Free Extension, Locked against Flexion	2-3	Tibia
3	Ankle	Pin Joint	Low Friction Rotation	3-4	Ground
4	Crutch Tip	Pin Joint	Low Friction Rotation	4-5	Crutch
5	Elbow	Constrained by pilot	Pilot's Muscles (small muscle groups)	5-6	Humerus
6	Shoulder	Constrained by pilot	Pilot's Muscles (large muscle groups)	6-1	Torso

During standup the exoskeleton transitions from seated position control to standup torque control and finally into standing position control (see Figure 51). Torque control during standup

allows the pilot to standup at a self-selected pace while receiving maximum assistance from the exoskeleton; pilot and exoskeleton are able to consistently work together as a team. Using torque control avoids the timing problems associated with the position control strategy of the previous method.

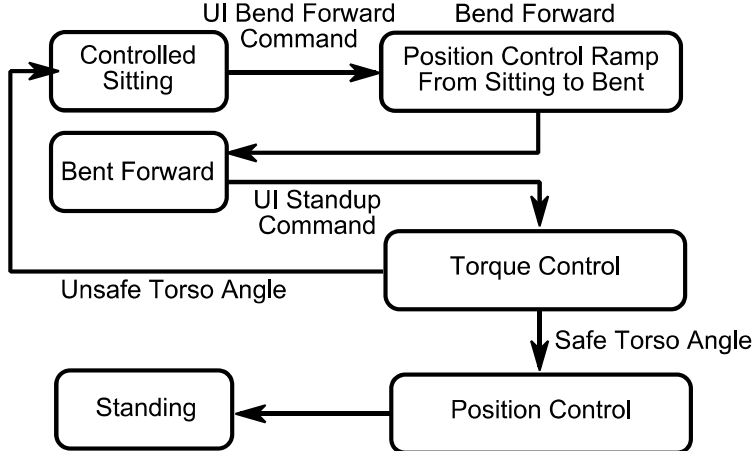


Figure 51 : State transition diagram for new standup procedure.

6.3.3 Ineffective Sit-down Trajectory

In the original approach to sit-down (proposed in [37]), the pilot would position himself in front of his wheelchair and position crutches behind him/herself for support. The knees unlocked and the hip motors followed a position controlled ramp from standing to sitting (illustrated in Figure 52). The motors turned off 1.5 seconds through descent to allow the user to freewheel until seated. The damping inherent to the hip actuator system aided the user into the seated position while providing freedom to move at a self-selected pace. It was observed however, that this approach was difficult to master as it required precise timing and required high pilot strength.

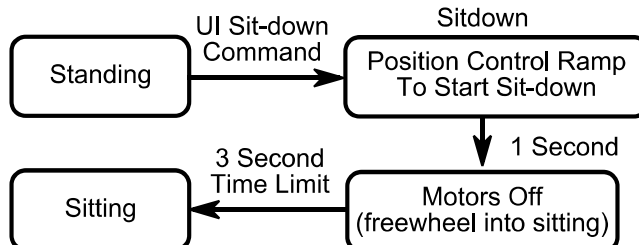


Figure 52 : State transitions for legacy approach to sit-down.

Furthermore, once the user is in the seated position crutches need to be quickly repositioned so that the user's torso is stabilized from falling forwards. Backward crutch placement is needed during sitting, and forward crutch placement is needed immediately after making contact with the seat. It is difficult for the user to rapidly move crutches after sitting which would often result in the pilot falling forward in his/her wheelchair. The entire movement was unpleasant, unpredictable, and potentially hazardous (as illustrated in Figure 53).



Figure 53 : User falling forward after making contact with wheelchair due to insufficient erector spinae musculature. 1) Begin sit-down. 2) Touchdown on wheelchair. 3) Pilot falls forward.

6.3.4 Developing a Better Method for Sit-down

In the current approach (illustrated in Figure 55), the pilot positions himself in front of his wheelchair, moves crutches into the support position and initiates sit-down as before. During sit-down the knees unlock, and the hips are position controlled until a predefined angle is reached. Once this angle is attained, the controller automatically switches to a torque control mode which works together with the muscle contributions from the user to sit down smoothly. Once the user reaches a seated position the controller automatically switches to a supported sitting posture which allows the user to reposition his/her crutches at any time (without feeling like he/she will fall forward) (see Figure 54).

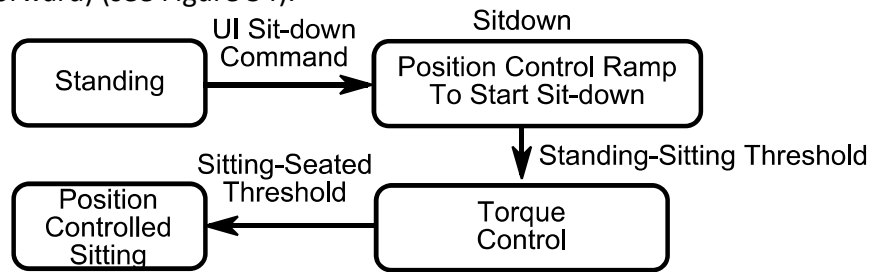


Figure 54 : State transitions for torque controlled sit-down method.

This method has been extremely well received by exoskeleton pilots. The elegance of this approach is that it allows the machine to work well with the pilot without requiring that the pilot perfectly time his/her contributions during sitting. Additionally, this approach can be easily tuned to provide more or less assistance depending on user strength and preference. Using this approach pilots are able to smoothly, safely, and gracefully sit-down without assistance.

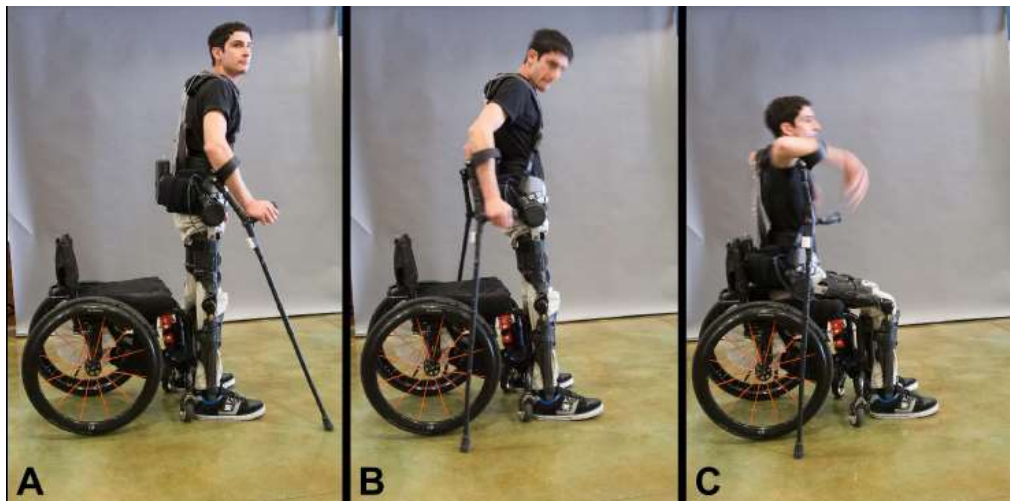


Figure 55: Sit down: A) Positioned relative to wheelchair. B) Crutches placed beneath seated COM. C) Sit-down completed without repositioning crutches to support torso. The pilot is able to complete this maneuver without the assistance of a spotter.

Chapter 7: Tailoring the Right Fit: Making an Exoskeleton Best Suit Its Pilot

The most advanced exoskeleton designs will suffer from poor performance if a proper fit is not tailored between suit and user. After initial fit is achieved by adjusting the size of the exoskeleton to a pilot, fit is maintained through soft human machine interface structures that reduce the impact of the device on the wearer. Improper fit can pose problems with skin integrity and can lead to restriction of a user's range of motion, agility, and balance. Ultimately the fit of an exoskeleton contributes to the success or failure of a system.

7.1 Mechanical Sizing

7.1.1 Exoskeleton Dimensions

A pilot's body dimensions (as illustrated in Figure 13) are first measured before fitting the exoskeleton. A pilot is asked to sit in his wheelchair with feet flat on the floor. Torso Length is measured from the top of the shoulder (where a backpack strap would sit) to the rotational center of the hip as viewed in the sagittal plane. Femur length is measured from the rotational center of the hip to the rotational center of the knee as viewed in the sagittal plane. Shank length is measured from the approximate rotational center of the knee to the floor. Hip width is measured from the bony protuberances of the pelvic bones as viewed in the coronal plane. These dimensions are used to roughly position the exoskeleton joints prior to donning the device.

7.1.2 Location and Construction of Key Pads

Padding is critical for keeping the pilot located in the exoskeleton safely and securely. As illustrated in Figure 56, the shoulder straps, lumbar pad, thigh pad, and knee pad are responsible for maintaining the colocation of pilot and exoskeleton joints while receiving assistance from the device. These pads represent the most efficient means of ensuring pilot and device alignment such that contact forces and pad surface area are minimized. The placements of all pads are adjusted so that pilot and exoskeleton joints are in alignment.

It is advantageous to minimize the size of support pads in order to reduce overall mass and insulating properties. For example, the Reciprocating Gait Orthosis (RGO) uses a custom molded rigid plastic shell padded by 1/4" foam to support the wearer's entire lower torso. By increasing contact area, it is possible to reduce tissue pressure and thereby reduce the odds of pressure sores. However, users quickly become too hot as a result of covering large regions of the body with foam.

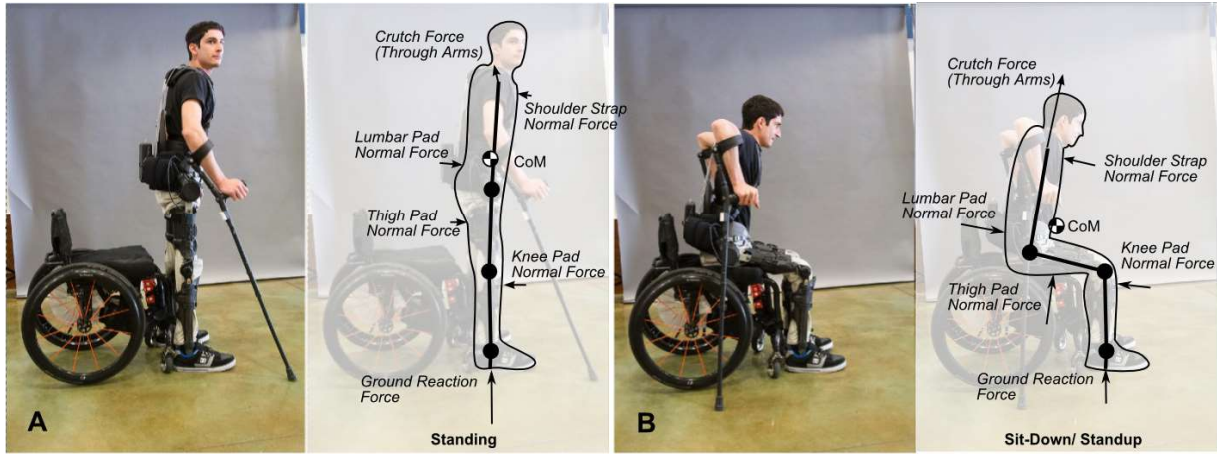


Figure 56: Pad forces acting on user to maintain posture while wearing exoskeleton. Pad forces are low when standing in an erect posture as loads are efficiently transferred through the pilot's skeletal structure. Pad forces increase during standup and sit-down.

7.1.2.1 Shoulder Straps

Shoulder straps are used to keep the pilot's shoulders aligned with the exoskeleton. Straps are attached to the exoskeleton above the shoulder to minimize strap pressure on the shoulder and pectoral regions as illustrated in Figure 57. Through the shoulder strap connection, the flexible exoskeleton spine is able to replace the atrophied erector spinae and rectus abdominis muscles. Shoulder straps may not be necessary for individuals with lower core muscle function, and can be removed if desired.

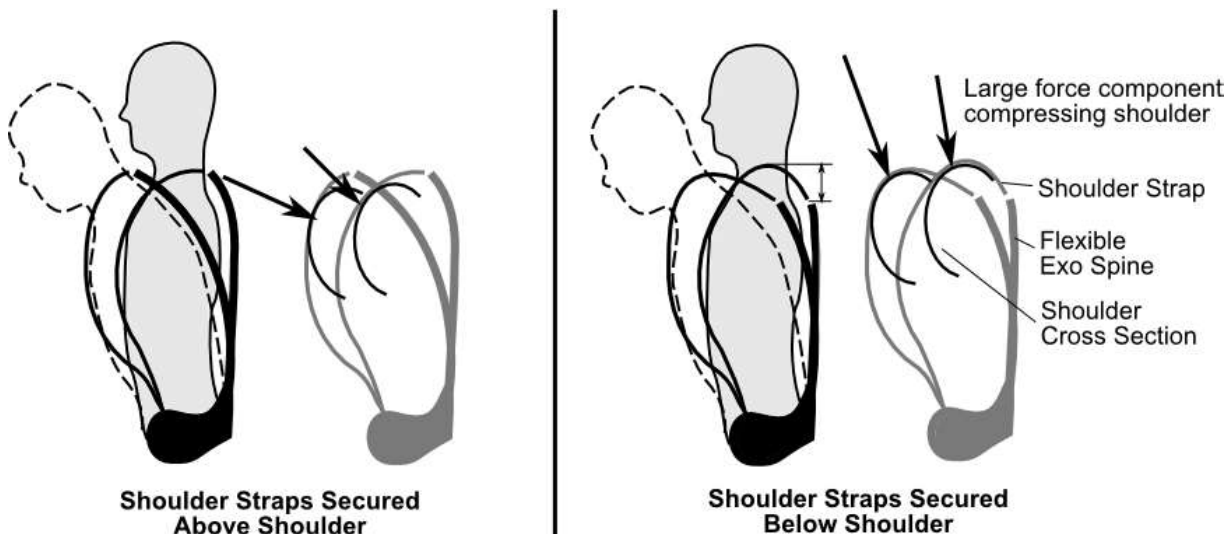


Figure 57 : Comparison of shoulder strap placement. Less tissue pressure and better control result from fixing straps above the shoulder.

7.1.2.2 Lumbar Pad

The lumbar pad is placed to support the lumbar sacral region and extends 2.5cm below the coccyx. It is important to minimize the risk of pressure ulcers by reducing pressure points for patients without sensation in this area. As illustrated in Figure 58, the lumbar pad is

constructed from a layer of EVA 30 foam to match the basic shape of the pilot's back, with a ROHO 14"x 8" inflatable pad (see Figure 59) to distribute pressure across the area. By using an inflatable pad as part of the support structure, pressure can be minimized across the bony spinous processes and sacral tuberosities of the lumbar region.

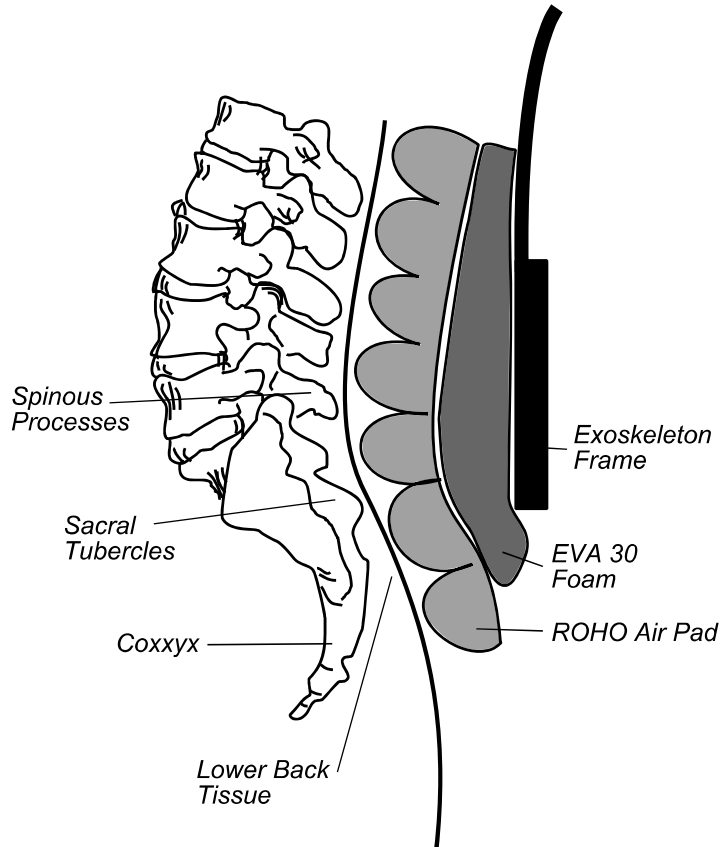


Figure 58: Cross section illustrating lumbar pad construction. Roho pad pressure should be minimized to minimize pad interface pressure.



Figure 59 : Multi cell Roho inflatable pad [71].

7.1.2.3 Thigh Pad

A thigh pad is positioned to maintain hip alignment during transitional periods such as standup and sit-down. As illustrated in Figure 56b, thigh pad force increases during periods of hip flexion

when the mass of the user is partially supported by the exoskeleton. The exoskeleton pilot will have a tendency to “fall out” of the exoskeleton during standup or sit-down if the thigh pad cannot provide adequate support.

7.1.2.4 Knee Pad

The knee pad should be positioned below the patella to ensure direct support of the tibial tuberosity (illustrated in Figure 60). This pad should be rigidly positioned so as to ensure colocation of exoskeleton and pilot knee joints. The knee pad is typically constructed of 1cm thick EVA 30 foam to ensure that the pilot’s knee tissues are safely supported during load bearing phases. The basic contour of the pad should match the tibial curvature as closely as possible to distribute forces and minimize pressure points.

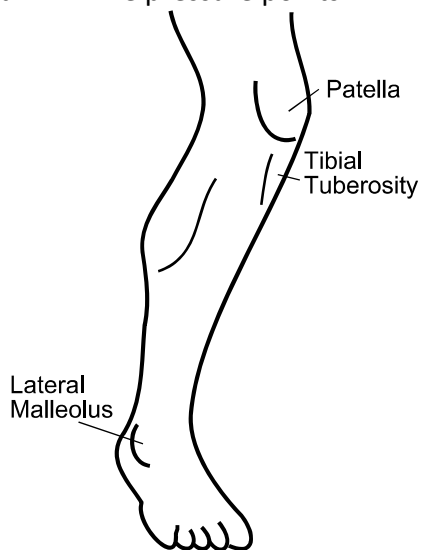


Figure 60: Tibial Tuberosity.

7.2 Posture While Seated

As discussed in section 6.2, the exoskeleton is capable of contributing to balance while in the seated posture. After first fitting the exoskeleton to a user, the erect and bent forward seated postures should be tuned according to pilot preference. Additionally, controller gains should be tuned to provide an appropriate level of hip stiffness while seated. These angles and gains are saved as controller set-points.

7.3 Posture for Static Balance and Walking

Humans are well equipped to balance in an erect posture. Even without the assistance of crutches, a typical paraplegic exoskeleton pilot is able to easily balance in a standing position soon after fitting to his/her dimensions, and tuning the system to a natural posture. The role of the exoskeleton is to minimize effort required to balance by stabilizing joints, and assisting posture.

Depending on the level and severity of a pilot’s injury he/she will feel a window of stability that can be maintained by adjusting his/her healthy upper body muscle groups. Typically users with higher (T3-T6) more severe (ASIA A) injuries will perceive a smaller stability window than those

with lower (T11-T12) less severe (ASIA C) injuries [14]. Hip and ankle angles are adjusted to maximize the window of stability while standing. With the Steven Exoskeleton the hip angle can be changed through actuator control while the ankle angle is adjusted with a setscrew. Typically ankle angle is adjusted so that the pilot is most comfortable during standing.

Using parallel bars for balance the exoskeleton and pilot are moved into a standing posture. With the knee fully extended, hip and ankle angles are adjusted so that the pilot's center of pressure is approximately centered near the shoe midsole (illustrated in Figure 61). With a correct adjustment of hip and ankle angle, the pilot's posture should be erect with shoulders back, head up, and hips forward.

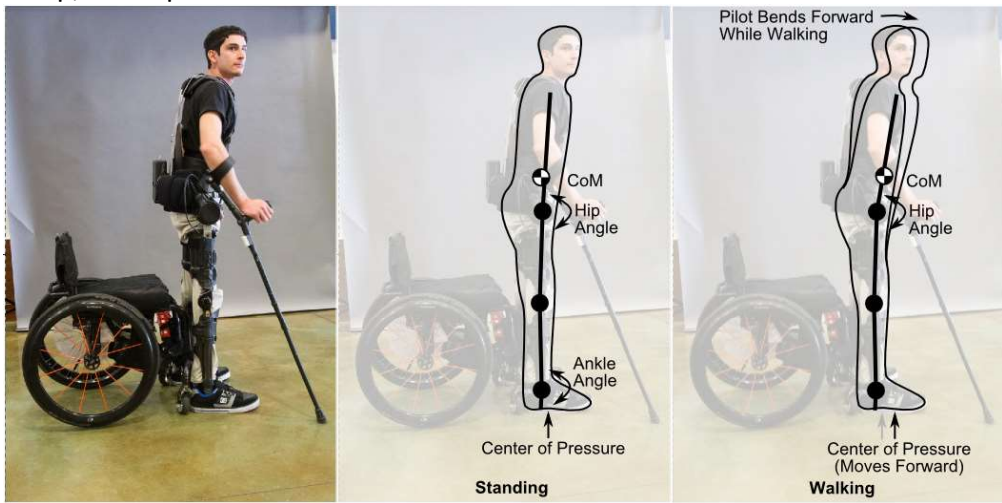


Figure 61: Tuning hip and ankle angles.

While walking the preferred posture is slightly forward (as illustrated in Figure 61) so that the center of pressure moves toward the toes. This position will allow the pilot to feel more stable while taking steps. These standing and walking tunings are saved as two separate control set-points in the FSM.

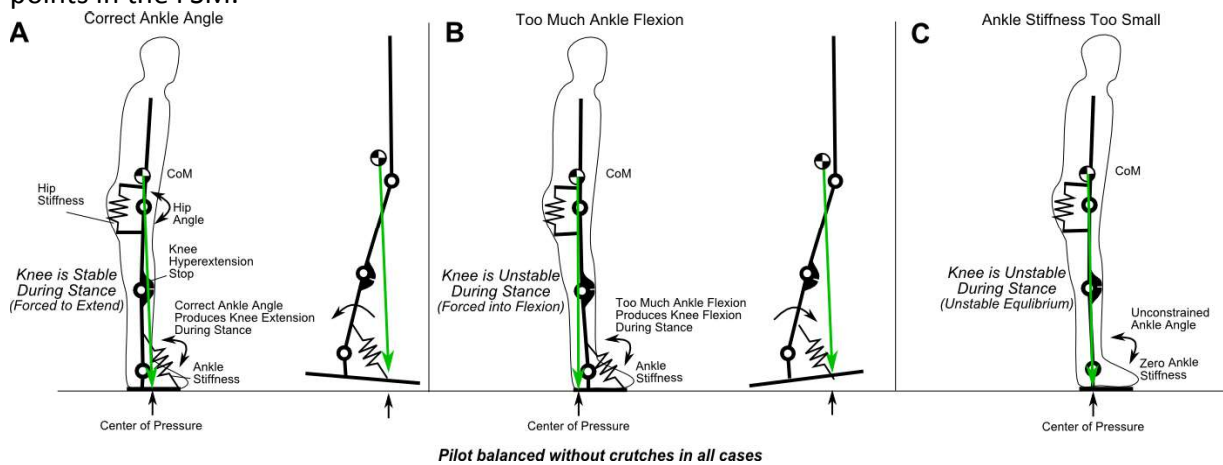


Figure 62 : Tuning of ankle angle for knee stability during stance phase.

Correct tuning of exoskeleton ankle angle increases knee stability during stance phase. As illustrated in Figure 62a, tuning the ankle angle to be slightly extended (toe down) creates a

knee extension moment during stance (extension is limited by a hyperextension hard stop). This extension moment means that zero knee torque is required to prevent knee buckling during stance. Conversely, the knee is unstable if the ankle is biased slightly flexed (toe up) as illustrated in Figure 62b. In this case, a knee flexion moment is created during early stance phase, requiring knee torque in order to avoid buckling. A third case shown in Figure 62c illustrates stance phase knee instability due to insufficient ankle stiffness. In this case, the center of mass passes through the knee resulting in an unstable equilibrium. This case is more difficult for the pilot to balance because there will only be one point of equilibrium.

7.3.1 Comparison of Standing Posture between Steven and Austin Exoskeletons

The standing posture of the Steven Exoskeleton was tuned to keep the pilot's center of mass over his feet. This effectively transfers the pilot's body weight through the legs and allows hands free balance while standing. With the Austin system the same posture is used for both standing and walking. This compromise means that the standing posture was tuned to a forward position which is more suitable for walking and transfers partial bodyweight through the hands at all times. This posture rapidly fatigues the pilot's hands and forearms.



Figure 63: Comparison of standing posture between Steven (left) and Austin (right) exoskeletons. Note the pilot of the Steven Exoskeleton can stand hands free.

Chapter 8: Electronics for Exoskeleton Systems

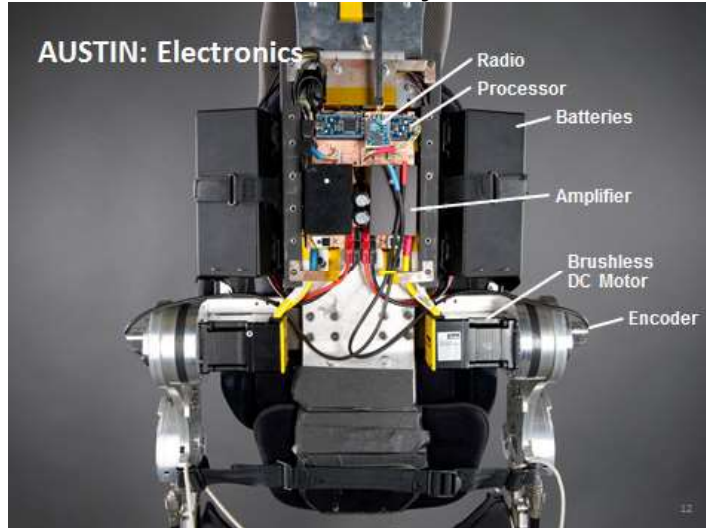


Figure 64 : Electronics for the Austin Exoskeleton.

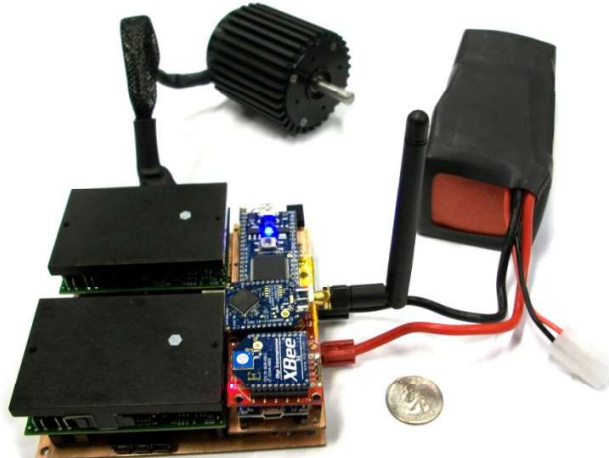


Figure 65 : Miniaturized electronics for the Ryan assistive exoskeleton system.

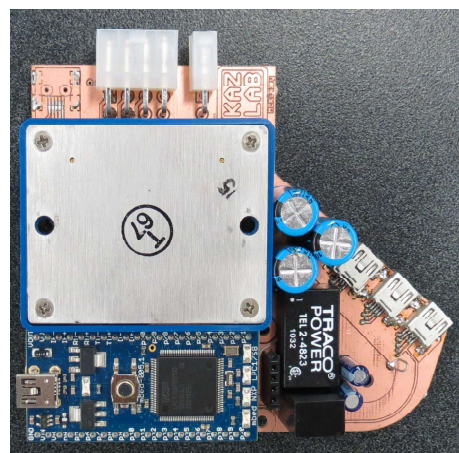


Figure 66 : Daniel Exoskeleton control module.

The author developed the electronics used in the Austin, Austin 2 (Figure 64), Ryan (Figure 65), Steven (Figure 23), and Daniel (Figure 66) exoskeletons. Over several iterations the process for designing power electronics for these mobile systems was refined and streamlined. The procedure used to develop these boards is outlined in the following sections.

8.1 Main Board Design

8.1.1 Constraints on Electronics Design

In order to protect pilot and engineer, operating voltages and motor power should be kept as low as possible, systems should be designed to fail gracefully, and schematics and code should be easy to understand. The exoskeletons discussed in this work are designed to push limits and try new ideas which require electronics and code to be easily adaptable. Two layer boards, standardized cables, and off the shelf parts were used as much as possible to ease manufacturing, inspection, and repair.

8.1.2 High Power Systems

Exoskeleton electronics design starts with the consideration of high power systems.

- 1 Motor and actuator requirements impose the largest design constraints on the overall system. After specifying desired maneuvers and operator weight, simulations were used to develop an understanding of torque and speed required of the actuators. Estimates of actuator performance requirements allow motor and transmission to be sized appropriately. The Maxon EC-90-flat electric motor and SHD-20-100-2SH 100-to-1 transmission Harmonic Drive have been sufficient for recent exoskeletons (Ryan, Steven, Daniel).
- 2 A bus voltage and motor winding are then selected; by changing motor winding it is possible to reduce motor current thereby reducing required amplifier current capacity. A bus voltage is selected to be as high as possible without jeopardizing pilot safety.
- 3 Batteries are selected that provide required bus voltage, continuous, and peak current ratings. Battery energy capacity is proportional to battery volume thereby making it advantageous to select the smallest possible battery for volume and weight savings. For recent exoskeletons a pair of 25.9v nominal 2.1Ah Lithium Polymer Battery packs connected in series were used to produce 51.8v nominal. These packs were specified to deliver enough power for approximately 4 hours of continuous walking or 8 hours of average use. Each pack weighs 0.9 lbs. and measures 5.9" x 4.25" x 1.0" (15cm x 10.8cm x 2.5cm).
- 4 Amplifiers are selected that meet the required motor performance and battery specifications (selecting the smallest possible amplifier that satisfies motor performance specifications). Copley Bantam BTM-090-10 amplifiers were selected for the Ryan, Steven, and Daniel exoskeletons based on their current and voltage ratings.
- 5 Polarity protection [72], current protection, and power switching electronics [73] are also designed around battery specifications and motor power requirements (see Figure 67).

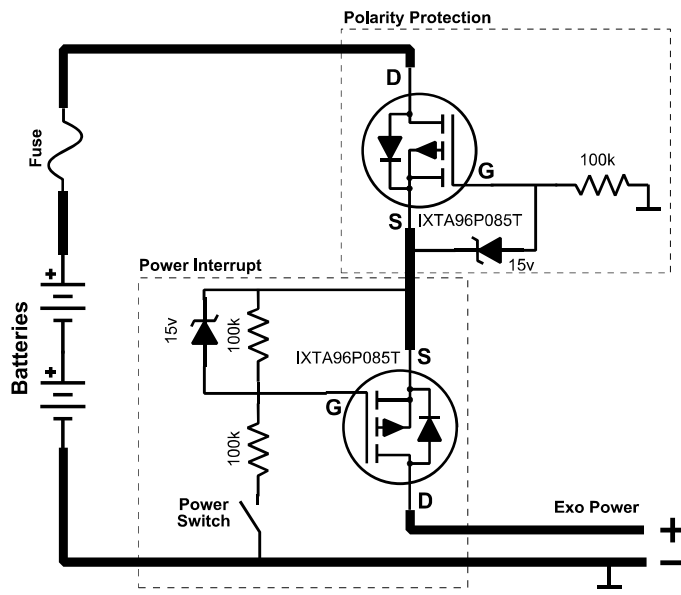


Figure 67 : Polarity protection and power switching. High efficiency P-channel MOSFETs used for polarity protection and power switching to minimize part count and resistive losses. Heavy and light line thicknesses used to denote high and low current pathways respectively.

8.1.3 Low Power Systems

Low power electronics including controllers and sensors are selected to meet the control objectives of a given exoskeleton design.

- 1 Processors are selected based on estimated control complexity and required communication busses. TheMBED prototyping board has offered sufficient processing power for the lightweight controllers used in most systems developed in the HEL.
- 2 Encoders are selected to measure hip angle. Generally, AS5145b 12bit Absolute Magnetic Encoders have been used for exoskeleton actuator position feedback as they offer high speed high resolution angle measurement in a tiny package.
- 3 Low power regulators are specified after summing the total low power system requirements (considering the needs of processors, wireless radios, sensors etc...).

The basic electronics system architecture is illustrated in Figure 68.

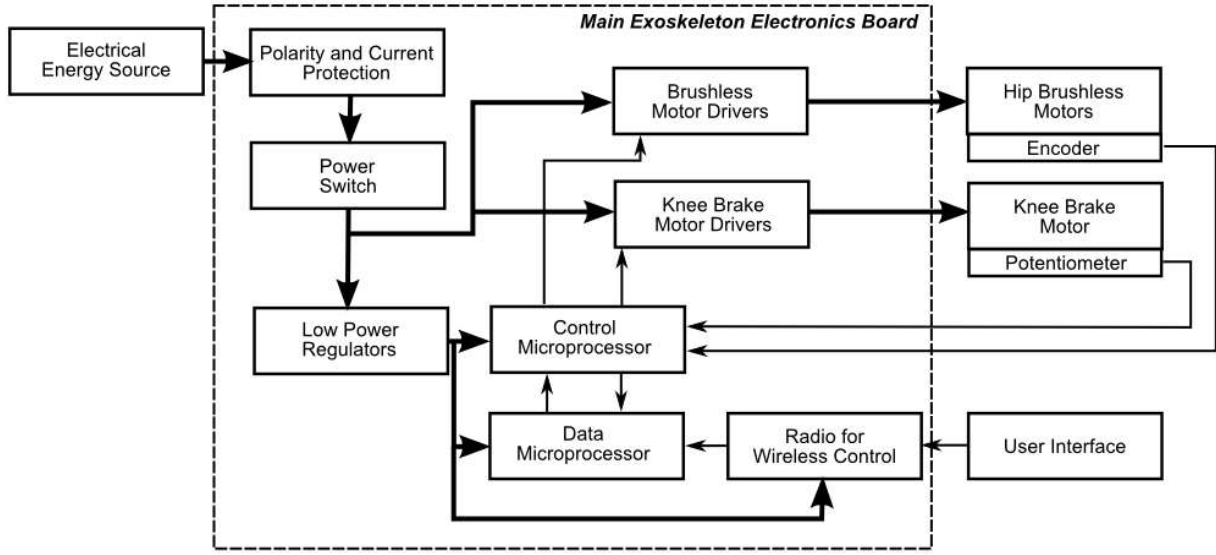


Figure 68: Exoskeleton Electronics System Configuration: Heavy lines indicate flow of power; light lines indicate flow of data.

8.1.4 Layout

Exoskeleton electronics boards are laid out to minimize routing complexity, minimize electrical interference, and minimize overall board dimensions. An excellent description of techniques for electronics layout can be found in [74]. Modular subsystems were used extensively in exoskeleton electronics including modules for microprocessors, amplifiers, and radios. This approach allows rapid identification of problems and easy replacement of parts should a component become mechanically or electrically damaged.

8.1.5 Keeping Track of Data on the Exoskeleton

Data is logged on the data management processor at a rate of 1 Hz in order to document system performance. A text file is updated with a record of system time, number of steps taken, battery pack voltage, and momentary commanded current. Total energy consumption is approximated by integrating the product of battery pack voltage and commanded current over time.

$$Energy\ Consumed \cong Battery\ pack\ Voltage * Commanded\ Current * \Delta time \quad (8-1)$$

At system startup, the most recent data file is parsed so that total energy consumption and steps taken can be recorded. Energy consumption and step counts are reset after each battery charge (battery charge is detected by a change in battery voltage from below 53v to over 55v as compared to the previous data file). By taking data regarding battery pack performance, we are able to better understand how far a pilot can walk, and whether he/she has enough energy to get home. Currently the Steven Exoskeleton is configured to sound an audible tone every 30 seconds if battery voltage drops below a preset threshold. A low pass filtered voltage divider (illustrated in Figure 69) is used to measure battery pack voltage. A schottky diode is used as a voltage regulator to safeguard microprocessor analog input pins against voltages above the expected range.

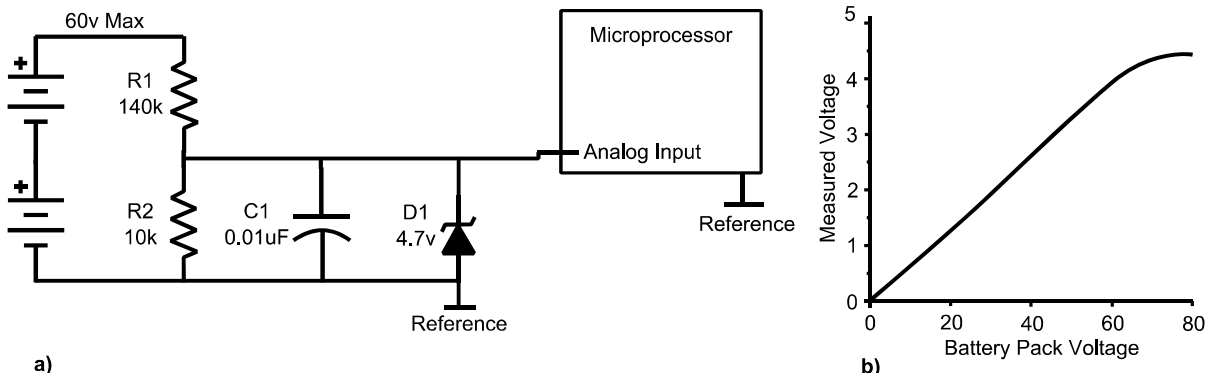


Figure 69: Exoskeleton battery pack voltage measurement. A) Voltage divider for monitoring pack voltage. B) Overvoltage protection of microprocessor analog input.

In designing exoskeletons, it is advantageous to increase bus voltage (to within safe limits) in an effort to reduce motor current which allows thinner conductors, and smaller amplifiers. The Steven Exoskeleton uses two 25.9V nominal 2.1Ah Lithium Polymer battery packs configured in series. These packs come with a built in protection board that automatically protects the cells should peak current or cell voltage exceed preset thresholds. One challenge associated with a series pack configuration is that should one of the two packs fail the whole system will shut down. Human Engineering Laboratory exoskeletons have been designed for this eventuality by defaulting to a braced configuration in the event of power failure. This allows the pilot to stabilize and find a way to sit-down.

8.1.6 Battery Charging

Presently batteries are disconnected and charged through an external battery charging system. An in-pack management board takes care of cell balancing and monitors cell voltage and current draw. This circuitry is included with the 25.9v nominal 2.1Ah Lithium Polymer Battery packs and is designed to safeguard the batteries against over charge/discharge and extreme current draw situations. In future revisions it would be helpful to have a better understanding of individual cell performance. This data would provide a level of pilot security as unexpected pack failures could be avoided. A custom battery management board would enable accurate monitoring of individual cell health and overall pack capacity. This information could be easily communicated with the control processor to warn the pilot before sit-down is required.

Chapter 9: Developing a Lightweight Handheld User Interface

The user interface (UI) plays a critical role in the overall safety, reliability, and performance of an exoskeleton system. The UI should not interfere with the user experience, that is to say it should not limit the user's range of motion or behaviors. A successful UI allows the user to intuitively control an exoskeleton without imposing cognitive or physical limitations on other activities. Without extensive training, the interface should be intuitive to use for a beginner without limiting the maneuvers of an advanced user. Reliability and minimal latency allow the user to trust the device in new terrain and tricky situations.

9.1 Comparison to Other User Interface Approaches

ReWalk, eLegs, Indego and Rex has developed a range of user interface designs. In comparing these approaches it is important to consider how the user commands steps and changes between modes. ReWalk uses a wrist mounted interface to change modes [30] while individual steps are commanded by leaning the torso forward to a threshold angle [75]. eLegs uses an IMU to measure of upper arm orientation to initiate steps. Sensors on crutch and foot act to filter out unwanted step commands. Modes are navigated with a tethered control box [76]. Vanderbilt's Indego uses estimated center of pressure as measured by a torso mounted accelerometer to control standing, sitting, and walking by estimating center of pressure motion[77]. This system allows the user to maintain control of the crutches or walker while changing modes which is an advantage over ReWalk's and eLeg's systems. Rex was designed to self-balance through numerous powered degrees of freedom [26]. Users command the system via control pad and joystick [27]. Although changing modes requires numerous keypad interactions, users have plenty of time to calculate their next move as mobility is limited by Rex's extremely slow speed [28].

9.2 User Interface Simplicity

Simplicity and predictability are the primary advantages of the crutch based user interface over other methods used by the state of the art. A button placed in a convenient location is natural to learn and can be operated with minimal latency. As described in chapter 3.3, the finite state machine has been designed to be controlled by two command signals. These signals can be generated through a multitude of possible approaches [45], however two crutch mounted buttons have been the most common method.

User interfaces designed for the Austin, Austin 2, Ryan, Steven, and Daniel exoskeletons have been designed to be as lightweight and unobtrusive as possible. From experimentation with the Austin and Ryan exoskeleton systems, it is clear that a tethered UI imposes unnecessary constraints on user performance. Common maneuvers such as standing to work at a counter and using handrails to walk on a ramp dictate that the exoskeleton pilot must switch the UI between hands, or let go of the UI altogether. Furthermore, while sitting it is common to store the crutches nearby. In all of these cases a wireless device eliminates the potential for tangled or broken cables, and allows the device to be naturally switched from one hand to the other to adapt to changing environments. Figure 70 illustrates how a wireless crutch mounted user interface allows the pilot to become easily hands free or maneuver in tight spaces such as a car.

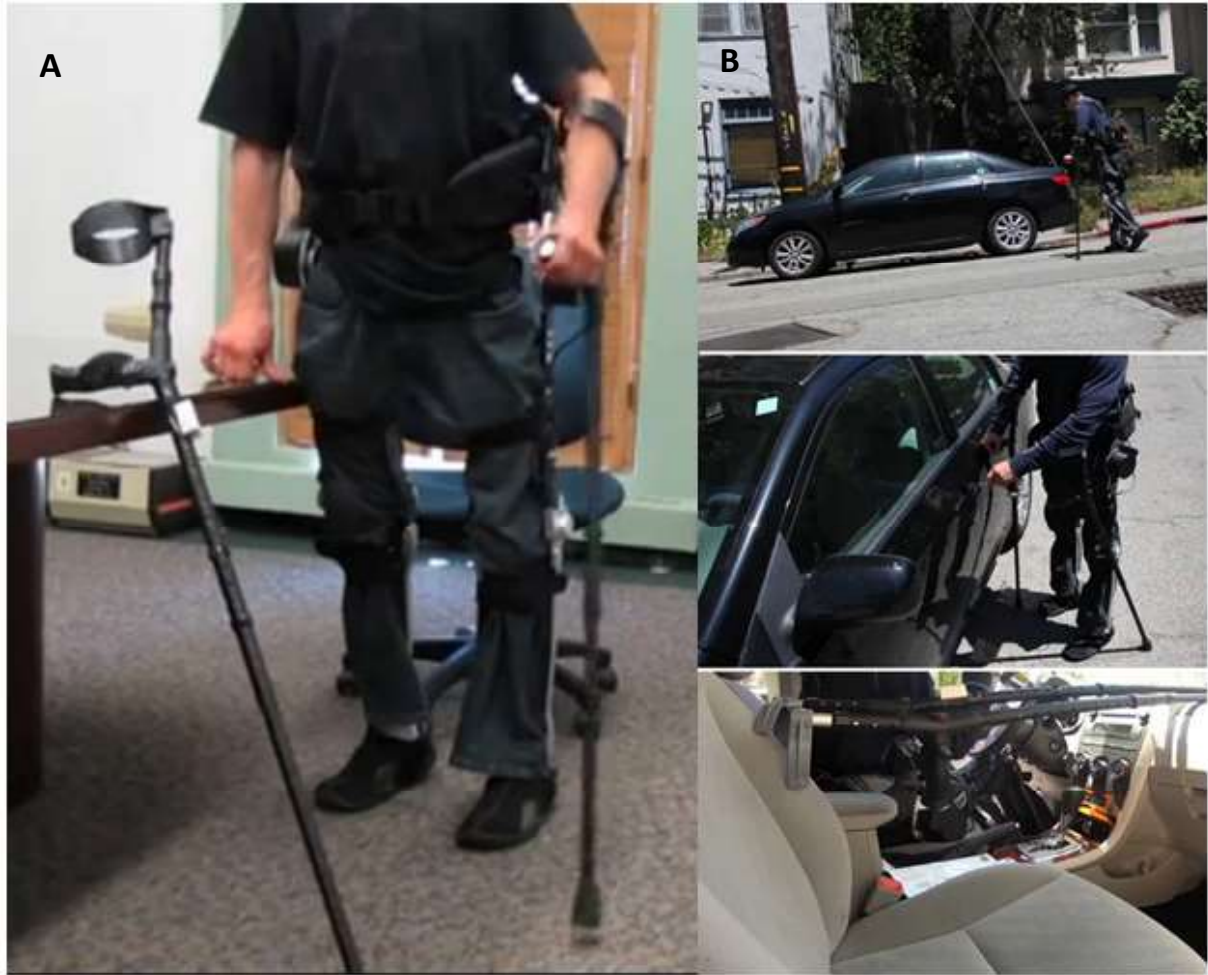


Figure 70: Freedom of motion afforded by a wireless User Interface. A) Leaning a crutch nearby to get hands free. B) Getting into a car and stowing crutches nearby.

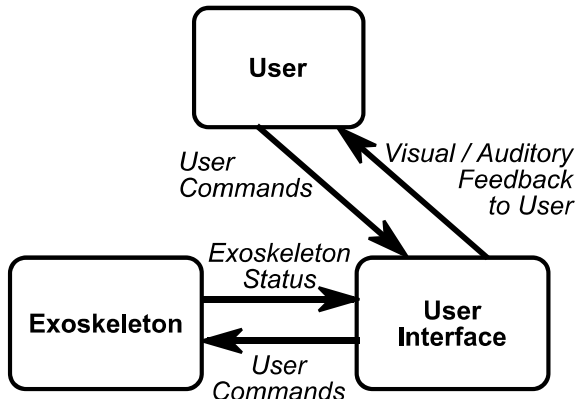
9.3 Impact of Power Requirements on User Interface Design

Previous iterations of the two button user interface relied on constant radio communication between crutch and exoskeleton to send and receive signals. This approach was exceedingly impractical as it required frequent charging of large batteries to meet power demands.

Constant average power consumption was approximately 0.64 Watts which depleted a 2Ah 7.4v rechargeable battery in approximately 12 hours of use.

The user interface and finite state machine were redesigned to minimize the amount of energy required for communication. By transmitting state changes only, the UI was kept in sleep mode for as much time as possible. Through this approach average UI power consumption was reduced from 0.644 Watts to 3.59×10^{-4} Watts (a 1000x reduction in power consumption). This enables the system to operate on one pair of AA batteries for approximately 290 days (or 9-10 months) before replacement is required. Table 1 offers a comparison of the two UI designs.

Feedback Provided to User Through UI



Feedback Provided to User by Exoskeleton

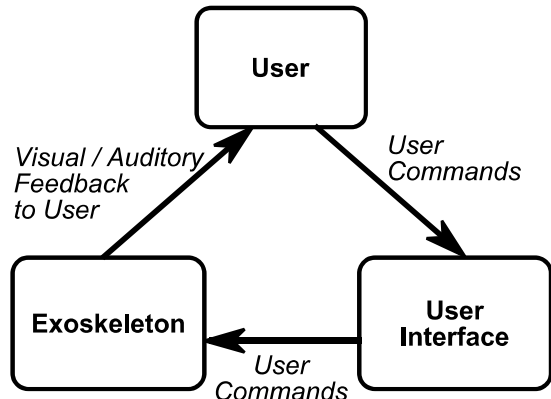


Figure 71: User interface information diagram.

Table 8: Comparison of Old and New UI.

	Previous User Interface	New User Interface
	UI always on to confirm status with exoskeleton	UI in sleep mode unless state transitions are commanded
Components	Xbee Pro 900MHz LDO Regulator Arduino Pro Mini	Xbee Pro 900MHz in sleep mode High Efficiency Regulator
Total Power Consumption	Approx. 0.64 Watts	3.6×10^{-4} Watts
Life from 2 AA Batteries	0.16 Days	290 Days

Figure 72 illustrates the high level schematic for the low power user interface. The Xbee module is programmed to stay in the sleep state until the DTR pin is pulled low. When one or both of the buttons are pressed the Xbee wakes from sleep and transmits the status of DIO0 and DIO1. The Xbee continues transmitting this signal until the button is released (the Xbee goes back to sleep mode upon button release). This approach has the added benefit of transmission redundancy as up to 100 transmissions can be sent in the period of a typical 500ms button click.

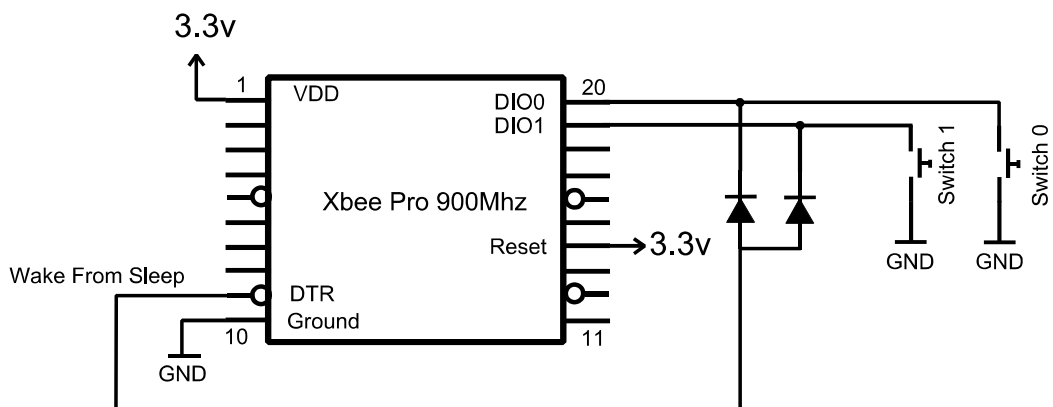


Figure 72: Schematic of low power wireless user interface.

The high efficiency regulator used for the UI is illustrated in Figure 73. The regulator chip automatically transitions to sleep mode during periods of low power draw, further increasing system efficiency.

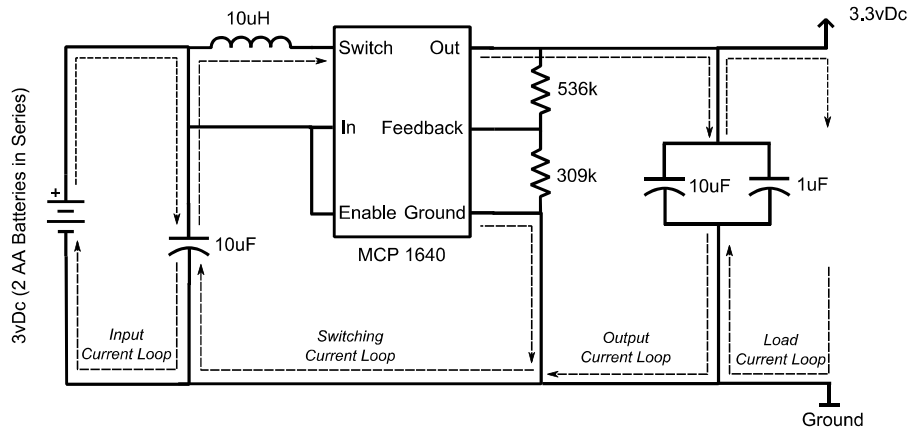


Figure 73: Schematic of high efficiency low power voltage regulator for wireless user interface.

The board illustrated in Figure 74 was laid out to minimize overall dimensions. Current loops (illustrated in Figure 73) were minimized to reduce electromagnetic interference[74].

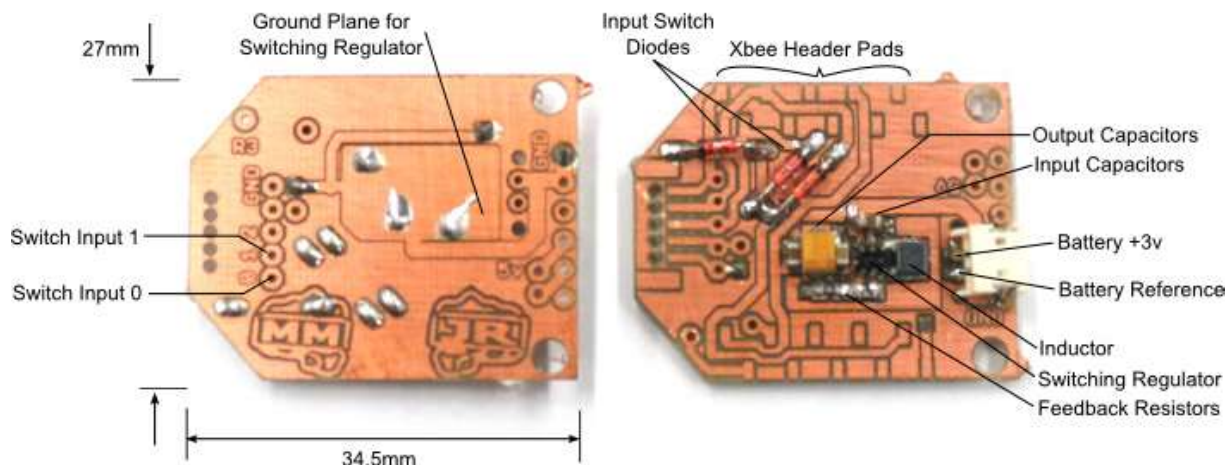


Figure 74: Physical Implementation of low power wireless user interface board.

Figure 75 illustrates the UI as attached to a standard forearm crutch. Two AA batteries are housed in the body of the crutch with the UI board housed in a plastic case (for radio transparency). Two control buttons are embedded in the crutch handle placed conveniently for pilot operation.



Figure 75: User Interface Embedded in Forearm Crutch.

This UI design has proven to be exceptionally reliable and robust. Batteries have been changed two times since it was first designed in fall of 2012 (an average of 9 months per set). Pilots have commented that they feel more secure knowing that the UI will operate predictably and remain undamaged when dropped on the floor.

Chapter 10: Taking the Next Steps



Figure 76 : A pilot of the Ryan Exoskeleton explores beyond the lab.

The utility of UC Berkeley Human Engineering Lab exoskeleton systems has improved dramatically over the last five years. These systems have evolved from cumbersome curiosities to nimble mobility tools. The Steven Exoskeleton is now capable of moving with more ease and grace than the Austin system ever could. Rethinking the approach to standing, sitting, and walking has moved the Steven Exoskeleton much closer to independent operation for paraplegic pilots. However, several areas of the Steven Exoskeleton could still be improved.

10.1 Reduction in Mass

System mass could be further reduced by redesigning hard and soft structures. Reducing system mass, (especially the mass of the torso unit) greatly simplifies difficult maneuvers such as standing and sitting. Lower torso mass also simplifies how the device is handled when stowing in a car, and when donning and doffing. Dead weight can be easily trimmed from several areas:

- The hip module and associated adjustment system could be redesigned for more efficient material placement.
- Protection for electronics and cabling can be improved, and material efficiency can be increased by incorporating this structure into the hip module. Electronics are currently

housed in an ABS enclosure (illustrated in Figure 23) which is unnecessarily heavy, and does not adequately protect connections.

- The exoskeleton uses a large volume of foam padding to securely match user and machine. A redesign of these structures for minimized foam thickness could result in a lighter system and would keep the pilot cooler.
- Current revisions of adjustable and fixed length leg braces (see Figure 15) are substantially overbuilt. Mass could be removed without compromising structural integrity.
- Additional weight could be removed through a redesign of the flexible spine support (see Figure 14).

10.2 Simplified Donning

Donning and doffing has been greatly simplified with the modular elements of the Steven Exoskeleton (illustrated in Figure 11). However, achieving alignment of the hip and torso during the donning process is physically demanding. The connection between the hip and torso could benefit from a mechanical redesign. A successful redesign would simplify alignment of the hip and torso in 6 degrees of freedom and reduce effort required to lock the adjustment mechanism while maintaining hip abduction/adduction flexibility (see Figure 14).

10.3 Working with Contracture and Spasticity

The dynamic approach to swing phase knee flexion used with the Steven Exoskeleton works most effectively with individuals exhibiting flaccid paralysis (no joint impedance from residual muscles). If the Steven Exoskeleton is to achieve widespread adoption, the knee needs to be redesigned to accommodate individuals exhibiting knee muscle spasticity or contracture. Serving these individuals may require the addition of an actuator at the knee in order to provide powered swing phase knee flexion.

10.4 Moving Faster

10.4.1 Hardware Modifications

The Steven Exoskeleton has exhibited the fastest walking speeds for an assistive exoskeleton developed at the UC Berkeley Human Engineering Laboratory. This increase in speed was made possible through gait modifications aimed at increasing stride length and smoothing out walking dynamics (see Chapter 5). At higher speeds, the walking gait was tuned to provide adequate toe clearance and knee extension while minimizing kinetic energy at terminal swing. Currently the top speed of the Steven Exoskeleton is limited by how well the pilot can balance between steps. Faster walking speeds could be achieved by redesigning the exoskeleton knee to provide better shock absorption at heel strike and controlled energy dissipation at terminal swing.

10.4.2 User Interface Modifications

Currently the user interface requires a command from the pilot to initiate each step. This approach is intuitive at slow walking speeds where foot placement is critical. A UI with a different command approach that requires fewer user inputs per step would be advantageous when traversing longer distances.

Chapter 11: Concluding Remarks

This dissertation focuses on the development of the minimally actuated Steven Exoskeleton as a practical mobility solution for paraplegics. This device was specifically designed to address shortcomings of previous exoskeleton designs that hinder independence and utility.

The Steven Exoskeleton is the first mobile assistive exoskeleton to assist the pilot while in the seated position. While seated, the exoskeleton acts as the pilot's absent core muscles providing postural stability and security. Additionally, the exoskeleton can be commanded into a reaching posture to effortlessly manipulate objects on the floor. This work also discusses a new approach to increase the reliability, and safety of standup and sit-down. Consistent standup and sit-down enables individuals to be self-sufficient and opens the possibility for full operation without a spotter.

Several improvements have been made to increase utility while standing and walking. Tuning and hardware refinements have allowed better balance adjustments for a broader range of SCI patients. Hardware modifications enable tunable hip and spine flexibility to improve performance and pilot adaptability.

This dissertation discusses a biologically inspired approach to gait scaling as a function of walking cadence. By smoothing hip trajectory and increasing average stride length it has been possible to increase walking speed and pilot comfort. Additionally, modifications to the finite state machine have enabled more intuitive modulation of speed.

Through hardware and control modifications maximum walking speed has been increased to 0.475m/s from a previous maximum of 0.27m/s. Increased walking speed makes the device more practical, and enables more independence in society. The discussed work was validated through extensive testing with a range of SCI patients in laboratory and real world environments. Device and associated control software adaptability has made it possible to test with pilots exhibiting a variety of medical conditions.

The Steven Exoskeleton has made great strides to improve the accessibility of assistive medical exoskeletons. Ultimately the true measure of success for these devices will be how well they serve as tools for independence. The Steven Exoskeleton is ready to step out of the laboratory. Hopefully, through future research, these tools will continue to be forged and honed until they are widely available for all.

Chapter 12: Bibliography

- [1] NSCISC, "Spinal cord injury facts and figures at a glance.," Mar-2014. [Online]. Available: <http://www.ncbi.nlm.nih.gov/pubmed/24559421>.
- [2] *International Perspectives on Spinal Cord Injury*. World Health Organization, 2014.
- [3] L. Phillips, M. N. Ozer, P. Axelson, H. Chizeck, C. W. Britell, J. Fonseca, M. E. Bayless, and H. E. Watson, "Spinal Cord Injury: A Guide for Patient and Family," *J. Spinal Disord. Tech.*, vol. 3, no. 3, p. 282, 1990.
- [4] T. Gordon and J. Mao, "Muscle atrophy and procedures for training after spinal cord injury.," *Phys. Ther.*, vol. 74, no. 1, pp. 50–60, Jan. 1994.
- [5] J. Little and P. Micklesen, "Lower extremity manifestations of spasticity in chronic spinal cord injury," *Am. J. Phys. Med. Rehabil.*, vol. 68, no. 1, p. 32, 1989.
- [6] L. Harvey and R. Herbert, "Muscle stretching for treatment and prevention of contracture in people with spinal cord injury.," *Spinal Cord*, vol. 40, pp. 1–9, 2002.
- [7] M. Bliss, "Aetiology of pressure sores," *Rev. Clin. Gerontol.*, vol. 3, no. 04, p. 379, Nov. 2008.
- [8] Y. Zehnder, M. Lüthi, D. Michel, H. Knecht, R. Perrelet, I. Neto, M. Kraenzlin, G. Zäch, and K. Lippuner, "Long-term changes in bone metabolism, bone mineral density, quantitative ultrasound parameters, and fracture incidence after spinal cord injury: a cross-sectional observational study in 100 paraplegic men.," *Osteoporos. Int.*, vol. 15, no. 3, pp. 180–9, Mar. 2004.
- [9] A. Esclarín De Ruz, E. García Leoni, and R. Herruzo Cabrera, "Epidemiology and risk factors for urinary tract infection in patients with spinal cord injury.," *J. Urol.*, vol. 164, no. 4, pp. 1285–9, Oct. 2000.
- [10] A. Lynch, A. Antony, B. Dobbs, and F. Frizelle, "Bowel dysfunction following spinal cord injury.," *Spinal Cord*, vol. 39, pp. 193–203, 2001.
- [11] R. Brown, A. F. DiMarco, J. D. Hoit, and E. Garshick, "Respiratory dysfunction and management in spinal cord injury.," *Respir. Care*, vol. 51, no. 8, pp. 853–68;discussion 869–70, Aug. 2006.
- [12] J. Myers, M. Lee, and J. Kiratli, "Cardiovascular disease in spinal cord injury: an overview of prevalence, risk, evaluation, and management.," *Am. J. Phys. Med. Rehabil.*, vol. 86, no. 2, pp. 142–52, Feb. 2007.
- [13] P. T. Katzmarzyk, T. S. Church, C. L. Craig, and C. Bouchard, "Sitting time and mortality from all causes, cardiovascular disease, and cancer.," *Med. Sci. Sports Exerc.*, vol. 41, no. 5, pp. 998–1005, May 2009.

- [14] C. Sadowsky, O. Volshteyn, L. Schultz, and J. W. McDonald, "Spinal cord injury.," *Disabil. Rehabil.*, vol. 24, no. 13, pp. 680–7, Sep. 2002.
- [15] G. Merati, P. Sarchi, M. Ferrarin, a Pedotti, and a Veicsteinas, "Paraplegic adaptation to assisted-walking: energy expenditure during wheelchair versus orthosis use.," *Spinal Cord*, vol. 38, no. 1, pp. 37–44, Jan. 2000.
- [16] M. Bernardi, I. Canale, V. Castellano, L. Di Filippo, F. Felici, and M. Marchetti, "The efficiency of walking of paraplegic patients using a reciprocating gait orthosis.," *Paraplegia*, vol. 33, no. 7, pp. 409–15, Jul. 1995.
- [17] L. Sykes, J. Edwards, E. S. Powell, and E. R. Ross, "The reciprocating gait orthosis: long-term usage patterns.," *Arch. Phys. Med. Rehabil.*, vol. 76, no. 8, pp. 779–83, Aug. 1995.
- [18] D. M. Hendershot and C. A. Phillips, "IEEE ENGINEERING IN MEDICINE & BIOLOGY SOCIETY 10TH ANNUAL INTERNATIONAL CONFERENCE--1577 1578--IEEE ENGINEERING IN MEDICINE & BIOLOGY SOCIETY 10TH ANNUAL INTERNATIONAL CONFERENCE," pp. 1577–1578, 1988.
- [19] a V Nene, H. J. Hermens, and G. Zilvold, "Paraplegic locomotion: a review.," *Spinal Cord*, vol. 34, no. 9, pp. 507–24, Sep. 1996.
- [20] R. Scelsi, "Skeletal Muscle Pathology after Spinal Cord Injury : Our 20 Year Experience and Results on Skeletal Muscle Changes in Paraplegics , Related to Functional Rehabilitation," pp. 75–85.
- [21] A. Yamane, "Reciprocating Gait Orthoses," in *Spinal Cord Medicine: Principles and Practice.*, et al. Lin VW, Cardenas DD, Cutter NC, Ed. Demos Medical Publishing, 2003.
- [22] "Bracing Options," *Post-Polio Heal.*, vol. 19, no. 1, 2003.
- [23] A. Esquenazi, M. Talaty, A. Packel, and M. Saulino, "The ReWalk powered exoskeleton to restore ambulatory function to individuals with thoracic-level motor-complete spinal cord injury.," *Am. J. Phys. Med. Rehabil.*, vol. 91, no. 11, pp. 911–21, Nov. 2012.
- [24] "Berkeley Bionics – eLEGS," 2011. [Online]. Available: <http://berkeleybionics.com/exoskeletons-rehab-mobility/> .
- [25] R. Farris, "Design of a powered lower limb exoskeleton and control for gait assistance in paraplegics," Vanderbilt University, 2012.
- [26] R. Little and R. A. Irving, "Self contained powered exoskeleton walker for a disabled user," US20110066088 A12011.
- [27] F. Almesfer and A. J. Grimmer, "Control system for a mobility aid," EP2448540 A12012.
- [28] K. H. Low, "Robot-assisted gait rehabilitation: From exoskeletons to gait systems," *2011 Def. Sci. Res. Conf. Expo*, pp. 1–10, Aug. 2011.

- [29] W. Tung, M. McKinley, M. Pillai, J. Reid, and H. Kazerooni, "Design of a Minimally Actuated Medical Exoskeleton With Mechanical Swing-Phase Gait Generation and Sit-Stand Assistance," *Proc. ASME 2013 Dyn. Syst. Control Conf.*, pp. 1–9, 2013.
- [30] G. Zeilig, H. Weingarden, M. Zwecker, I. Dudkiewicz, A. Bloch, and A. Esquenazi, "Safety and tolerance of the ReWalk™ exoskeleton suit for ambulation by people with complete spinal cord injury: a pilot study.," *J. Spinal Cord Med.*, vol. 35, no. 2, pp. 96–101, Mar. 2012.
- [31] E. Strickland, "Good-bye, Wheelchair," *IEEE Spectrum*, pp. 30–32, 2012.
- [32] J. Contreras-Vidal, A. Presacco, H. Agashe, and A. Paek, "Restoration of Whole Body Movement," *IEEE Pulse*, no. February, p. 34, 2012.
- [33] J. Stallard, R. E. Major, and J. H. Patrick, "A review of the fundamental design problems of providing ambulation for paraplegic patients.," *Paraplegia*, vol. 27, no. 1, pp. 70–5, Feb. 1989.
- [34] W. Tung, "DESIGN AND OPERATION OF MINIMALLY ACTUATED MEDICAL EXOSKELETONS FOR INDIVIDUALS WITH PARALYSIS," University of California at Berkeley, 2013.
- [35] M. G. McKinley, "Design of a Novel Orthotic Knee Joint for Use in an Assistive Exoskeleton for Paraplegics," University of California at Berkeley, 2011.
- [36] J. Reid, M. McKinley, W. Tung, M. Pillai, and H. Kazerooni, "A Method of Swing Leg Control for a Minimally Actuated Medical Exoskeleton for Individuals With Paralysis," *Proc. ASME 2013 Dyn. Syst. Control Conf.*, pp. 1–9, 2013.
- [37] J. Reid, "Control Strategies for a Minimally Actuated Medical Exoskeleton for Individuals with Paralysis," University of California at Berkeley, 2012.
- [38] P. E. Barnes, "Design of a Modular Human Exoskeleton Torso," University of California at Berkeley, 2011.
- [39] J. T. Kahle, "Comparison of nonmicroprocessor knee mechanism versus C-Leg on Prosthesis Evaluation Questionnaire, stumbles, falls, walking tests, stair descent, and knee preference," *J. Rehabil. Res. Dev.*, vol. 45, no. 1, pp. 1–14, Dec. 2008.
- [40] D. Gagnon, C. Duclos, P. Desjardins, S. Nadeau, and M. Danakas, "Measuring dynamic stability requirements during sitting pivot transfers using stabilizing and destabilizing forces in individuals with complete motor paraplegia.," *J. Biomech.*, vol. 45, no. 8, pp. 1554–8, May 2012.
- [41] M. Arazpour, M. a Bani, S. W. Hutchins, S. Curran, and M. a Javanshir, "The influence of ankle joint mobility when using an orthosis on stability in patients with spinal cord injury: a pilot study.," *Spinal Cord*, vol. 51, no. 10, pp. 750–4, Oct. 2013.
- [42] Stephen McKinley, "Design and Control of a Continuously Variable Brake for use in an Assistive Orthotic Device," University of California Berkeley, 2013.

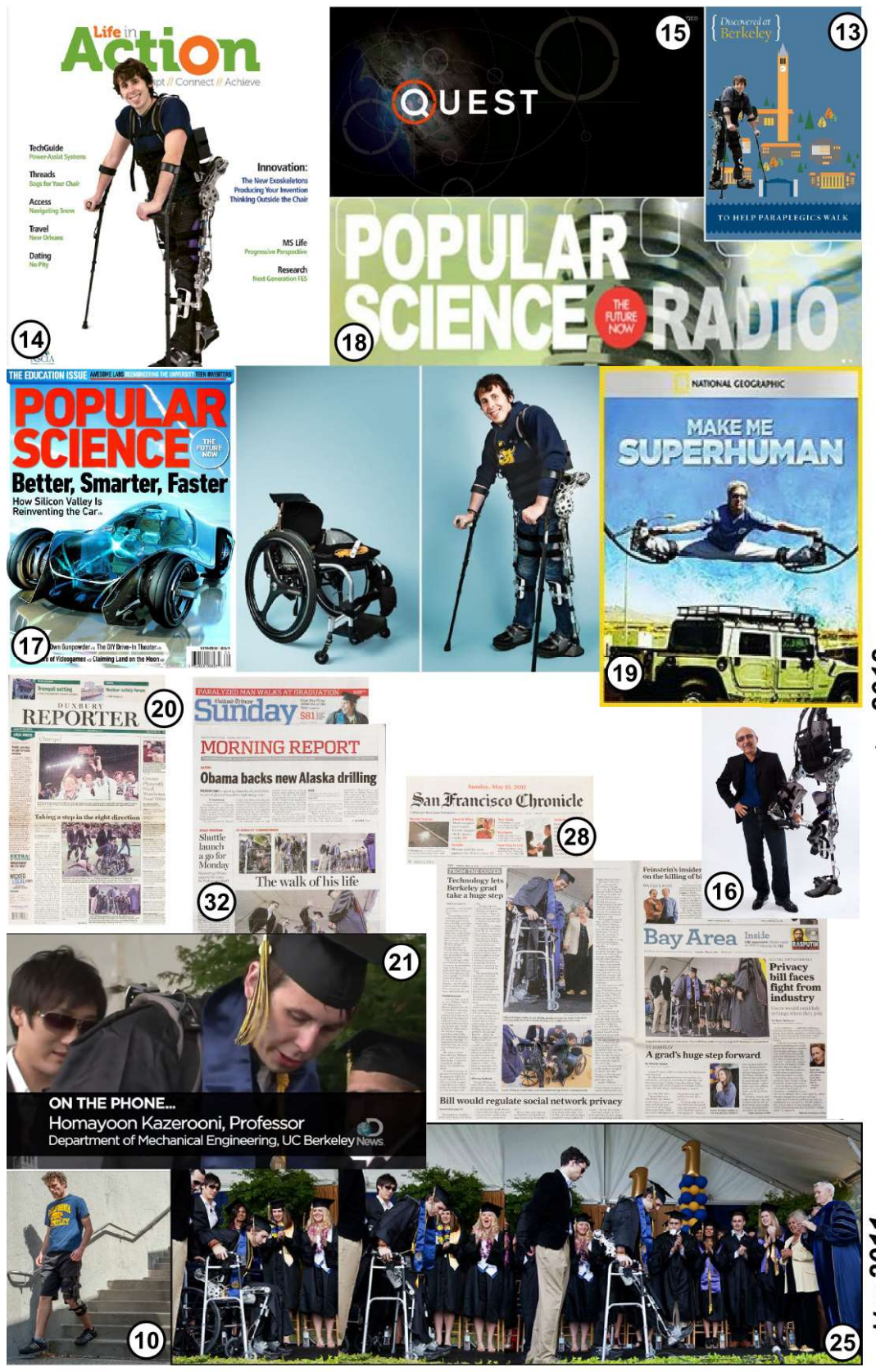
- [43] D. Hoffman, L. M. Sheldahl, K. J. Buley, P. R. Sandford, and A. P. Med, "Above-Knee Amputee and Able-Bodied Subjects , and a Model to Account for the Differences in Metabolic Cost," vol. 78, no. April, 1997.
- [44] Y. J. Wu, S. Y. Chen, M. C. Lin, C. Lan, J. S. Lai, and I. N. Lien, "Energy expenditure of wheeling and walking during prosthetic rehabilitation in a woman with bilateral transfemoral amputations," *Arch. Phys. Med. Rehabil.*, vol. 82, no. 2, pp. 265–9, Feb. 2001.
- [45] W. Y. Tung, *ORTHESIS SYSTEM AND METHODS FOR CONTROL OF EXOSKELETONS*, vol. 1, no. 61. 2013.
- [46] M. J. R. Sutherland D. H., Kaufman K. R., "Kinematics of normal human walking," in *Human walking*, J. Rose and J. Gamble, Eds. Williams & Wilkins, 1997.
- [47] D. Winter, "Biomechanical Data Resources: 2D Gait Data." [Online]. Available: <http://isbweb.org/data/>.
- [48] R. L. Waters, B. R. Lunsford, J. Perry, and R. Byrd, "Energy-speed relationship of walking: standard tables.," *J. Orthop. Res.*, vol. 6, no. 2, pp. 215–22, Jan. 1988.
- [49] M. Morris, R. Iansek, T. Matyas, and J. Summers, "Abnormalities in the stride length-cadence relation in parkinsonian gait.," *Mov. Disord.*, vol. 13, no. 1, pp. 61–9, Jan. 1998.
- [50] C. BenAbdelkader, "Stride and cadence as a biometric in automatic person identification and verification," *Autom. Face ...*, 2002.
- [51] R. Tanawongsuwan and A. Bobick, "A Study of Human Gaits across Different Speeds," pp. 1–13.
- [52] Chris Kirtley, *Clinical Gait Analysis Theory and Practice*. Elsevier, 2006.
- [53] C. Kirtley and M. W. Whittle, "INFLUENCE OF WALKING SPEED ON GAIT," *J. Biomed. Eng.*, vol. 7, 1985.
- [54] M. R. Pierrynowski and V. Galea, "Enhancing the ability of gait analyses to differentiate between groups: scaling gait data to body size.," *Gait Posture*, vol. 13, no. 3, pp. 193–201, May 2001.
- [55] Hof, "Scaling gait data to body size," *Gait Posture*, vol. 4, pp. 222–223, 1996.
- [56] A. W. Andrews, S. A. Chinworth, M. Bourassa, M. Garvin, D. Benton, and S. Tanner, "Update on Distance and Velocity Requirements for Community Ambulation," vol. 27244, pp. 128–134, 2010.
- [57] B. J. Mohler, W. B. Thompson, S. H. Creem-Regehr, H. L. Pick, and W. H. Warren, "Visual flow influences gait transition speed and preferred walking speed.," *Exp. brain Res.*, vol. 181, no. 2, pp. 221–8, Aug. 2007.
- [58] T. A. Swift, "Control and Trajectory Generation of a Wearable Mobility Exoskeleton for Spinal Cord Injury Patients," U.C. Berkeley, 2011.

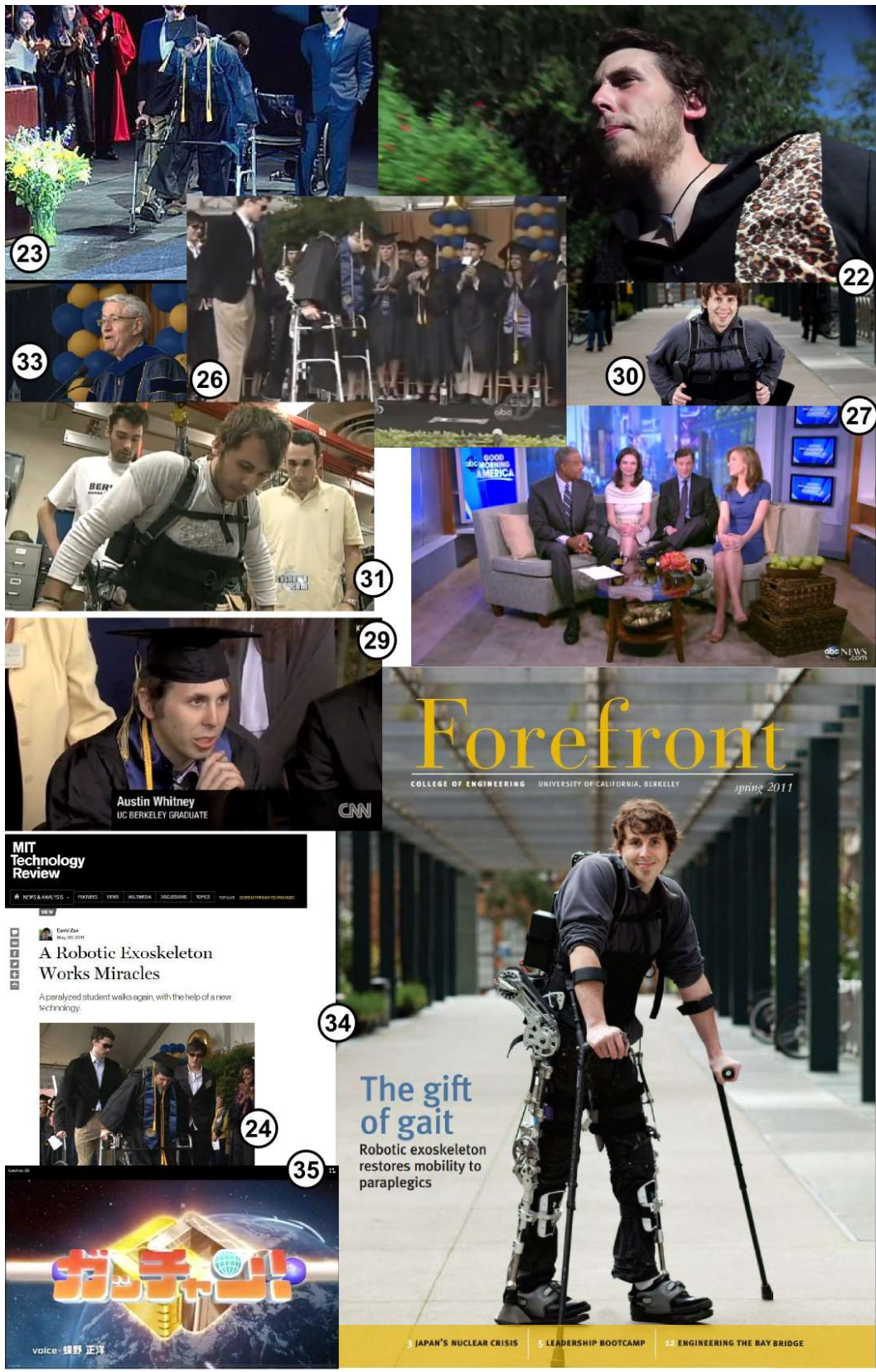
- [59] "Speed of Animals." [Online]. Available: <http://www.infoplease.com/ipa/A0004737.html>. [Accessed: 07-May-2014].
- [60] R. M. Glaser, M. N. Sawka, S. W. Wilde, B. K. Woodrow, and a G. Suryaprasad, "Energy cost and cardiopulmonary responses for wheelchair locomotion and walking on tile and on carpet.," *Paraplegia*, vol. 19, no. 4, pp. 220–6, Jan. 1981.
- [61] E. Jarosz, "Determination of the workspace of wheelchair users," *Int. J. Ind. Ergon.*, vol. 17, no. 2, pp. 123–133, Feb. 1996.
- [62] J. W. Kozey and B. Das, "Determination of the normal and maximum reach measures of adult wheelchair users," *Int. J. Ind. Ergon.*, vol. 33, no. 3, pp. 205–213, Mar. 2004.
- [63] K. a Curtis, C. M. Kindlin, K. M. Reich, and D. E. White, "Functional reach in wheelchair users: the effects of trunk and lower extremity stabilization.," *Arch. Phys. Med. Rehabil.*, vol. 76, no. 4, pp. 360–7, Apr. 1995.
- [64] H. a Seelen, Y. J. Potten, a Huson, F. Spaans, and J. P. Reulen, "Impaired balance control in paraplegic subjects.," *J. Electromyogr. Kinesiol.*, vol. 7, no. 2, pp. 149–60, Jun. 1997.
- [65] H. A. Seelen and E. F. Vuurman, "Compensatory muscle activity for sitting posture during upper extremity task performance in paraplegic persons.," *Scand. J. Rehabil. Med.*, vol. 23, no. 2, pp. 89–96, 1991.
- [66] S. Nuzik, R. Lamb, a VanSant, and S. Hirt, "Sit-to-stand movement pattern. A kinematic study.," *Phys. Ther.*, vol. 66, no. 11, pp. 1708–13, Nov. 1986.
- [67] E. Papa and a Cappozzo, "Sit-to-stand motor strategies investigated in able-bodied young and elderly subjects.," *J. Biomech.*, vol. 33, no. 9, pp. 1113–22, Sep. 2000.
- [68] H. Burger, J. Kuželički, and Č. Marinček, "Transition from sitting to standing after trans-femoral amputation," *Prosthet. Orthot. Int.*, vol. 29, no. 2, pp. 139–151, Jan. 2005.
- [69] a Kralj, R. J. Jaeger, and M. Munih, "Analysis of standing up and sitting down in humans: definitions and normative data presentation.," *J. Biomech.*, vol. 23, no. 11, pp. 1123–38, Jan. 1990.
- [70] W. Mathiyakom, J. L. McNitt-Gray, P. Requejo, and K. Costa, "Modifying center of mass trajectory during sit-to-stand tasks redistributes the mechanical demand across the lower extremity joints.," *Clin. Biomech. (Bristol, Avon)*, vol. 20, no. 1, pp. 105–11, Jan. 2005.
- [71] "The ROHO Group - High Profile Quadtro Select Cushion." [Online]. Available: http://www.therohogroup.com/products/seat_cushions/high_profile_quadtro_select_cushion.jsp. [Accessed: 30-Apr-2014].
- [72] P. M, "Reverse Battery Protection," *Solutions*, no. May. pp. 1–6, 2005.

- [73] Vishay, “P-Channel MOSFETs , the Best Choice for High-Side Switching,” pp. 1–5, 1997.
- [74] H. W. Ott, *Electromagnetic Compatibility Engineering*. John Wiley & Sons, 2011.
- [75] A. Goffer and C. Zilberstein, “LOCOMOTION ASSISTING DEVICE AND METHOD,” US8348875 B22013.
- [76] K. a. Strausser and H. Kazerooni, “The development and testing of a human machine interface for a mobile medical exoskeleton,” *2011 IEEE/RSJ Int. Conf. Intell. Robot. Syst.*, pp. 4911–4916, Sep. 2011.
- [77] M. Goldfarb, R. Farris, and H. Quintero, “MOVEMENT ASSISTANCE DEVICE,” US20130197408 A12013.

Appendix A: Media Featuring My Work







Patents and Publications

- P1) McKinley. "Design of lightweight assistive exoskeletons for individuals with mobility disorders", UC Berkeley Ph.D. Thesis, 2014.
- P2) Tung, McKinley, Pillai, Kazerooni. Design of a minimally actuated Exoskeleton with mechanical swing-phase gait generation and sit-stand assistance. ASME DSCC 2013.
- P3) Reid, McKinley, Tung, Pillai, H. Kazerooni. A Method of swing leg control for a minimally actuated medical exoskeleton for individuals with paralysis. ASME DSCC 2013.
- P4) Tung, McKinley, Reid, Kazerooni. Patent Application. "Controllable Passive Artificial Knee" Berkeley. Sep. 2012.
- P5) McKinley. "Design of a Novel Orthotic Knee Joint for Use in an Assistive Exoskeleton for Paraplegics", UC Berkeley MS Thesis, Dec 2011.
- P6) Tung, McKinley, Reid, Kazerooni. Aug 2011. Patent Application #20130158445. Orthosis system and methods for control of exoskeletons.
- P7) Reid, McKinley, Tung, Kazerooni. Patent Application. Method and device of human machine interface for exoskeleton. May 2011
- P8) Tung, McKinley, Reid, Kazerooni, Patent Application. Exoskeleton with Coupled Knee and Hip Joint. Jan 2011.

Media Featuring My Work

- 1) *Public Transit*. University of California. 1 May 2014. Billboard. Billboard featuring the Steven Exoskeleton near Oracle Arena in Oakland California. Visible from Interstate 880 South.
- 2) *I'm Not The Robot: Exoskeletons For Paraplegics*. Jan Sturmann. US Bionics, 6 Apr. 2014. Web. Film introducing the Steven and Daniel Exoskeletons. Shows exoskeleton pilots walking together through unstructured environments.
- 3) *At Berkeley*. Prod. Frederick Wiseman. 26 Feb. 2014. Film. Early prototypes of the Austin Exoskeleton featured in Frederick Wiseman's Documentary "At Berkeley"
- 4) *Thats Berkeley*. <https://www.youtube.com/watch?v=prCKZg5ONGg>. UC Berkeley, 9 Jan. 2014. Web. Austin Exoskeleton featured in UC Berkeley Promotional video.
- 5) *Science of Innovation: Bionic Limbs*. NBC Learn. <http://www.nbclearn.com/portal/site/learn/cuecard/62946> Web. 4 Feb. 2013. Steven Exoskeleton featured on NBC Learn.
- 6) *2012 Chancellor's Holliday Card*. UC Berkeley. 12 Dec. 2012. Human Engineering Laboratory and Austin Exoskeleton Featured on UC Berkeley Chancellor's Holiday Card.
- 7) *The Berkeley Way*. US Airways Magazine. Dec. 2012. Human Engineering Laboratory and Austin Exoskeleton Featured in an article highlighting research at UC Berkeley.

- 8) *The Cure*. David Alvarado. <https://www.youtube.com/watch?v=wLz9H5pleIE>. 26 Nov. 2012. Web. Featuring the Steven Exoskeleton. Filmmaker David Alvarado tells the remarkable, behind-the-scenes story on the founding of the Silicon Valley Institute of Regenerative Medicine.
- 9) *Richard Hammond's Miracles of Nature*. Episode 3. BBC1. Aired 19 Nov. 2012. The Steven Exoskeleton Featured in Richard Hammond's Miracles of Nature.
- 10) *Demonstration of the Steven Exoskeleton*. Stanford University, Palo Alto. 16 Nov. 2012. Presentation. Invited Demonstration at the Stanford Conference on Spinal Cord Injury: Symposium on regeneration, repair and restoration of function after spinal cord injury.
- 11) *Welcome to Berkeley*. UC Berkeley Promotional Video. 23 Aug. 2012. Austin Exoskeleton Featured in "Welcome to Berkeley" an introduction to UC Berkeley.
- 12) *Accessible Exoskeleton Systems: Takin' It To The Street*. Jan Sturmann. 17 Jun. 2012. A Documentary on the Passive dynamic exoskeleton project by Jan Sturmann.
- 13) *2011 Chancellor's Holliday Card*. UC Berkeley. 16 Dec. 2011. Austin Exoskeleton Featured on UC Berkeley Chancellor's Holiday Card.
- 14) *From Science Fiction to Reality*. Life in Action Magazine, United Spinal Association, Dec. 2011.
- 15) *QUEST TV Exoskeletons Walk Forward*. KQED 9, Aired 16 Nov. 2011. The Austin Exoskeleton featured on QUEST TV documentary on bionics.
- 16) *Discussion of Bionics at Berkeley*. Kazerooni, H. UC Berkeley College of Engineering Homecoming. 106 Stanley Hall, Berkeley. 15 Oct. 2011. Lecture.
- 17) *First Steps of a Cyborg*. Popular Science Magazine, Sep. 2011. Austin Exoskeleton featured in Popular Science Magazine.
- 18) *Exoskeletons for Paraplegics*. Popular Science Radio. 27 Aug 2011.
- 19) *Naked Science: Make me a superhuman*. The National Geographic Channel. Aired 11 Aug. 2011. Early prototype of the Austin Exoskeleton featured in documentary about assistive robotics.
- 20) "Taking a Step in the Right Direction." Koch, Kathryn. Duxbury Reporter 17 June 2011: 1. Print.
- 21) *Paralyzed Student, Austin Whitney, Walks at Graduation Explained*. <https://www.youtube.com/watch?v=3Q3DVAEplbc>. Discovery News. 6 Jun. 2011. Web. Four years after being paralyzed in a car accident, UC Berkeley graduate Austin Whitney was able to walk again thanks to a new robotic exoskeleton. Jorge Ribas finds out how it works.
- 22) *What If?* Jan Sturmann. 3 Jun. 2011. A documentary on the Austin Project by Jan Sturmann.
- 23) *Paraplegic Student Walks at College Graduation*, Inside Edition. 19. May 2011.

- 24) *A Robotic Exoskeleton Works Miracles*. MIT Technology Review, May 2011
- 25) *Paralyzed Berkeley grad's small steps highlight giant bionic leap*. USA Today. 16 May 2011.
- 26) *Graduation Walk*. ABC 7 News, 15 May 2011.
- 27) *Miracle Walk*. Good Morning America. ABC. Aired 15 May 2011.
<http://abcnews.go.com/GMA/video/graduation-miracle-walk-1360688>. Austin's Graduation Walk featured on Good Morning America.
- 28) *Exoskeleton lets UC Berkeley grad take a huge step*. San Francisco Chronicle, 15 May 2011.
- 29) *Exoskeleton Helps Student Walk*. CNN News, 15 May 2011.
<http://www.cnn.com/video/?/video/us/2011/05/15/dnt.ca.paralyzed.grad.walks.kgo>
- 30) *Paraplegic student stands tall and walks at commencement*. UC Berkeley. News center Berkeley. 14 May 2011. Web.
- 31) *Exoskeleton lets paralyzed walk again*. CBS News, 14 May 2011.
<http://www.cbsnews.com/video/watch/?id=7366088n&tag=exclsv>.
- 32) *Robotic exoskeleton helps UC Berkeley paraplegic make short -- but triumphant -- walk for diploma*, The Oakland Tribune. 14 May 2011.
- 33) *Engineers to Help Paraplegic Student Walk at Graduation*. UC Berkeley. News center Berkeley. 12 May 2011. Web.
- 34) *The Gift of Gait*. Forefront Magazine, Apr. 2011. Austin Exoskeleton featured as cover story for Forefront Magazine.
- 35) *Mechatronics at Berkeley*, Gatchan. Aired on NHK. 4 Feb. 2011. Austin Exoskeleton featured on Japanese technology and education show Gatchan!

Appendix B: The Austin Exoskeleton

AUSTIN: System



Figure 77 : System overview of the Austin Exoskeleton.



Figure 78 : Austin Exoskeleton crew April 2011. (Left to right) Jason Reid, controls; Austin Whitney, pilot; Michael McKinley, hardware and electronics design; Wayne Tung, hardware and padding design.



Figure 79 : Austin Exoskeleton mechanical gait generation MGG. Knee trajectory encoded in hardware.

Standing



Figure 80 : Austin Exoskeleton Standup - Trajectory encoded in hardware.